כנס החברה הגיאולוגית

אשקלון | 2012

תקצירים

2012 ASCALON

כנס החברה הגיאולוגית אשקלון

ABSTRACTS

Editors:

Lea Feldman

Oz Dror

Ashkelon

13.3 - 15.3.2012

החברה הגיאולוגית הישראלית מודה למוסדות הבאים
על תמיכתם ותרומתם לכנס השנתי באשקלון:


המכון הגיאולוגי לישראל


המכון הגיאופיסי לישראל


אבנר חיפושי נפט ש"מ


גיאו מג


רותם אמפרט נגב בע"מ


נגב מינרלים


מכון צוקרברג לחקר המים, המכון לחקר המדבר ע"ש י. בלאושטיין, המחלקה לגיאולוגיה והסביבה, אונ' בן גוריון בנגב


האוניברסיטה העברית, המכון למדעי כדור הארץ


Israel Energy Initiative


גיאו-פרוספקט בע"מ


נשר מפעלי מלט ישראליים בע"מ


אקולוג הנדסה


בית הספר למדעי הים, אוניברסיטת חיפה


גיאוכום


מ. לוין סקרים גיאולוגים וגיאוטכנים


גיאו-לוג


מודיעין אנרגיה


Globe Oil Exploration


יהוא חרסיות בע"מ


אלדן ציוד אלקטרוני


דלק קידוחים


Adira Energy


הכשרת הישוב בישראל - אנרגיה בע"מ


רציו חיפושי נפט בע"מ


גוליבר אנרג'י בע"מ

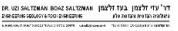
ד"ר עוזי זלצמן ובועז זלצמן


נובל אנרג'י


המחלקה לגיאופיסיקה ומדעים פלנטריים, אוניברסיטת ת"א

Contents

Immature high sulfurous asphalts in the Jordan rift valley: In memory of Dr. Eli Tannenbaum 15
Aizenshtat Z., Amrani A., Tannenbaum E. (PM)*

Anatexis in K-poor and Si-rich migmatites, Roded massif, Israel 16
Anenburg M., Katzir Y.

Re-examination of correlation coefficients of earthquake source parameter 17
Ataev G., Shapira A., Hofstetter A.

Eastern Interceptor Wells forBrackish water Desalination as a key component for the Southern and Central Israeli Coastal Aquifer Rehabilitation and Restoration Plan 18
Avital A., Lumelsky S., Matmon D., Gev I.

The paleogeographical significance of Lower Eocene crocodilian relics discovered north of Ramon anticline, southern Israel 20
Avni Y., Lewy Z

Monitoring the geomorphic evolution of the Nahal Ze'elim fan - a vital step toward proper planning of new infrastructures, Dead Sea, Israel 21
Avni Y., Filin S., Arav R., Zilberman E.

Carbon isotopic exchange in hypersaline groundwater 23
Avrahamov N., Sivan D., Yechieli Y., Lazar B.

Intra-formational mass-movement phenomena in the avedat group (eocene) of the avedat plateau, negev, israel. 25
Ayali B., Eyal Y., Benjamini C.

An assessment of the distribution, concentration and transport processes of mercury offshore from Haifa based on sediment cores 26
Bareket M., Bookman R., Herut B.

Detrital zircon U-Pb-Hf systematics of Israeli coastal sands: Novel perspectives on erosion in the Nile source regions 27
Be'eri-Shlevin Y., Avigad D., Gerdes A., Zlatkin O.,

In situ U–Pb dating of zircon by LA-ICP-MS at the Institute of Earth Sciences, Hebrew University 28
Be'eri-Shlevin Y., Dvir O., Gerdes A., Zlatkin O., Avigad D.

Considerations on engineering intervention along the friable dynamic Mediterranean Seashore Cliffs **30**
Ben-David R.

Mud Diapirs in the Deep Levant Basin – A Proposed Mechanism for the evolution of the Gas-Bearing Tertiary Structures **31**
Ben-Gai Y.

The Geology of the Elat Sheet **33**
Beyth M., Eyal Y., Garfunkel Z.

Artificial islands offshore Israel- Dutch/Israeli feasibility study **34**
Beyth M., Ben-Elyahu H.

Controls on the sedimentary system of evaporitic half-graben basins, Late Triassic Mohilla Fm of the Ramon basin **36**
Bialik OM., Korngreen D., Benjamini C.

Anisotropy of Magnetic Susceptibility (AMS) as a tool for evaluating strain field around faults **37**
Braun D., Eyal Y., Weinberger R., Levi T.

Geological Characterization, Capacity Estimates of CO_2 Storage in the Two Elk Energy Park Pilot Test site, Powder River Basin, Wyoming **38**
Calvo R.

Variations in soil CO_2 concentrations and isotopic values in a semi-arid region due to biotic and a-biotic processes in the unsaturated zone **39**
Carmi I., Yakir D., Yechieli Y., Kronfeld J., Stiller M.

Bedload transport by flashfloods: a comparison of wadis across the semi-arid/arid environmental spectrum **40**
Cohen H., Laronne J. B., Reid I.

Spatial and temporal trends of groundwater salination at the Sulam-Tsor basin, western Galilee **41**
Dafny E.

Geological Constraints on the Location of Natural Gas Treatment and Transmission Facilities on the Israeli Continental Shelf **43**
Dor O., Bruner I., Harari D., Lerman G., Ben-Shushan M., Klein M.

Prospect for Commercial Gas Discovery in the Hula Valley **45**
Dor O., Hazan N., Bruner I., Almog D., Bruner O., Erez I.

3D digital geological setting of the Mediterranean Israeli Ports areas **46**
Doudkinski D., Frid V., Averbakh A., Liskevich G.

A new technique for direct analyses of C-H-O liquids coexisting with mantle material **47**
Dvir O., Angert A., Kessel R.

Boron content and isotope ratio as tracers of serpentinization in the Troodos ophiolite, Cyprus **48**
Elisha B., Katzir Y., Samuele A., Meir A.

Rock formations and fluid flow along the northern slope of the Palmahim Disturbance **49**
Ezra O., Makovsky Y., Ben Avraham Z., Austin J., Coleman D., Tchernov D., Tezcan D., Spiro B., Hübscher C., and Project Nautilus participants.

The Transition from aggradation to incision in the Late Pleistocene in the Negev Highlands. **50**
Faershtein G., Matmon A., Porat N., Avni Y.,

Genetic Groups of Oil Samples from the Southern Israel and SE Mediterranean Continental Margin - Revisit **51**
Feinstein S., Aizenshtat Z., Miloslavsky I., Goldberg M., Obermagher M.

111 Years of Seismic Monitoring or Israel and adjacent regions **52**
Feldman L., Reich B., Avirav V., Hofstetter R.

Engineering geophysical methods for Israeli road industry **53**
Frid V., Averbakh A., Liskevich G., Titov V.

Origin of the Andromeda Mound Complex in the Lower Pliocene Yafo Sand Member, Southeastern Levantine Basin **54**
Fuhrmann A., Weimer P., Bouroullec R., Gardosh M., Pettingill H., Hurst A.

Mantle aspects of oil/gas forming **55**
Galant Y.B.

Acceleration of ureolytic CaCO3 precipitation by non-ureolytic bacteria **57**
Gat D., Tsesarsky M., Ronen Z.

The Mottled Zone Event – the scale of system closure **58**
Geller Y.I., Burg A., Halicz L., Kolodny Y.

Reservoir mapping and characterization for hydrocarbon exploration, enhanced oil recovery and geological natural gas and CO_2 storage **60**
Gendler M.

Investigation of shallow gas and fluid migration within the Pleistocene-Holocene sedimentary section of the southeastern Levant basin using 3D seismic data 61
George S., Makovsky Y., Ben Gai Y., Tezcan D.

The oil-shale survey at the HaShfela basin: hydrogeological properties of the Santonian-Maastrichtian sequence 62
Gersman R., Bartov Y.

Pleistocene lakes in southern Israel and Jordan: paleogeography, paleohydrology and paleoclimate implications 63
Ginat H., Mischke S., Al-Saqarat B.

Some features of seismic, acoustic waves and craters for Sayarim surface explosions 64
Gitterman Y.

The pH of the Dead Sea - A liquid junction independent determination 65
Golan R., Gavrieli I., Lazar B., Ganor J.

Characterizing rock varnish developed on earliest Holocene Negev flint artifacts as a potential paleoenvironmental or paleoclimatic indicator 67
Goldsmith Y., Enzel Y., Stein M.

Diurnal Geochemical Fluctuations of the Effluents in the Infiltration basins of the Shafdan plant 69
Goren O., Gavrieli I., Burg A., Lazar B., Negev I., Guttman J., Kraitzer T.

Determination of site response in Timna using microtremor and seismic events 71
Gorstein M., Zaslavsky Y., Kalmanovich M., Perelman N.

Measuring near-equilibrium rates of silicate mineral dissolution and secondary phase precipitation using silicon isotopes 72
Gruber C., Zhu C., Jiwchar G.

Pseudo-Deterministic Seismic Hazard Analysis for the Dead Sea Basin Area 73
Harari D., Dor O., Ben-Nun O.

Complex landscape evolution of the central Coastal Plain (Israel) based on buried and relict surfaces 74
Harel M., Amit R., Enzel Y., Porat N.

Magnetic Properties of Carbonate Rocks as a Tool for Estimating the Strain field near the Dead Sea Transform, Northern Israel 76
Issachar R., Levi T., Weinberger R., Marco S.

Meso-scale fault geometry in the Lisan Formation 77
Jacoby Y.*, Weinberger R., Marco S.

Uplift and exhumation of Mount Hermon: insights from the first (U-Th)/He cooling ages along the northern Dead Sea Transform 78
Joseph - Hai N., Haviv I., Eyal Y., Weinberger R., Benjamini C., Farley K. A.

Observation of Site Effects at the Schools of Qrayot and Earthquake Hazard Assessment 79
Kalmanovich M., Zaslavsky Y., Gorstein M., Perelman N., Giller V., Aksinenko T., Ataeva G., Dan H., Giller D., Shvartsburg A.,

Sediment reworking events as possible indicators for seismic activity in the Northern Gulf of Aqaba-Eilat 80
Kanari M., Bookman R., Ben-Avraham Z., Tibor G., Niemi T.M., Goodman Tchernov B. , Hartman G., Galloway J.L., Al-zoubi A.[6], Abueladas Abdelrahman M.S.

Methane bubble growth and migration within shallow muddy aquatic sediments: a theoretical study 82
Katsman R., Makovsky Y.

Re-evaluation of the inland retreat rate of Israel's Mediterranean coastal cliff 83
Katz O., Mushkin A.

Oil sand exploration project in Inner Mongolia, China 84
Kolodner K., Barun D.

Groundwater recharge in the southern coastal aquifer: soil and vadose-zone point of view 86
Kurtzman D., Turkeltaub T.*, Baram S., Dahan O.,

The late Pleistocene hydrological history of Lake Kinneret based on Sr/Ca and $^{87}Sr/^{86}Sr$ in ostracods from Ohalo shore, Israel 88
Lev L.* , Almogi-Labin A., Stein M., Ben-Avraham Z.

Reliable Monitoring of Fresh-Saline Water Interface in Coastal Aquifers 89
Levanon E.*, Yechieli Y., Salev E., Friedman V., Gvirtzman H.

Developing new earthquake scenarios for Israel using Hazus loss-estimation software 90
Levi T., Katz O., Bausch D.

Late Pleistocene palaeoclimate of the Dead Sea area (Israel): speleothem and stromatolite records 92
Lisker S., Vaks A., Bar-Matthews M., Porat R., Frumkin A.

The Meged Oil Field – Introduction **93**
Luskin T., Shteingolts V., Soferstein M.

Pervasive evidence of methane seepage along the base of Israel's Mediterranean slope – preliminary results of E/V Nautilus 2011 cruise **94**
Makovsky Y., Ben Avraham Z., Ballard R.D., Austin J., Coleman D., Almogi-Labin A., Tchernov D., Tezcan D., Spiro B., Ezra O., Antler G., Rubin M., Tsadok R., Fuller S.A., Phillips B., Qupty N., Sade H., David N., Scheinin A., Sivan O., Hübscher C., and Project Nautilus participants.

Liquefaction on the Mediterranean shore of Israel: possible onshore evidence for past tsunami **96**
Marco S., Katz O., Dray Y.

Observations of seismic activity in Southern Lebanon **97**
Meirova T., Hofstetter R.

Seismic attenuation in Israel from coda waves **98**
Meirova T., Pinsky V.

Tsunami Early Warning and Mitigation System in Israel **99**
Meirova T., Rosen D., Salamon A.

Evolution of the Arabian-Nubian Shield and the provenance of Paleozoic sandstones in Southern Israel and Jordan: Zircon U-Pb-Hf perspectives **100**
Morag N., Kolodner K., Avigad D., Gerdes A., Belousova E., Harlavan Y.

The role of extreme winter storms in the overall retreat pattern of an actively eroding eolianite coastal cliff-line in the eastern Mediterranean **101**
Mushkin A., Katz O.,

Direct dating of late-Pleistocene activity along the Qiryat Shemona fault, the Dead Sea Transform in northern Israel **102**
Nuriel P., Weinberger R., Rosenbaum G.

Experimental assessment of dynamic characteristics of two monuments in Avdat national park. **103**
Perelman N., Zaslavsky Y.

Thermal and optical luminescence of fault gouge: preliminary experimental results **104**
Philip E., Porat N., Agnon A., Reches Z.

Detailed mapping of deep Jurassic structures in the Eastern LevantBasin with multi-azimuth seismic data **105**
Politi M., Agnon A., Reshef M.

Data Exchange Improves Regional and Global Seismic Monitoring **106**
Reich B., Feldman L., Avirav V., Hofstetter R.

Precipitation Kinetics of Sulfate-Bearing Minerals under Environmental Condition of CO_2 Geological Storage **107**
Rendel P., Wolff-Boenisch D., Gavrieli I., Ganor J.

High resolution magnetic survey in lake Kinneret (Sea of Galilee) **108**
Rofe M., Ben-Avraham Z., Tibor G., Rybakov M.

Stratigraphy and lithology of the Neogene sedimentary sequence in Nahal Tavor area **109**
Rozenbaum A.G., Sandler A., Zilberman E., Stein M.

The effect of coastal groundwater salinization and freshening on nutrient behavior, experimental study **110**
Russak A.′, Yechieli Y., Lazar B., Herut B., Sivan O.

Where is the Carmel Fault? **111**
Salamon A., Aksinenko T., Zaslavsky Y., Kalmanovich M., Shvartsburg A., Giller V., Dan H., Giller D., Zviely D., Ankori E. Medvedev B. Frieslander U. Zilberman E., Baruch O.

Disharmonic structures along the arava valley. A key for understanding the tectonic activity along the dead sea rift valley. **113**
Salmon M., Ginat H., Eyal Y.

A revised chronostratigraphy of the Neogene sequence in the eastern Lower Galilee **114**
Sandler A., Zilberman E., Rozenbaum A.G.′, Stein M.′, Jicha B., Singer B

Structure of the Levant Basin based on residual gravity anomalies **116**
Segev A., Rybakov M.

Coastal-cliff retreat dynamics at Olga beach characterized through monthly high-resolution ground based LiDAR campaigns **117**
Shahar N., Katz O., Mushkin A.

Quantitative Analyses of Macrofauna and Depositional Environments of the Bira Formation at Nahal Tavor **118**
Shaked-Gelband D.′, Edelman-Furstenberg Y., Mienis H. K., Sandler A., Zilberman E., Stein M.′, Starinsky A.

Geometrical Focusing as a Mechanism for Significant Amplification of Ground Motion in Sedimentary Basins **119**
Shani-Kadmiel S., Tsesarsky M., Louie J. N., Gvirtzman Z.

Deep percolation of nitrate, under citrus orchards: vadose zone observations and modeling **120**
Shapira R., Kurtzman D.

Probability based estimation of earthquake risk parameters to be used in earthquake preparedness operations. **122**
Shapira A., Steinberg D. M., Begin Z. B.

The emergence of collapsed sinkholes on mudflats along the shore of the Dead Sea **123**
Shoval S., Kaz G.

Study the long-term re-hydroxylation and rehydration in pottery of different archeological ages in view of re-hydroxylation dating **124**
Shoval S., Paz Y.

Pseudo-amorphous and crystalline phases in the ceramic composition of noncalcareous pottery **125**
Shoval S., Paz Y.

The emergence of collapsed sinkholes on mudflats along the shore of the Dead Sea **126**
Shlomo S., Paz Y.

Geomorphological settings of wave-shape notches, developed on the carbonate slopes of Mt. Carmel, Israel **127**
Shtober Zisu N., Amasha H., Frumkin A.

The small scale structure and roughness of carbonates fault mirrors **128**
Siman-Tov S., Aharonov E., Emmanuel S., Sagy A.

Corroboration for the influence of a component of solar irradiance on subsurface radon signals **130**
Steinitz G., Sturrock P., Martin C., Piatibratova O., Kotlarsky P.

Hydrocarbon Potential and Prospectivity of the Southern Dead Sea - Results of an Integrated Basin Analysis **131**
Tannenbaum E., Gardosh M., Bruner I., Kremien R.

Master plan for floodwater utilization in the Central and Northern Arava Valley **132**
Tatarsky B., Simon E., Iviansky Y., Agbaria R.

Lithological constrains for gas hydrate distribution on the mid-Norwegian margin: influencing slope stability and geo-hazard through time **134**
Waldmann N., Haflidason H.

A Holocene record of tectonic activity in Tierra del Fuego, Southernmost South America (54°S) **135**
Waldmann N., Ariztegui D., Austin Jr. J., Anselmetti F., Moy C.

Late Holocene sediment cycles and vegetation change in the Zraq Qa'a Jordan **136**
Woolfende W., Ababneh L.

Constraining regional paleo peak ground acceleration from back analysis of prehistoric landslides: Example from Sea of Galilee, Dead Sea transform **137**
Yagoda - Biran G., Hatzor Y.H., Amit R., Katz O.,

About "myth" accompanying the results obtained from the ambient noise measurements for the microzoning of an earthquake hazard **138**
Zaslavsky Y., Gorstein M., Ataeva G., Aksinenko T., Kalmanovich M., Perelman N.

Quantification of the site effects in the Israeli building code, using the Vs,30 parameter. – A seismological view **139**
Zaslavsky Y., Gorstein M., Perelman N., Ataev G., Aksinenko T., Shapira A.

Neoproterozoic basement and Lower Paleozoic siliciclastic cover of the Menderes Massif (Western Taurides): coupled U-Pb-Hf zircon isotope geochemistry **140**
Zlatkin O., Avigad D., Gerdes A.

Visual methodology for identifying damage of historical earthquake: the case of 1927 in old photographs of Jerusalem **142**
Zohar M., Rubin R., Salamon A

S-shape distribution of the longshore sand transport at the Mediterranean coast of Israel **143**
Zviely D., Kit E.

Immature high sulfurous asphalts in the Jordan rift valley: In memory of Dr. Eli Tannenbaum

Aizenshtat Z.[1], Amrani A.[2], Tannenbaum E. (PM)*

1 The Hebrew University of Jerusalem Institute of Chemistry Israel 91904
2 The Hebrew University of Jerusalem Institute of Earth Sciences Israel 91904

Asphalt shows from Hatzbia in the north to the Dead Sea (Perlmuter) in the south were studied employing variety analytical tools. All showed two common properties: 1. Abundant organically bonded sulfur and 2. their biomarkers indicate low maturity. Tannenbaum in his Ph.D. thesis compared these immature asphalts to related Senonian (Ghareb) kerogens and suggested these to originate from early stages of catagenesis. Critics who claimed asphalts to be remnants of either bio or thermal degradation of petroleum confronted these conclusions. Later studies, including various pyrolysis analyses of both kerogens and asphalts were complemented by sulfur and carbon isotopes, and show that under certain conditions, parts of the immature kerogen cleave off to yield asphalt. The residual kerogens/asphalts were examined for structural changes using closed and open system experiments. Bulk parameters were recorded as well as gas chromatograms of the trapped pyroproducts. Thermal and structural changes of the organic matter were followed through analyses of gases, condensates, and extracts. It has been shown that high concentrations of organic sulfur bonded (8.0–12.9% S) compared with low concentrations (1.5–2.1% S) has a significant influence on the thermal behavior of kerogen and asphalt samples from the Dead Sea Rift Valley and Green River Shale Gilsonite. The results obtained indicate very similar thermal behavior and biomarkers distribution for kerogen-immature asphalts pairs. There were marked differences between various modes of thermal treatment and surprisingly marginal differences between hydrous/ nonhydrous, closed system experiments. Hydrous pyrolysis (HP) experiments were reinforced by Tannenbaum and Amrani's works using the USGS laboratories in Denver (with Dr. Mike Lewan).These scientific innovative studies, initiated by Tannenbaum, laid the foundation for better correlation between HP expelled oils and Dead Sea Basin oils and asphalts .HP studies of the Senonian (Ghareb) bituminous rock provided valuable information for basin evaluation. Carbon and Sulfur transformations can explain the mechanisms prevailing during oil generation processes. Thermal parameters for Type II-S kerogens can now be applied to better correlate source rock to petroleum.

Anatexis in K-poor and Si-rich migmatites, Roded massif, Israel

Anenburg M., Katzir Y.

Department of Geological and Environmental Science, Ben Gurion University of the Negev, Beer Sheva 84105, Israel

---

The Roded migmatites of southern Israel were previously thought to form by subsolidus metamorphic differentiation based on the lack of K-feldspar in leucosomes and similarity of plagioclase compositions in coupled leucosomes and melanosomes. Geochemical analysis of carefully sampled palaeosomes shows that the protoliths of Roded migmatites were K-poor and Si-rich metapelites. Rocks of this chemical composition are not expected to have clear mineralogical indicators for anatexis because of the limited number and abundance of peritectic phases. Additionally the products of the melting reactions tend to be erased by retrograde deformation and recrystallization. Thus, the pre- and post-peak assemblages may be almost identical and evidence for migmatization might be overlooked. Nonetheless relict textural evidence for melting is found in the Roded migmatites including quartz-filled embayments and rounded quartz inclusions in leucosome plagioclase crystals, and newly formed euhedral crystals of plagioclase. Likewise lenticular K-felsdpar occurs within melanosome biotite indicating muscovite dehydration melting. Thermodynamic analysis of specific rock compositions show that anatexis should have occurred at peak P-T conditions estimated for the Roded migmatites (4.5 kbar; ~650^{o}C). Petrographic and microstructural observations suggest that potassium was mobilized from the leucosomes to the melanosomes during melt crystallization: Leucosome K-feldspar was replaced by myrmekite and melanosome sillimanite was replaced by symplectites of muscovite and quartz. Wider neosomes are characterized by diatexitic microstructures and by lower amount of myrmekite suggesting channeled influx of water resulting in higher degree of anatexis and dilution of potassium in the melt. Subsequent deformation homogenized the plagioclase compositions.

The Roded migmatites are shown to form by two different processes: migmatites from the western exposures (Mt. Shlomo) formed largely by muscovite-dehydration melting with additional minor neosomes facilitated by small amounts of melting during vapor-saturated conditions. The eastern migmatites (Mt. Yedidya) formed by high-degree melting during influx of large amounts of H_2O.

Re-examination of correlation coefficients of earthquake source parameter

Ataev G.[1], Shapira A.[2], Hofstetter A.[1]

1 Geophysical Institute of Israel, P.O.Box 182, Lod 71100, Israel
2 National Steering Committee for Earthquake Preparedness

We have analyzed 1018 digital records from 100 local and regional earthquakes in the magnitude range Mw=2.7-7.2, occurring in a distance range of 4.5 km to 550 km during 1995-2011. The source parameters were estimated from S-wave spectra using Brune's seismic source model (Brune 1968, 1970 and 1971). We obtained a distance correction parameter, $D=R^{0.8333}e^{0.00365R}$ for the low frequency amplitude and $f_0 = f'_0 e^{4.3610\text{-}4R}$ for corner frequency. Both distance dependent parameters are in good agreement with those obtained by Shapira and Hofstetter (1993). This attenuation model was used to determine the source spectrum of the ground displacement, the seismic moment, M0, moment magnitude, Mw, source radius, r, and stress drop for each earthquake.

The analyzed earthquakes have the seismic moment between $1.28*10^{13}$ and $7.67*10^{19}$ (Nm), moment magnitudes in a range 2.7-7.2, the corner frequencies between 0.15 and 5.17Hz, stress drop between 10^{-1} MPa and 44 MPa. The scaling relation between the seismic moment and stress drop indicates a tendency of increasing seismic moment with stress drop. The empirical correlations between kinematic source parameters obtained in this study can be used in the SEEH procedure to assess the uniform hazard (Shapira and van-Eck, 1994). The results better facilitate routine analysis of the Israel Seismic Networks data.

Eastern Interceptor Wells forBrackish water Desalination as a key component for the Southern and Central Israeli Coastal Aquifer Rehabilitation and Restoration Plan

Avital A.[1], Lumelsky S.[1], Matmon D.[1], Gev I.[2]

1 TAHAL Consulting Engineers Ltd. 154 Menachem Begin Road, Tel Aviv 64921 Israel
2 The Israeli Water & Sewage Authority, Hamasger 14,BOX 20365,Tel Aviv 61201.

The Southern and Centarl Coastal Aquifer of Israel, between Ashdod and Nir-Am and Ashdod-Rishon Le Tziyon , serves as a major operative storage for the National water System as well as for local consumers. This aquifer is threatened by over-exploitation and successive years of drought, resulting in storage depletion, and water quality deterioration due to salination processes, predominantly by saline water inflow along the eastern boundary from the adjacent Eocene aquitard, intensive irrigation with sewage effluent.

In order to arrest the salination processes and allow replenishment of the aquifer a rehabilitation plan has been designed introducing the concept of brackish water desalination as key component of aquifer rehabilitation in this area.

The two main components of this plan are:

(a) "The Eastern interceptor" - a battery of wells located along the brackish-fresh water interface (400-900 mg/L chloride) in the eastern boundary of the aquifer. The water will be pumped continuously in order to prevent saline water inflow to the fresh water storage in the west. The pumped water will be treated in local brackish water desalination plants (BWRO), and in Ashdod-Rishon Le Tsiyon Area either by desalination, dilution with fresh water wells orwill be conveyed to the Shafdan Supply system to the Negev. Finally the desalinated product water will be supplied to consumers within the area and for Ashdod- Rishon Le Tsiyon aquifer the brackish water may be to the Shafdan supply System

(b) A balanced regime pumping plan from both Aquifers based on the annual aquifer recharge replenishment rate. This plan is based on a rigid pumping regime of 30-40 MCM and 20 MCM in the Eastern interceptor and redistribution of groundwater extraction from the low saline operative storage in the west, of an average of 35 MCM and 20 MCM, in Ashdod Nir- Am Aquifer and Ashdod- Rishon Le Tsiyon aquifer, respectively.

The performance of this rehabilitation plan as well as other engineering components and their influence on salinity rehabilitation rate of the operative storage has been studied by a detailed flow and mass-transport hydrological model for a planning period of 45 years. The model results for both aquifer areas indicate that each Eastern interceptor eliminates 15,000-

17,000 tons of salt per year from flowing to the west. The balanced pumping plan enabled the storage and groundwater level restoration. Moreover, the reuse of the desalinated water in the rehabilitation area producing low salinity effluent that in turn is used for irrigation, is contributing to additional elimination of salt inflow to the aquifer.

Brackish water desalination is a key component to the success of the plan facilitating the management of these important aquifers as an annually regulative storage for the National water System.

The paleogeographical significance of Lower Eocene crocodilian relics discovered north of Ramon anticline, southern Israel

Avni Y., Lewy Z

Geological Survey of Israel, 30 Malkhe Israel, Jerusalem 95501, Israel

Bone fragments embedded in hard brownish-pink limestone of the lower part of the Lower Eocene Avedat Group weathered out on top of a mountain plateau northeast of Mizpe Ramon near Nahal Mahmal (near elevation point 720 m; coord. 1409/0136). The corroded fragments preserve part of an external bony (vesicular) envelop and two longitudinal bony (fibrous) canals along 25 cm of the restored specimen. It was identified as the upper jaw of a crocodilian long snout belonging to the Dyrosauridae. The family is known from the Cenomanian to the Lutetian (L. Eocene) successfully surviving the K-T boundary biological turnover. It is characterized by a long and narrow subparallel snout comprising 60-70% of the skull length resembling Indian extant Gavialis. Another triangular fragment belongs to the posterior expanding part of the snout. The present elliptical shape of the circular canals attests to compaction to half their height. Accordingly, the width of the subparallel part of the snout was about 5 cm. Compared to a complete skull of D. phosphaticus (Thomas) from North Africa the reconstructed skull would be 80-90 cm long, and the body 6-7 m long like adult Paleocene-Lower Eocene dyrosaurids.

The limestone is a lithified pelagic chalk consisting of Lower Eocene planktonic foraminifera with lenses of nummulitic (large benthic foraminifera) limestone transported from shallow marine environments. The Lower Eocene limestone unconformably overlies chert of the Upper Campanian Mishash Formation as part of the general onlap on the Ramon anticline since Late Coniacian times.

Earlier, during Cenomanian-Coniacian times, the Ramon region was part of an elevated and periodically exposed carbonate platform belt at the shelf edge as attested by hardground levels, clastic sediments and silicified wood found within the Zafit, Avnon and Tamar formations in outcrops surrounding the present Ramon monocline. Horizontal Eocene beds onlap Upper Cretaceous inclined sediments (ranging 2-5°; Avni, 1991) around the Ramon structure, but whether and when they completely covered the structure is still speculative. The crocodilian relics occur in 200-300 m deep (or more) pelagic sediments about 10-12 km northwest of the anticline crest. These marine reptiles were breeding on land, suggesting that a Lower Eocene landmass was not far, whereas the coast of the main continent was far to the south (in Sudan). The discovery of the crocodilian relics evidences that the Ramon anticline, the largest structure of the Syrian Arc fold belt in the Negev, continued to be partly exposed during the Early Eocene, and may have been completely transgressed during later Eocene times.

Monitoring the geomorphic evolution of the Nahal Ze'elim fan - a vital step toward proper planning of new infrastructures, Dead Sea, Israel

Avni Y.[1], Filin S.[2], Arav R.[2], Zilberman E.[1]

1 Geological Survey of Israel, 30 Malkhe Israel, Jerusalem 95501, Israel
2 Technion-Israel Institute of Technology, Haifa 32000

Nahal Ze'elim is one of the largest drainage basins along the western coast of the Dead Sea, occupying an area of more than 250 km2. During the last decades the outlet of Nahal Zeelim to the Dead Sea has been heavily incised forming deep gullies, which developed on the eastern proximal edge of the recently exposed Holocene alluvial fan. These gullies are gradually migrating upstream toward the western part of the fan, endangering modern infrastructures. Recently, this process became extremely important due to new large-scale infrastructures which are being planned in the fan region. Therefore, detailed and accurate monitoring of the fan evolution is vital to ensure proper planning of the fan area.

Till the first half of the 20th century Nahal Ze'elim had a single, wide (300-400 m), braded stream channel, which was located at the northern sector of the fan. During the 1960's, gravel quarrying from the fan has modified the natural drainage pattern. As a result, large portion of the Nahal Zeelim flood water were diverted towards the southern edge of the fan, generating massive incision and forming large gullies.

During the years 2005 and 2011, the fan evolution has been monitored, combining field observations and high resolution laser-scanning (LiDAR) campaigns.The monitoring indicates that:

1. Despite of the massive past anthropogenic modification of the fan morphology, the Ze'elim fan is gradually restoring its northern historical channel, transporting the majority of the flood water to the northern sector of the fan.

2. Simultaneously with the fluvial channeling, two major sinkholes fields were developed in the northern sector of the fan, trapping large quantities of flood water. Thereby they prevent most of flood water from reaching the eastern segments of the gullies and therefore the incision rates at the eastern sector of the fan are decreasing.

3. Between 2005 and 2011, a decrease of ~40% in the number of the active gullies was observed. Most of the inactive gullies are located in the southern and central sector of the fan.

4. Along the most active gullies, annual rates of backward incisions are not exciding 67 m/y during the 2005-2011 interval. However, last years observations indicate that the incision rates are decreasing.

The diverting of the floods to the northern sector of the Ze'elim fan is associated with declining of the fluvial activity in its southern sector. This ongoing process open an opportunity to place the new infrastructures on the eastern part of the central sector of the fan, south of the active zone, while the northern active sector will remain untouched allowing the restoration of the Nahal Ze'elim outlet to the Dead Sea following its historical pattern.

Carbon isotopic exchange in hypersaline groundwater

Avrahamov N.[1,2], Sivan D.[1], Yechieli Y.[2], Lazar B.[3]

1 Department of Geological and Environmental Science, Ben Gurion University of the Negev, Beer Sheva 84105, Israel

2 Geological Survey of Israel, 30 Malkhe Israel, Jerusalem 95501, Israel

3 Institute of Earth Sciences, The Hebrew University, Jerusalem 91904, Israel

---

Radiocarbon as a dating tool for groundwater is widely used in a variety of aquifers around the world. Dissolution of carbonate minerals during the recharge of CO2 enriched groundwater into limestone/dolomite aquifers is known to interfere with 14C dating of groundwater due to addition of "dead" dissolved inorganic carbon (DIC), until reaching CaCO3 saturation. Further complication to 14C dating of groundwater may stem from recrystallization of aquifer's carbonate rocks during the flow of the saturated groundwater within the aquifer. During this water/rock interaction process, isotopic exchange between the solid phase and the dissolved phase (DIC) decreases the DI14C until reaching inter-phase isotopic equilibrium. The potential effect of such radiocarbon exchange reaction on groundwater dating was investigated mainly by laboratory experiments with fresh or low salinity water. The aim of this research was to estimate the effect of radiocarbon exchange reaction on the dating of hypersaline groundwater in the Dead Sea rift valley.

In order to simulate the effect on DI14C dating of hypersaline brines, we conducted sediment/water batch experiments with brines enriched with DI13C with two types of solids and solutions. The solids were: alluvial sediments from Arugot Wadi on shore of the Dead Sea; and high purity CaCO3 powder (98%). The solutions were: freshwater from Ein Gedi springs; and hypersaline Dead Sea brine. The solids and solutions were placed in bottles that were rotated very slowly during the whole duration of the experiments (up to 6 months). Before closing the bottles all (except of controls) solutions were spiked with solutions highly enriched with DI13C (13C /12C ratio of about two fold the natural 13C /12C ratio) with DIC similar to that of the original solutions. Throughout the experiments, water samples for isotopic and DIC analyses were taken at predetermined time intervals. Several of the bottles were consecutively re-spiked another two times when the 13C/12C ratio of the DIC seemed to level off.

The preliminary results indicate that the solids/solution isotopic exchange process in hypersaline water is slower than in freshwater. According to a heterogenic recrystallization model developed in this study we estimate the isotopic exchange rate constant for hypersaline brines to be ~10 times smaller than that for freshwater. In addition, the time elapsed until the isotopic ratio leveled off decreased for each consecutive spiking. We estimate that just

a minute fraction of the solid phase (~10-4) effectively participated in the recrystallization process. It appears that water/rock interaction has an “aging” effect on radiocarbon dating of fresh and saline groundwater during the first stage of groundwater recharge. If recharge condition stay constant over thousands of years, the groundwater may equilibrate with the rather small effective recrystallization volume of the solid, and radiocarbon dating yields reliable age estimates.

Intra-formational mass-movement phenomena in the avedat group (eocene) of the avedat plateau, negev, israel.

Ayali B., Eyal Y., Benjamini C.

Department of Geological and Environmental Science, Ben Gurion University of the Negev, Beer Sheva 84105, Israel

---

Middle Eocene rocks belonging to the Horsha, Matred and Nahal-Yeter formations formed the Avedat Plateau, located on the northern flank of the Ramon anticline. The pelagic chalk of the autochthonous local sedimentary environment formed in an oceanic environment in the Eocene. Allochthonous limestones of various compositions were emplaced among the chalks, derived from different, more shallow environments. Transport was mostly as debris flows and by slumping. Field measurements of slide planes, small thrusts and fold axes taken on surfaces from the allochthonous limestones indicate two main directions of movement, towards the NNE to NW, and westwards.

Microfacies of the limestones from the allochthonous units indicate considerable compositional and textural diversity, reflecting diverse facies in the source area, but all are of outer shelf origin. The nature of the macroscopic and microscopic features of structural origin indicate both plastic and partially brittle deformation, that occurred during failure, syn-sedimentary transport and emplacement, of partially lithified sediments. Ultimately, limestones of a variety of origins and stages of consolidation were brought together, sometimes intimately mixed in conglomeratic facies. The Avedat region represents the toe-of-slope environment where the limestone lithofacies came to rest among pelagic chalk sediments.

An assessment of the distribution, concentration and transport processes of mercury offshore from Haifa based on sediment cores

Bareket M.[1], Bookman R.[1], Herut B.[2],

1 The Dr. Moses Strauss Department of Marine Geosciences, Haifa University, Mt. Carmel, Haifa 31905, Israel

2 Israel Oceanographic & Limnological Research Ltd., Tel-Shikmona, P.O.Box 8030, Haifa 31080, Israel

---

The Haifa Bay region is affected by industrial and municipal discharges introducing mainly particulate matter, nutrients and heavy metals. Mercury (Hg) that has potentially severe health consequences for the marine environment was detected above eastern Mediterranean background levels in the Haifa Bay surface sediments. Hg levels in shallow water sediments and biota are monitored by the Israel Oceanographic and Limnological research as part of the Israel's National Monitoring Program, showing elevated levels compared to the rest of the coast and few cases in which Hg levels in fish exceeds the safety standards. Two main point sources of Hg pollution were found in Haifa Bay: (1) a chlor-alkali plant effluent discharge at the northern part of the bay that was operated until 2004; and (2) the Qishon estuary which contains effluent from nearby industries. These are in addition to diffusive sources as atmospheric deposition and runoff. Though Haifa Bay is considered a terminal basin for sediments being supplied from the Nile delta, it is possible that sediments are eroding and continuing further, carrying pollution on. In this study, geographically representative sediment cores and grab samples in and off Haifa Bay area were collected and analyzed for Hg concentrations to assess Hg re-distribution and transport.

Two cores were collected by box corer in 2009-2010 from Bustan HaGalil calcareous ridge north of the bay (B3, water depth 36m) and from the continental shelf off Haifa bay (G1, water depth 66m). A third core (ST9, water depth 6m) was collected by divers using Perspex tube in 2011 at the northern part of Haifa Bay.

The core from inner part of the bay shows a decrease of Hg content in the upper few centimeters with respect to last years' concentration in the same station. Its Hg profile demonstrates the decreasing trend of anthropogenic Hg in the bay. On the other hand, the other two cores taken outside of the bay, show significant Hg enrichment (6-fold and 2-fold of background levels) towards the upper few centimeters, reflecting the re-suspension and seaward transport of enriched Hg particles.

Hg analysis of grab samples which were collected this year, will give more information on Hg distribution in the surface sediment at the bay and offshore. Further Lead-210 dating and grain-size analysis will enable calculating changes in Hg fluxes in time and reveal transport mechanisms.

Detrital zircon U-Pb-Hf systematics of Israeli coastal sands: Novel perspectives on erosion in the Nile source regions

Be'eri-Shlevin Y.[1], Avigad D.[1], Gerdes A.[2], Zlatkin O.[1],

1 Institute of Earth Sciences, The Hebrew University, Jerusalem 91904, Israel
2 Goethe University, Frankfurt am Main D-60438, Germany

The Nile, the longest river on Earth, accumulates its sediments within the ~3 km-thick Nile delta and these are partly swept westwards, to the Israeli coast. Of the Niles' main tributaries, the White Nile supplies <5% of the overall sediment load. The Blue Nile and Atbara rivers, which are currently the main sediment suppliers to the Nile, drain the Ethiopian plateau uplifted since ~29 Ma. The latter comprises juvenile Arabian-Nubian Shield basement (ANS; 580-870 Ma), Paleozoic-Mesozoic sediments, and Oligocene flood basalts.

Here we present new LA-ICP-MS, U-Pb ages coupled with Hf isotopic data for detrital zircons from Israeli coastal sands. Three samples from Palmahim-Nitzanim coast were collected at the waterline, and ~ 30 m inland. For each sample ~130 zircons were analyzed for U-Pb and ~ 100 were analyzed for Lu-Hf within the dated domains. Despite some variations in size, shape and modes of the heavy minerals, all three samples yielded similar ranges of detrital zircon U-Pb-Hf values.

The vast majority of the detrital zircons cluster within ~520-1100 Ma with major peaks at 620-680, 780-820 and 900-1080 Ma. Paleoproterozoic to Archean-aged detrital zircons, and a minor population of Phanerozoic-aged zircons, comprise <20-30% of the overall zircon populations. The main 520-1110 Ma zircon group displays a wide range of epsilon Hf(T) values (+13 to -25), with a distribution of high (>5) versus moderate to negative (<5) values indicating a ~1:1 mixture of juvenile versus non-juvenile sources.

Although the Blue Nile and Atbara rivers incise the Ethiopian plateau into ANS basement, our new data imply that ANS is neither the sole nor the dominant source for the Nile's quartz-rich sediments. ANS basement possesses a restricted age range and a clearly juvenile isotopic signature. Thus erosion of this material can not explain the significant amount of Stenian and older zircons in the Israeli coastal sands. Moreover, the ubiquitous presence of detrital zircons portraying negative epsilon Hf values negates ANS as a provenance for much of these sands.

On the other hand, the detrital zircon U-Pb-Hf spectra of the Israeli coastal sands exhibits a marked similarity with detrital zircon patterns of Paleozoic-Mesozoic cover sediments of NE Afro-Arabia. It may thus prove that Nile's sediments issued from the erosion of older siliciclastic sediments residing beneath the Tertiary flood basalts in Ethiopia.

The fact that the three samples studied by us display similar U-P-Hf patterns, indicates no differential sorting of detrital zircons by wave action on the coast.

In situ U–Pb dating of zircon by LA-ICP-MS at the Institute of Earth Sciences, Hebrew University

Be'eri-Shlevin Y.[1], Dvir O.[1], Gerdes A.[2], Zlatkin O.[1], Avigad D.[1]

1 Hebrew University, Edmond J. Safra Campus, Jerusalem, 91904, Israel
2 Goethe University, Frankfurt am Main D-60438, Germany

Laser Ablation Inductively Coupled Plasma Mass Spectrometry (LA-ICP-MS) is emerging as a promising technique for rapid, sufficiently precise, and accurate in-situ U–Pb dating of accessory minerals including zircons.

Successful U-Pb dating by LA-ICP-MS requires sustaining high analytical stability, careful monitoring of depth-dependant U/Pb fractionation, and instrument drift, calibration versus standards, and selecting appropriate common Pb corrections.

The LA-ICP-MS laboratory at the Institute of Earth Sciences, Hebrew University includes an Agilent quadruple mass-spectrometer coupled with a New-Wave 193fx Excimer laser ablation system and a teardrop-shaped, low-volume sample cell.

Following experimentations over the last year, we report optimal analytical conditions for zircon U-Pb dating in our lab with the following protocol:

(a) Lasing is performed with 35 to 25 micron spots, at 7 Hz repetition rate, and 4-5.5 J/cm2 fluency. In most cases this enables analysis of more than one domain within a typical zircon grain.

(b) Ar (ICP) and He (sample chamber) gas flows are set to 0.98-1.04 and 0.26-0.31 l/min respectively.

(c) Background collection, ablation, and washout times are set to 35, 25, and ~5 seconds respectively.

(d) Time resolved data acquisition in peak hopping mode is used with a set dwell time of 0.01 seconds for: 202Hg, 204Pb, 206Pb, 207Pb, 208 Pb, 232Th, 235U and 238U.

Alongside analytical calibrations of the instruments, several data-reduction softwares have been tested. Of these, an Excel based software by A. Gerdes best fits our system as it offers independent assessment of the U/Pb fractionation trend for individual analyses, a straightforward evaluation of standard behavior during the session and a variety of common Pb correction paths.

Finally, we report results from some recent analytical sessions. The ~1095 Ma FC-1 zircon

standard yielded weighted mean 206Pb/238U ages in the range of 1110-1093 Ma, although variable 2 sigma errors (± 18 Ma to ± 34 Ma) and MSWD values (<1 to >6) characterized different sessions. Other results include concordia ages of 624± 7 Ma (MSWD=1.5) for the Shahmon meta-basite (Elat), 597± 8 Ma (MSWD=2.0) for the Sharm pluton and 604± 7 Ma (MSWD=1.8) for the Sama pluton (Sinai). Zircons from these samples have been previously dated with SIMS to 624± 4 Ma, 596± 6 Ma and 608± 4 Ma, respectively. Overall, the results indicate that our LA-ICP-MS system can produce sufficiently accurate and precise U-Pb ages with 2 sigma errors well below 3% as expected for quadruple LA-ICP-MS systems.

Considerations on engineering intervention along the friable dynamic Mediterranean Seashore Cliffs

Ben-David R.

Roved Geology

General geological background – The geological section of the Seashore cliffs is composed mostly of party cemented calc-sandstone (kurkar) as well as clay-sand soil units (Hamra). Outcrops are seen along many km of the Israeli sea shore forming cliffs reaching to about +35. The thickness of sections and their spatial dispersion vary along the exposures, influencing the general stability of the cliffs. The cliffs slope changes from vertical to about 1v:1h. The width of the shores varies on rather short distances. In places the seashore is very narrow (example: Apolonia seashore) but in other places it may reach to several tens of meters at the most (example: Tel-Aviv): it is clear that anthropogenic interventions have a major impact on seashore width. The top of the cliff forms in many places a plateau which is cut by rather small drainage systems carrying water to the sea shores and eventually to the sea.

Destructive forces - There are two main destructive forces affecting the seashore cliffs – runoff due to natural and anthropogenic sources, and high waves hitting the base of the cliffs. These combined forces cause extensive retreat of cliffs by mass landslides or by continuous erosion. Therefore, by eliminating these two forces, the major destructive forces are neutralized.

The Seashore cliffs environment as a natural value – the state and municipalities consider the seashore and cliffs as an important environment: it has been declared that "The Seashore cliffs existence, continuity and its wholeness has a major value for the city of Herzliya. Therefore, development and land use will be planned according to sustainable principles"(Herzliya city policy). This declaration forces the use of rather moderate engineering procedures when dealing with its long term stability which keep the natural aspects of the cliffs.

Authorities will act along this fragile environment when a. massive land use is planned; b. real risk for life exists, or c. severe damage to property may occur.

Only a comprehensive approach, considering the mentioned above sustainable planning principles may arrive to suitable solutions.

The presentation will argue with engineering solutions made along the seashore area and suggest possible solutions to be applied according to sustainable values and principles mentioned above.

Mud Diapirs in the Deep Levant Basin – A Proposed Mechanism for the evolution of the Gas-Bearing Tertiary Structures

Ben-Gai Y.

Genesis Energy Ltd.

The recent gas discoveries in the deep Levant basin are associated with Miocene age folded structures, so far assumed to result by rejuvenated contraction activity due to relative movement of Africa and Europe. This study suggests that they are in fact a result of mud upwelling and diapirism, associated with fast Tertiary subsidence of the basin.

The history of the Levant margin and basin can be briefly summed up to comprise of four major steps: Early Mesozoic rifting, Jurassic to Late Cretaceous passive margin, Late Cretaceous to Early Cenozoic contraction and Tertiary to present subsidence and filling.

The third stage is associated with the conspicuous Syrian Arc inverted structures, mapped onshore and throughout the shelf and slope of the basin. The structures in the deep basin have been described as a rejuvenation of this phase during the Miocene and even been named "Syrian Arc II". The problem is that they do not at all portray the mechanism associated with the original Syrian Arc system.

The main observations associated with this phase are as follows:

1. The older structures on the Levant margin and slope do not indicate any sign of being rejuvenated post-Late Eocene (post Base Saqiye unconformity).

2. The deep-water structures, in most cases, are not associated with older, Late Cretaceous or Early Cenozoic inverted structures.

3. The deep-water structures are symmetric in nature.

4. No reverse faults are observed at any level in the vicinity of these structures; they are dissected by normal faults of pre-Messinian age.

5. Some of the structures are associated with severe disruption of the strata at their core, sometimes piercing all the way to the top.

Three possible scenarios can be suggested: Magmatic (or volcanic) intrusions, salt upwelling or mud diapirism, all must have been elevated from the deep-lying Early Mesozoic strata or below. Magmatic intrusions can be rejected on the basis of the magnetic data; only one, the Jonah structure, is associated with positive magnetic anomaly. Salt presence, although might have been deposited during the rifting stage, can be rejected based on absence of any evidence in

boreholes or seismic sections. Mud diapirism is thus suggested to be the likely cause.

If this scenario is correct, it can be explained by gravitational instability of unconsolidated sediments during the fast subsidence of the basin since Early Tertiary, which resulted in a thick Oligo-Miocene section. This section accommodates the recently discovered thick gas-bearing sand bodies. As these structures ceased to evolve prior to the Messinian, it is assumed that the intrusive material reached a state of equilibrium during the Late Miocene. Mud diapirs are known in other basins that experience plate's collision, such as the South Caspian Sea.

The Geology of the Elat Sheet

Beyth M.[1], Eyal Y.[2], Garfunkel Z.[3]

1 Geological Survey of Israel, 30 Malkhe Israel, Jerusalem 95501, Israel
2 Department of Geological and Environmental Science, Ben Gurion University of the Negev, Beer Sheva 84105, Israel
3 Institute of Earth Sciences, The Hebrew University, Jerusalem 91904, Israel

---

A new 1:20,000 geological map of the Elat area, including explanatory notes in Hebrew and English is presented.

The extensive research done in the Elat area has turned this region into a field laboratory for geosciences students. The Elat Sheet geological map prepared as part of the 1: 50,000 scale geological mapping project of the Geological Survey of Israel is based on previous maps updated by field work of the present study. This very detailed mapping was carried out on 1:10,000 average scale using GIS and orthophoto as the base map.

Three major processes controlled the geological and geomorphological evolution of the Elat area: 1) The creation of the Arabian-Nubian Shield during the Neoproterozoic as part of the East African Orogen and the enclosure of the Mozambique Ocean between the east and west Gondwana plates; 2) Accumulation of the Cambrian to Eocene sedimentary sequence on the Arabian Plate at the south-east margins of the paleo-Tethys and Tethys sea; 3) The Oligocene-Miocene to Recent regional uplift and the evolution of the sinistral Dead Sea Transform which is the plate boundary between the eastern Arabian Plate and the western African Plate.

The well exposed stratigraphy and structure of the Elat area due to extreme arid desert climate document the evolution of these three processes and thus make the geology of the Elat Sheet so unique.

Artificial islands offshore Israel- Dutch/Israeli feasibility study

Beyth M.[1], Ben-Elyahu H.[2]

1 Geological Survey of Israel, 30 Malkhe Israel, Jerusalem 95501, Israel
2 Private consultant, Atlit

The fast growing population along the coast of Israel has motivated feasibility studies of offshore solutions for future infrastructures required.

This study which was carried out by professional Dutch/Israeli teams during the late 1990's, to investigate the environmental, technological and economic and legal feasibility of constructing artificial islands off the coast of Israel. This is especially relevant for uses that impose restrictions on their surroundings such as airports and infrastructure facilities. The environmental feasibility is contingent on continuing maintenance to prevent damage to the coast, to the continental shelf and to the water body. Constructing islands will obligate sand by-pass as mitigating measures. The results presented are mainly based on the report published on February 2000.

The simulation study was conducted for three scenarios:

• Rectangular artificial, regional airport island 2,900X800 meters at a distance of 2,000 meters from Tel-Baruch shore totaling 40,000 to 150,000 cubic meters of sand accumulating behind the island annually.

• 2,000 dunam drop-shaped, residential and commercial island, at a distance of 1,250 meters from Bat-Yam with 50,000 to 200,000 cubic meters annual accumulation of sand.

• A chain of three drop-shape islands, of 2,000 dunam each, at a distance of 1,250 meters from the Ga'ash coast that would accumulate between 40,000 to 150,000 cubic meters of sand per year.

For the construction of the airport island ~100 million cubic meters of suitable fill material are required. For the submerged breakwater and rocks in different weights from 1 to 10 tons each and concrete cubes from 20 to 45 tons each are required. The estimated cost of constructing the airport island including its connection to the coast by means of a bridge was estimated at 1.35-1.85 billion US$ (2000 prices).

The inventory of the fill material namely sand in the continental shelf was based on seismic survey carried out at water depth from 30 to 70 meters between Zikim in the south and Hadera in the north as well as boreholes drilled to depths of 12 meters. Estimated potential reserves are between 100 to 400 million cubic meters dredgeable appropriate fill material, including Kurkar at a cost of 5-15 US$ per cubic meter.

Alternative methods were also considered for construction of islands such as:

1. Floating Island.

2. Pile Based Island.

3. PSP Floating Islands

In Israeli the three Earth Sciences governmental institutes and the Technion played a major rule and all the relevant government planning authorities approved and signed the report.

Controls on the sedimentary system of evaporitic half-graben basins, Late Triassic Mohilla Fm of the Ramon basin

Bialik OM.[1,2], Korngreen D.[2], Benjamini C.[1]

1 Department of Geological and Environmental Science, Ben Gurion University of the Negev, Beer Sheva 84105, Israel

2 Geological Survey of Israel, 30 Malkhe Israel, Jerusalem 95501, Israel

---

The Late Triassic (Carnian) Mohilla Fm was deposited within small (10-20 km wide, 20-60 km in length) half-graben basins situated in a chain along the Levant shelf-edge of the Triassic. Common patterns of sedimentation were found in the Ramon outcrops and in the Kurnub and Qanaim basins known from boreholes. Basin fill is characterized by two main end member facies: an evaporite-rich succession ca. 200m thick in the basin center, and a carbonate succession of up to 100 m near the barrier. These end members are sometimes juxtaposed in proximity to basin-edge faults, with the evaporite facies on the hanging wall side and the carbonate facies on the footwall side. The evaporite succession commences with dolomite near the base, overlain by a middle, evaporite-rich unit, and terminated by a rather monotonous limestone. The upper and lower carbonates are mainly microbialites, truncated by subaerial exposure horizons and with some more fossiliferous marine intercalations.

The Mohilla Fm in the half-graben basins situated near rift-edge faults were found to record signals from repeated structural movements, from sea level change, and from a climate signal, often rhythmic. High sensitivity carbonate-evaporite successions respond to each of these signals as the basin evolves. The controls on fill patterns of multiple orders as the small basins evolved, may be traced to eustatic change, climatic rhythms and local tectonic movements, some of which affected the flux of fresh water into these basins, and others affecting connectivity of the marine system. Basin fill processes recorded in the Mohilla Fm are of three orders: a) Long term eustatically-related restriction and reflooding; 2) Intermediate scale fill patterns, with carbonate/evaporite ratios controlled by climate, evident also in distribution of siliciclastics and carbon isotope ratios in the carbonates; and 3) Short term effects of movement on basin edge faults. Lowering of the barrier floods the basin, but tectonic lowering of the barrier region is generally a one-way, short-term process.

Flooding of the basin, whether during high sea levels or by tectonic movement on the barrier ,results in domination of carbonates from the barrier edge to the basin center. When restriction, usually due to sea level change, causes the barrier region to be exposed, meteoric diagenesis affects the carbonates, while evaporites are deposited in the basin center.

Anisotropy of Magnetic Susceptibility (AMS) as a tool for evaluating strain field around faults

Braun D.[1], Eyal Y.[1], Weinberger R.[2], Levi T.[2]

1 Department of Geological and Environmental Science, Ben Gurion University of the Negev, Beer Sheva 84105, Israel

2 Geological Survey of Israel, 30 Malkhe Israel, Jerusalem 95501, Israel

One of the main problems in structural geology is determining the stress field along faults that lack stress indicators such as slickolites or veins. To overcome this difficulty the present study tests the applicability of the anisotropy of magnetic susceptibility (AMS) method as strain proxy in carbonate rocks. The AMS of carbonate rocks is influenced by their magnetic properties, and the directions of calcite/dolomite c-axes. The shape of the AMS ellipsoid is described by its principal susceptibility values, k1 (maximum), k2 (intermediate) and k3 (minimum). The method is based on laboratory tests and field measurements, showing that the minimum k3 axes of the calcite/dolomite crystals are parallel to the maximum shortening direction in the rocks (i.e., k3?c-axes). In an undisturbed "sedimentary" rock fabric the orientation of k1 and k2 axes would be parallel to the bedding plane, and k3 axes would be orthogonal to the bedding plane (i.e., parallel to the direction of rock compaction). In a "tectonic" fabric, under shortening or elongation conditions, the principal AMS axes would be parallel to the principal strain axes, whereas k3 axes are well-grouped and parallel to the maximum shortening axis. In the current study we measure the AMS along faults planes and from rocks located further away from these planes, in order to compare their magnetic fabrics and associated AMS parameters as a function of strain. For the measurements we sampled the dolomitic Tamar Formation, which contains a very low content of iron. This selection assures that the AMS signals are mainly the result of c-axes distribution in the rocks and are not due to iron-bearing minerals. We collected a total of 116 samples from 4 sites. Our preliminary results reveal that "sedimentary" AMS fabric (k3 perpendicular to bedding) were found in samples that are far (>1 km) from faults, whereas "tectonic" fabrics were found in samples close (<10 m) to the fault plane. These results should be verified in other localities and faults.

These preliminary results show that AMS can be served as a tool for evaluating strain field around faults, especially where other traditional methods cannot be used, and can help determining fault nature in the absence of strain indicators.

Geological Characterization, Capacity Estimates of CO_2 Storage in the Two Elk Energy Park Pilot Test site, Powder River Basin, Wyoming

Calvo R.[1,2]

1 Geological Survey of Israel, 30 Malkhe Israel, Jerusalem 95501, Israel
2 Stanford University, Palo Alto, CA

The Energy Park (North America Power Group) is a commercial-scale demonstration project planned as a series of renewable and other electric power generation, carbon capture, sequestration and related facilities, located in the eastern side of the Powder River Basin, northeastern Wyoming. The site is located on top of several deep saline aquifers, depleted oil reservoirs, and coal seams. The Powder River basin was identified by NETL and Big Sky partnership as having high potential for CO_2 sequestration. The aims of our current study were to identify and describe all porous sections below the proposed site, to estimate the capacity of each unit, and to conduct simulations to better understand the faith of injected CO_2 between those different layers. The storage goal of the project is 3 Mt/year for 50 years of operation. The project is supported by the DOE.

Detailed geological characterization of the section between the Madison Formation and the Mowry Shale was based on two wells, located ~10 km from the proposed site. Porous sandstone layers were identified in the Minnelusa, Spearfish, Sundance, Morrison, Lakota, and Dakota formations. Average porosity in all of those units is between 8 to 15%. These formations consist of interbedded sandstone and shale, with some anhydrite and dolomite layers in the Minnelusa Formation. Our interest was to examine the ability of these impermeable layers (shale, anhydrite, and dolomite) to act as local seal to the different porous units. Other shale dominant formations also occur in the section (Opeche, Fuson, Skull, and Mowry formations) and will act as major seals to the whole porous section.

The complex stratigraphy and relatively low permeability of the rocks at this site appear to preclude identification of a single unit that can be used for CO_2 storage. Instead, the most promising option is to inject CO_2 into large thickness of sediments, resulting in the injection of a relatively small amount of CO_2 into a number of formations isolated from each other by low permeability shale, anyhydrite and dolomite layers. The benefits and drawbacks of storage in this type of setting for injectivity and long term storage security are examined using the TOUGH2-ECO2N simulation model. Additionally, CO_2 capacity was calculated, using NETL equations and range for storage efficiency, and compared to estimates based on the TOUGH2-ECO2N simulation model.

Variations in soil CO_2 concentrations and isotopic values in a semi-arid region due to biotic and a-biotic processes in the unsaturated zone

Carmi I.[3], Yakir D.[1], Yechieli Y.[2], Kronfeld J.[3], Stiller M.[2]

1 Weizmann Institute of Science
2 Geological Survey of Israel, 30 Malkhe Israel, Jerusalem 95501, Israel
3 Tel Aviv University

Interactions of biological processes and a-biotic carbonate chemistry affect the isotopic composition of soil CO_2 and have implications for groundwater dating and on ecosystems carbon fluxes. These interactions were investigated in the semi-arid Yatir forest in southern Israel (290mm mean annual precipitation), which is characterized by shallow soil overlying a carbonate base rock. PVC tubes for sampling of soil gas, open at both ends, were inserted into the unsaturated zone (USZ) at depths of 30cm, 60cm, 90cm, 120cm, 200cm and 250cm. Profiles of soil gas in the USZ were collected from the tubes five times between October 2007 and September 2008. Measurements of the collected profiles of soil gas included CO_2 (ppm), δ13C (‰) and, in one profile 14C (pmc). In the uppermost layer (30cm deep) the concentration of CO_2 in the soil gas was at least 2 times higher than in surface air (CO_2 ~ 390ppm,) and the δ13C was lower (about -16‰) than in the atmosphere (~-8‰). 14C (77 pmc) was lower than the atmosphere and the biosphere. Throughout the USZ down to depth of 250cm , the CO_2 increased with depth, up to ~9,500 ppm, and the δ13C(‰) became more negative (-17‰ to -21‰, at 250cm depth). Apparently, the main source of CO_2 in soil gas is release from the roots. In fall-winter the release of this biologically-derived CO_2 is lowest, increasing in the spring and reaching the highest values in the summer with the δ13C closest to that of a C3 plant. While the main source of CO_2 must be at the root zone, it fills up the profile to basis at or below 250cm (data from deeper level is not available). The decrease in CO_2 with diminishing depth may be due to two processes: CO_2 may be lost from the USZ into the atmosphere and lost due to dissolution into sediment water in the USZ. In the period of high production in the summer δ13C values indicated a mixture of the soil gas with the prevailing atmosphere of the USZ. In the early spring, the 14C (77 to 91pmc) throughout the profile was lower than both the atmosphere and biosphere (~100 pmc) indicating a contribution of a-biotic carbonate from the sediment (2.8 pmc). These biological/geochemical interactions have implications for the isotopic signal of soil CO_2 emitted to the atmosphere or dissolved in soil water to reach groundwater

Bedload transport by flashfloods: a comparison of wadis across the semi-arid/arid environmental spectrum

Cohen H.[1], Laronne J. B.[1], Reid I.[2,1]

1 Department of Geography and Environmental Development, Ben-Gurion University of the Negev, P.O.B 653, Beer-Sheva, 84105, Israel.

2 Department of Geography, Loughborough University, Loughborough LE11 3TU, UK

Semi-arid desert margins are amongst the most sensitive environments to global/regional climatic fluctuations and desertification. A comparison of bedload transport rates/processes in gravel bed wadis along an arid to semi-arid environmental gradient is used ergodically to examine the impact of environmental change. Continuous bedload transport observations for flood flow segments in four gravel-bed wadis in southern Israel (Eshtemoa, Yatir, Rahaf and Qanna'im) reflect a range of climatic conditions from semi-arid to hyper-arid.

These wadis have produced the highest recorded bedload transport rates and the bedload/suspended load ratio is shown to increase with aridity. Bedload transport rates are correlated with reach characteristics such as channel width, slope and bed texture, but there is no apparent correlation with climatic gradient.

In comparison to Qanna`im (hyper-arid) bedload rates in Eshtemoa (semiarid) are higher at lower shear stresses due to a lower armoring index, lower cluster frequency and higher presence of granule-sized flats. The common bedload magnitudes at higher shear in these channels exception the Rahaf justifies a unified empirical non-dimensional linear bedload flux response for gravel bed rivers in deserts. In the wider, oft-braided Rahaf channel bedload flux varies at a given local shear stresses due to a variable pattern of texture, topography variations and a complex flow pattern.

Spatial and temporal trends of groundwater salination at the Sulam-Tsor basin, western Galilee

Dafny E.

Ecolog Engineering Ltd.

During the last decades, ongoing salination was observed at several wells along the north-western border of Israel ("Sulam-Tsor basin"), as well as at a local spring (Ein Masrefot). At its peak, several pumping wells were temporarily shut down. Previous studies (Reference below) that were aimed to detect the saline water body and study the salination process, shed much light upon the local hydrogeology and concluded that (1) a confined saline water-body is found in-vicinity to the wells, within the Bezet syncline at the south, and that (2) over-exploitation leads to movement of this saline water-body northward, i.e. toward the radius of influence of the wells.

The present study is based on the geochemical analysis of 8 wells, located along a W-E section, as far as 10Km eastward to the Mediterranean coastline, collected during the last 2 decades (1991-2010). Several ongoing geochemical processes are proposed. Among, is a mixing process between two end-members that take place both in time and space. This process is well indicated by ionic ratios diagrams. Further analyses of geological and hydrological data, including the preparation of a new geological cross-section, strengthens the conclusions of previous studies, while at the same time refine the conceptual hydrogeological understanding.

Based on the present study it can be determined that the natural (pre-exploitation) flow-field in the Sulam-Tsor basin follows the local topography, i.e., groundwater flows radially from the mountain crest, where in the study area it flows to the south- and south-west. The existing recharge is dominant only in the upper part of the aquifer (the exact formation is pending upon local structures); in the lower parts of the aquifer the existing recharge is not as dominant, thus remnants of trapped saline water that invaded the sub-surface during past high-stand (sea levels) periods are present. Isotopic analysis (Sr, H, O, C) may help revealing the origin (source and period) of the saline water body. Exploitation at the Shlomi and Ya'ara well fields resulted in the reduction of the pressure of the fresh-water body, and the up-coning/ movement of the saline-water body toward the pumping wells, and overall salination. However, under current exploitation this process is still reversible.

THIS WORK WAS FUNDED BY MEKOROT, THE NATIONAL WATER COMPANY.

1. Shachnai E. and Guttman J., 1993. Sulam-Tsor basin – analysis of the hydrogeological model and salination phenomena. TAHAL, rep. 01/93/88 (In Hebrew).

2. Rosenthal E., 1998. Report on the hydrological state and salination processes at the Sulam-Tsor basin (Cell 340). The Hydrological Service of Israel, rep. Hydro/1/1998 (in Hberew).

3. Guttman J., 2011. Management and utilization of a fresh water body adjacent to saline water bodies in fracture and karstic aquifers in Israel. EGU General Assembly

Geological Constraints on the Location of Natural Gas Treatment and Transmission Facilities on the Israeli Continental Shelf

Dor O.[1], Bruner I.[1], Harari D.[1], Lerman G.[2], Ben-Shushan M.[2], Klein M.[3]

1 Ecolog Engineering Ltd
2 Lerman Architects
3 Department of geography and environmental studies, University of Haifa

---

The National Gas Authority is developing a National Master Plan (NMP) to facilitate a transmission of natural gas from Israel's offshore discoveries to the onshore gas distribution system, complementing the existing southern Treatment & Transmission System (TTS) offshore Ashkelon. The TTS requires the construction of a gas treatment rig and facilities on the continental shelf. Here we examine the geological and seismic hazard considerations in selecting location alternatives for the system.

The continental shelf was built by a massive Pliocene and younger clastic sedimentary column overlaying the Messinian evaporates. The shelf slopes westward 10m/km on average to a distance of >20km off central Israel, but narrows northward and in places were the Palmachim & Dor slumps developed. Off-Haifa the shelf morphology is disturbed by the tectonic activity of the Carmel fault system.

Of the various seismic hazards, ground displacement on an active fault and seismically triggered slumps (disturbances) due to thin-skin, salt-related deformation, were identified as the major affecting factors on the selection of location alternatives for the TTS. Several faults, primarily offshore Haifa and the Galilee, were identified as potentially active and were marked on a hazard map as elongated, 600m wide "high risk areas" centered on the fault's trace to allow for mapping errors and the presence of subsidiary active fault branches.

Sedimentological overabundance on the evaporate layer, its thickness, slope inclination, lubricating clay layers, saturation and discontinuities are not mapped systematically in the shelf, hereby deterministic prediction of future slumping sites is currently impossible. However, the occurrence of tsunamogenic slumping in the area suggest that much of the shelf-edge mass is in a critical equilibrium with respect to slumping. Consequently, a predicted framework for the development of seismogenic slumping was developed based on the following observations and assumptions: the head-scarp of the Dor disturbance, not controlled by a local fault system, is at a water depth of ~100 m, probably reflecting the minimum depth (maybe as a proxy for minimum inclination) for the development of non-structurally controlled slumps along the shelf. The head-scarp of the fault-controlled Palmachim disturbance is at a water depth of ~60 m, which is assumed to be the minimum depth for fault-controlled slumping development. It

was accordingly determined that areas deeper than 100 m or that are situated less than 2km east of a clear head-scarp are designated "high risk" for TTS installation; areas at depths of 60 to 100 m were designated "intermediate risk"; and areas shallower than 60 m were designated "low risk". It is possible that the definitions of the safety zones may be adjusted should a higher resolution data (i.e. multibeam) be examined. The NMP planning team has decided to select location alternatives within the "low risk" zone only.

Prospect for Commercial Gas Discovery in the Hula Valley

Dor O.[1], Hazan N.[1], Bruner I.[2], Almog D.[2], Bruner O.[2], Erez I.[1]

1 Ecolog Engineering Ltd
2 Coalbed Gaz Hachula Ltd

The Hula valley was developed between two left stepping faults of the Dead Sea Transform system in northern Israel during the last 4.1 Ma, accumulating more than 3.5 km of sediments. The ~150 km2 flat valley floor is bounded on the east and west by fault-controlled steep slopes. Its southern and northern geomorphic and tectonic boundaries are less distinct. The narrow outlet of the basin on its southeast corner, and the differential subsidence of its floor allowed the development of a fluvio-lacustrine system with expanding and retreating lakes alternating with marsh conditions. The fluctuations in the climatological conditions resulted in cyclic depositional pattern of primarily organic-rich marl, chalk, limestone and peat. With burial depth, the peat developed into lignite and coal, which is the source rock for two related gas systems ("plays"): A. Coal Bed Methane (CBM): gas that is absorbed and trapped within the crystal structure of the source rock itself. It migrates within the coal layer in a liquid state, dissolved in groundwater, and only minimal reduction of the hydrostatic pressure allows its effective extraction. The coal can store six to seven times as much gas as a conventional natural gas reservoir of equal rock volume. CBM become in recent decades an important source of energy in United States, Canada, and other countries. This play was evaluated by an independent international firm (NSAI) as a profitable resource in the Hula Basin; B. Shallow porous reservoirs: the shallow subsurface (down to ~200 m) of the Hula Basin includes porous reservoir rocks such as fluvial sand bodies and lacustrine limestones. Gas from the underlying coal source rocks migrates upward and fills pores where these rocks are in a trapping configuration.

Almost all 42 gas exploration wells and 20 lignite test boreholes drilled in the Hula Valley encountered gas. Most wells were drilled to shallow (~200 m) targets; five wells were drilled to the sub-bituminous coal section. The Ester 1+2 and the Notera 3 wells produced CBM for extended periods, with Notera 3 producing 12,000 MCFD for 15 months.

The primary objective of current exploration activities in the Hula Valley is the main coal layer that was identified in Notera 3 at depths of 838 to 866 m. The plan is to drill or deepen appraisal wells in the vicinity of Notera 3 for reservoir testing by means of reducing the hydrostatic pressure in the layer via pumping out water.

3D digital geological setting of the Mediterranean Israeli Ports areas

Doudkinski D., Frid V., Averbakh A., Liskevich G.

Isotop Ltd, 20 HaYarok, Canot Industry Zone, 70700

The geological – geotechnical models of the Israeli ports is highly required for the new designing and construction works for the different port structures (quays, terminals etc.). More than 1500 boreholes were previously drilled in the area of the Mediterranean Israeli Ports. The motivation of the investigation was to fully use more these boreholes to derive a 3D digital geological-geotechnical model, which will be used for geological –geotechnical cross sections building and will allow one to reduce the need for additional borings and laboratory investigations.

Our investigation consisted of geological-geotechnical data analysis, data filtering and processing of geological information from boreholes drilled in the area of Ashdod, Hayovel, Haifa and Kishon ports. Two-stage geological analysis of the data base was performed. The first level, which we arbitrarily called the "Stratigraphic" level, was consisted of the building of geological – geotechnical units. Soils and rocks similar by their genesis or/and similar in their geological and tectonic position or/and similar in their composition were integrated in the same geological – geotechnical units. The second level of analysis, which we arbitrarily called the "Lithological" level, was used to distinguish rocks and soils by their lithological and structural features within the frame of a specific geological – geotechnical unit. This approach enables us to build the combined "Stratigraphical – Lithological" model, geological – geotechnical cross-sections and maps with additional USCS information and different technical data (scale, layer's roof / bottom depth, cross-section position etc.). Rockworks software was used for 3D modeling and cross sections building. The main achievement and advantage of the 3D digital models built for Israeli ports area is ability to construct the geological-geotechnical cross sections and maps for any part of the Ports following to the investigator will.

A new technique for direct analyses of C-H-O liquids coexisting with mantle material

Dvir O., Angert A., Kessel R.

Institute of Earth Sciences, The Hebrew University, Jerusalem 91904, Israel

Carbon and hydrogen residence are controlled by complex phase equilibria in the Earth's interior. H_2O and CO_2 are introduced into the new formed oceanic lithosphere in mid-ocean ridges while H_2O- and CO_2-rich liquids are released from the subducting slab into the overlying mantle wedge where they trigger volcanism forming the continental crust. Accurate determination of the composition and nature of C-H-O liquids in the mantle is necessary to advance our understanding of the physical processes involved in melt generation at convergent plate margins.

We have developed a new analytical technique, the Quartz Tube System (QTS) for direct analyses of high-pressure, high-temperature fluid and melt compositions in equilibrium with mantle material. In the QTS, the capsule is frozen prior to opening and placed inside a N2-filled quartz tube closed by valves at both ends. One end of the tube is connected to a N2 gas cylinder and the other is connected to an Infra Red Gas Analyzer (IRGA) that analyzes the amount of CO_2 and H_2O. Experiments were conducted at pressure of 3, 4, 6 GPa and temperatures between 1000–1200 °C in a 675-ton rocking multi-anvil apparatus. 3 sets of experiments containing SiO2 and CaCO3 powders were used test and calibrate the technique. These experiments demonstrated that when diamond-trap capsules are prepared in air-free environment, using N2-bubbled di-ionized water, the H_2O and CO_2 content in the sample can be directly and accurately analyzed.

Another set of experiments contained synthetic carbonated lherzolite doped with 50 ppm Th, ~10 wt% H_2O, and a layer of diamond aggregates serving as a fluid/melt trap. A pair of capsules was run in each experiment. One capsule was analyzed for CO_2 and H_2O following the QTS technique. The other capsule was analyzed for total dissolved solids in the liquid following the cryogenic technique. The composition of the residual peridotite minerals was measured by electron microprobe.

In the new technique, a direct analysis of C-H-O fluid or melt in equilibrium with mantle material is possible. This allows us to perform a wide rang of P-T experiments on mantle systems, and to study the mobility of species in aqueous solutions in the mantle.

Boron content and isotope ratio as tracers of serpentinization in the Troodos ophiolite, Cyprus

Elisha B.[1], Katzir Y.[1], Samuele A.[2], Meir A.[3]

1 Department of Geological and Environmental Science, Ben Gurion University of the Negev, Beer Sheva 84105, Israel

2 IGG-CNR, Via Moruzzi 1, 56124 Pisa, Italy

3 Geological Survey of Israel, 30 Malkhe Israel, Jerusalem 95501, Israel

---

Seawater is much richer in boron and has significantly higher values of δ11B relative to peridotite (5 vs. 0.1 ppm; +40 vs. -4‰). Since boron is incorporated into tetrahedral sites in the serpentine lattice during hydration, boron contents of serpentinies are expected to be much higher than those of peridotite and its δ11B should reflect large contribution of water-derived boron. The history of alteration of the Troodos ultramafic section to serpentinite is studied here using coupled O and B isotope ratios in serpentine. Bimodal spatial distribution of

δ 18O values in the Troodos serpentine indicated overprinting of early oceanic, fault-localized 'high temperature' serpentinization (δ18O = 4 to 6‰)by widespread late hydration at lower temperatures forming abundant chrysotile veins (δ18O = 12 to 14‰) [1]. Early serpentinization was interpreted to occur during exhumation of peridotites in an oceanic core complex of a slow spreading ridge. Boron contents and δ 11B positively correlate with δ 18O in the Troodos serpentinites: B-poor (<10 ppm), low δ 11B (-3 to +3‰) serpentine is preserved along the inferred oceanic detachment and significantly differs from the late, asbestos-rich serpentine (40-60 ppm, 7-13‰). Serpentine samples with intermediate B-O isotope ratios indicates mixing and superposition of sequential serpentine generations. However, while δ 18O values of the fault-related oceanic serpentine in Troodos are similar to those of serpentinites from modern oceanic core complexes(e.g. the Atlantis Massif) they have an order of magnitude less boron and lower δ 11B (~0 vs. 10-15‰). Boron loss and lowering of δ 11B might have occurred by late interaction with lower pH solutions of meteoric origin destabilizing the tetraborate ion and preferentially leaching out the heavier isotope.

[1] Nuriel et al., 2009; EPSL 282, 34-46.

Rock formations and fluid flow along the northern slope of the Palmahim Disturbance

Ezra O.[1], Makovsky Y.[1], Ben Avraham Z.[1], Austin J.[2], Coleman D.[2], Tchernov D.[1], Tezcan D.[1], Spiro B.[1], Hübscher C.[3], and Project Nautilus participants.

1 Charney School of Marine Sciences (CSMS), University of Haifa, Haifa 31905, Israel.
2 Sea Research Foundation Institute for Exploration, Institute for Exploration, Mystic, RI, USA.
3 Institute for Geophysics, Center for Marine and Climate Research, University of Hamburg, 20146 Hamburg, Germany.

In the 2010 and 2011 side-scan sonar and remotely operated vehicle (ROV) surveys of the E/V Nautilus offshore Israel we have discovered enigmatic rock formations along the northern slope of the Palmahim Disturbance. The surface expression of the rocks ranges in size from sub-meter up to a few meters, some of the rocks were found to be settled by cold-water corals which were not previously known in this region. A preliminary examination of the rock samples give evidence that the rocks were formed due to a local methane fluid flow, supported by our discovery of gas seeps farther west. We created a geo-referenced data base corroborating previous high resolution academic (e.g R/V Meteor sub-bottom profiles acquired in 2002) and commercial surveys that were performed in the Palmahim Disturbance region during the past decade, and E/V Nautilus 2010 and 2011 finds. Our preliminary mapping results show rocks extending over ~3.5 km in the east-west direction and ~600 m in the north-south direction at a depth range of 650 - 790 m. The rocks are distributed along the northern slope of the Palmahim Disturbance ramp, from its bottom almost to its top. All rocks are distributed to the south and up 1 km away of the northern bounding fault of the Disturbance, as defined by Garfunkel et al. (1979), and within the perimeters of their 'northern graben'. This finding raises the question regarding the possible fluid flow path-ways that lead to the surface of the northern slope. Assuming that the reefs represent past fluid flow, our finding constrain the possible pathways of the fluids to the surface.

The Transition from aggradation to incision in the Late Pleistocene in the Negev Highlands.

Faershtein G.[1], Matmon A.[1], Porat N.[2], Avni Y.[2],

1 Institute of Earth Sciences, The Hebrew University, Jerusalem 91904, Israel
2 Geological Survey of Israel, 30 Malkhe Israel, Jerusalem 95501, Israel

---

One of the most significant indicators of the change in environmental conditions in arid and semi-arid regions at the end of the late Pleistocene is the sharp transition from a regime of fine-grained sediment deposition to one that is controlled by intensive incision, which forms alluvial channels that dissect the late Pleistocene sediments. This incision, which has intensified through the Holocene, seriously harms the agriculture and pasture potential and the modern infrastructures in these desert regions. This phenomenon is known world-wide and was documented in many arid regions from the low-mid latitudes in both hemispheres. This study aims at understanding when this important transition occurred in the Negev Highlands, and what is the mechanism that generates it is.

Recent developments of luminescence dating methods (such as luminescence measurements of single grains) now enable to date the fluvial sediments deposited before and after this transition. In the past years, large numbers of OSL ages have been published from various sites around the world. These ages allow to compare between different sites, and to answer the question whether the transition from aggradation to incision in the late Pleistocene was synchronous on a local or even global scale.

Three low order drainage basins of relatively large wadies (Nahal Nizzana, Nahal Loz and Nahal Arod) in the Negev Highlands were selected for this study. Morphostratigraphic mapping shows that similar sedimentary units are present in all three basins. These include a lower late Pleistocene fluvial loess unit, overlain and truncated at different heights by a gravel unit. This transition between fine and coarse sediments represents the beginning of incision. In all the basins the gravel unit is covered by another loess unit, probably of aeolian origin. The following incision is expressed by lower, younger terraces which are mostly gravelly.

Preliminary OSL ages show that the lower fluvial loess was deposited between ~70 ka to ~30 ka; however, the top of the sequence is eroded. The overlying gravely unit was deposited between ~14 ka and ~9 ka. The uppermost aeolian loess was dated to ~10-6 ka. The lower terraces are all younger than ~9 ka. The time interval between 30 ka and 14 ka brackets the transition from fine-grain loessic sediment deposition to major erosion and incision in the Negev Highlands. Further OSL age determinations will better constrain this event.

Genetic Groups of Oil Samples from the Southern Israel and SE Mediterranean Continental Margin - Revisit

Feinstein S.[1], Aizenshtat Z.[2], Miloslavsky I.[2], Goldberg M.[3], Obermagher M.[4]

1 Department of Geological and Environmental Science, Ben Gurion University of the Negev, Beer Sheva 84105, Israel

2 Department of Organic Chemistry, the Hebrew University of Jerusalem, Jerusalem 91904, Israel

3 Geological Consulting and Services

4 Geological Survey of Canada - Calgary, 3303-33rd St., NW, Calgary, Alberta T2L 2A7, Canada

---

Saturated and aromatic hydrocarbon molecular characteristics and δ13C data taken from oil samples from producing wells and shows in southern Israel and the eastern Mediterranean offshore show clear clustering into four different genetic groups. The clustering is concordant with their geographic distribution, namely, the inland Dead Sea and Coastal Plain groups, and the continental margin Yam and Mango groups. Differences in samples composition within groups are mainly confined to the light-end n-alkane compounds whereas heavier alkanes and aromatic parameters show consistent correlation. Hence the differences observed are attributed to selective post-generational modification, mainly by biodegradation. The clear distinction in biomarker characteristics between samples from different groups, and consistent similarity within each group, including thermal maturity levels, suggest that each genetic group represents a single source rock and generation kitchen. Furthermore, differences in biomarker characteristics and d13C in the saturated and aromatic fractions suggest that the Dead Sea and the Coastal Plain oil samples were generated from different marine, probably carbonate-rich, source rocks. The Mango oil was originated from a clastic source rock, probably with an input of some terrestrial organic matter. Biomakers and aromatic compound ratios of the continental margin Yam oil reveal distinctly different and more mature oil, but the source rock and depositional environment signals are ambiguous.

111 Years of Seismic Monitoring or Israel and adjacent regions

Feldman L., Reich B., Avirav V., Hofstetter R.

Geophysical Institute of Israel, P.O.Box 182, Lod 71100, Israel

Seismic monitoring of Israel and adjacent regions started in the beginning of the 20th century, using a few regional stations that operated in the Middle East, i.e. Helwan, Egypt, and Ksara, Lebanon, and from 1953 using 2 WWSSN stations in Jerusalem and Eilat. The Israel Seismological Network (ISN) started operating in a continuous mode in 1981, providing abundance of useful seismological data. The main tasks of the Seismological Division, GII, are: 1) operation and maintenance of the Israel Seismological Network; 2) rapid determination of epicenters of strong and felt earthquakes in Israel and adjacent regions; 3) routine determination of earthquakes in Israel and adjacent regions; 4) operation and maintenance of seismological database as a source for information to the public, civil authorities and seismological studies; 5) operation and maintenance of database of explosions and seismoengineering measurements; 6) providing seismological expert advice for improving the Israel Building Code. The ISN comprises 42 short-period stations (including Meron Array), 8 broadband stations, 57 accelerometers, and 10 infrasound stations. In the last 30 years a total of about 19,000 local earthquakes in Israel and adjacent more than 7,000 regional events and more than 14,500 teleseismic events regions were recorded by the ISN

Engineering geophysical methods for Israeli road industry

Frid V.[1], Averbakh A.[1], Liskevich G.[1], Titov V.[2]

1 Isotop Ltd, 20 HaYarok, Canot Industry Zone, 70700.
2 National Roads Company, 29 Yahadut Canada, 60371

The aim of the investigation was to identify the range of geophysical methods employment in the road industry. Our investigation was supported by the National Roads Company (project 120/09) and consisted of two stages as follows: bibliography scrutiny and in situ investigations. The bibliography investigation included the analysis of world and Israeli experience of geophysical methods employment for soil/rock exploration. It was found that the approach in choosing the most relevant geophysical method in the road industry is similar to that of shallow geophysics, rock mechanics and environmental industry. Three methods were found to be the most fitted to the soil/rock studies for the Israeli road industry as follows: electrical resistivity tomography (ERT), ground penetrating radar (GPR) and seismic refraction (SRfr) method. These methods were tested in different Israeli conditions including in the regions of Negev/Arava deserts, Jerusalem mountains, in the zone of Mediterranean and Dead seas, in the central region and on the Northern Israel.

As a result of our field investigations, it was found that GPR is useful only when the needed measurement depth is less than 10m. In such a condition, 250-100 MHz antennae could be used. Our investigations also showed that GPR applications is highly problematic if clay/marls layers of the thickness larger than 3 m exist near the Earth surface.

It was also shown that the SRfr depth (with 5kg hammer source) is less than 15-20 m. The mandatory condition for the SRfr method employment is an increase of rock density with the rock depth rise. The second essential condition is the contrast of elastic properties of nearby rock/soil layers. The distance from the source of acoustic noise is also very important for the good data quality acquisition.

Analysis of ERT data shows that all experiments carried out with this method were successful. The depth of the ERT surveys was maximal amongst all three investigated methods and mainly depended only on the length of the measurement line. However, it is necessary to note that the accuracy of the ERT measurements was highly depended on the inter electrode distance and the depth of measurements.

Careful analysis of the investigation results enables us to develop the first version of the Technical Requirements of the application of geophysical methods for the Israeli road industry including the novel quantitative methodology, which consists of the quantitative assessment of the geophysical survey task, the region of its application, the proposed geophysical method restrictions and conditions on the site under study.

Origin of the Andromeda Mound Complex in the Lower Pliocene Yafo Sand Member, Southeastern Levantine Basin

Fuhrmann A.[1], Weimer P.[1], Bouroullec R.[1], Gardosh M.[2], Pettingill H.[3], Hurst A.[4]

1 Energy and Mineral Applied research Center, Department of Geological Sciences, University of Colorado, Boulder, CO , USA
2 Ministry of Energy and Water, 234 Jaffa St, Jerusalem, Israel
3 Noble Energy, 100 Glenborough Drive, Houston, TX, USA
4 Department of Geology, University of Aberdeen, Scotland UK

A series of wells drilled in the southeastern Levantine basin, offshore Israel penetrated thick sand layer at the base of the Plio-Pleistocene sedimentary wedge. This siliciclastic unit termed the Yafo Sand Member was deposited in submarine turbidite fans and lobes at the mouth of the Afiq and el-Arish canyons, during the rise of the Mediterranean that followed the Messinian salinity event. Part of the Yafo sand layer was later remobilized, resulting with the formation of large mounded complexes. The Andromeda-1 dry hole that was drilled into one of these mounds, penetrated 400 m thick section of very fine to fine-grained quartz sand with some interbedded claystone. 3D seismic volume that covers the Andromeda area and one well log suite were used for a detailed study of the morphology, structure and evolution of this unusual feature.

The Andromeda Mound Complex is composed of fifteen individual or small groups of mounds. All of the mounds are confined to the lower Pliocene Yafo Sand Member stratigraphic interval. The fifteen large, high net-to-gross mounds are separated into three distinct groups, based on both their internal and external seismic farcies.

Our model for the genesis of the Andromeda sand complex is based on the combined effects of several factors: (1) the formation of pre-Messinian pockmarks, (2) more extensive up-dip initial Messinian Evaporite deposition, (3) the deposition of the turbidite sands of the Yafo Sand Member above the low gradient top Messinian surface, (4) lower Pliocene Syrian Arc uplift, which created conduits for undersaturated, low-salinity fluid migration into the Messinian Evaporites, (5) variable rates of evaporite dissolution within the study area, (6) mass-movement of individual block of the Yafo Sand Member along the basal detachment surface into collapse features associated with evaporite dissolution, (7) and continued Syrian Arc uplift and Messinian Evaporite dissolution resulting in the inversion of the mounded portions of the Yafo Sand Member and overlying sediments.

Mantle aspects of oil/gas forming

Galant Y.B.

This Report completed the set of investigations so called statistic characteristics i.e. that existence now. This research concentrates all former investigations on elucidation regularity between main parameters inorganic oil forming and accent on Mantle Characteristics. Among other aspects of magmatic oil - there is most important factors so called initial characteristics of Mantle: 1.compozitions, 2.melting, 3.age/period of raising, 4.roof/depth, and so on.

In this report investigate Regularity: Age of Rift/ Roof (Depth of Mantle).

Regularity considered for: mix (oil/gas bearing basins + not productive basins,) and separately for oil/gas bearing basins and not productive basins.

The Roof of mantle is an important characteristic because it tightly connected with development of rift oil/gas basins. It is known rift oil/gas basins initiated by inserting of Mantle diapir into Earth Crust. While Mantle diapir is inserting, Earth Crust is breaking and synchronically go on accumulations of sediments and degassation of Mantle diapir. But practically there are both oil/gas bearing and not productive basins. Which of Mantle factors are responsible for forming oil/gas fields?

For mix oil/gas basins + not productive basins .Relativity AGE of Rifts/ Roof of Mantle = 8, 7. Coefficient Correlation = 0, 39.

For oil/gas basins. Relativity Age of Rifts/ Roof of Mantle = 11, 2. Coefficient Correlation = 0, 53.

For not productive basins. Relativity Age of Rifts/ Roof of Mantle = 4, 1. Coefficient Correlation is negative = - 0, 62.

Connection oil/not =11, 2/4, 1=2, 73; Connection oil/mix=11, 2/8, 7=1, 29; Connection not/mix= 4, 1/8, 7=0, 47.

Revealed Regularities quiet different for oil/gas basins and for not productive basins.

So synchronous and high number of Age of Rifts and high number of Roof of Mantle, and high number of Relativity Age of Rifts/ Roof of Mantle, and > 1 Connection oil/not =11,2/4,1=2, 73 and Connection oil/mix=11,2/8,7=1, 29, and positive high Coefficient Correlation = 0, 53 are favorable sign of oil/gas forming.

Mentioned above model can serve for estimate of perspectives of territory where sedimentary layers absence or developed poorly. In World there are a lot of oil/gas fields in such conditions.

A world oil bearing basin in which oil/gas is associated with volcanogeneous rock is 60 out of general amount of 160 (37, 5 percent). And practically System of estimate perspective of oil/gas bearing for such areas has not been created yet.

Mentioned above model are Regional and Inorganic. So system of estimate perspective of oil/gas bearing is the same - Regional and Inorganic. Such prospecting method has not been created yet.

Acceleration of ureolytic CaCO3 precipitation by non-ureolytic bacteria

Gat D.[1], Tsesarsky M.[2,1], Ronen Z.[3]

1 Department of Geological and Environmental Science, Ben Gurion University of the Negev, Beer Sheva 84105, Israel

2 Department of Structural Engineering, Ben Gurion University of the Negev, Beer-Sheva 84105, Israel

3 The Zuckerberg Institute for Water Research, the J. Blaustein Institute for Desert Research, Ben-Gurion University of the Negev, Sede-Boqer Campus

---

Microbially induced CaCO3 precipitation (MICP) is recently being studied due to its various potential applications, e.g. sequestration of soil contaminants and mitigation of seismic liquefaction, among others. Some of these applications involve in-situ treatment of soils, and therefore require a better understanding of the interactions between microbial ecology and aquatic geochemistry.

Hydrolysis of urea, catalyzed by the enzyme urease, is one of the most common pathways for MICP. Hydrolysis of urea produces ammonium and carbonate thus increasing surrounding alkalinity. In the presence of dissolved calcium this process will result in the precipitation of CaCO3.

In order to study the interactions between ureolytic and non-ureolytic bacteria we performed a MICP experiment in artificial groundwater medium, inoculated with two model bacteria: S. pasteurii (ureolytic bacteria) and B. subtilis (non-ureolytic bacteria), and supplemented with Nutrient Broth and urea. Control was inoculated with S. pasteurii alone. The experiment lasted 10 days, during which NH4+, Ca2+, pH, dissolved inorganic carbon and optical density (OD) were measured.

Our results show that most of the CaCO3 precipitation took place until the 80th hour of the experiment. During which time, pH values and carbonate ion concentrations in the presence of non-ureolytic bacteria were lower than in their absence. However, measured Ca2+ concentrations indicate that CaCO3 precipitation was accelerated in the presence of non-ureolytic bacteria, despite less favorable chemical conditions. Bacterial growth in our experiment, as infferred from OD measurements, was significantly higher in samples containing non-ureolytic bacteria, and was attributed to the rapid growth of the non-ureolytic bacteria. Therefore, we suggest that the presence of the non-ureolytic bacteria, B. subtilis, accelerated MICP process, through the addition of nucleation sites in the form of bacterial cells.

The Mottled Zone Event – the scale of system closure

Geller Y.I.[1,2] Burg A.[2], Halicz L.[2], Kolodny Y.[1]

1 Institute of Earth Sciences, The Hebrew University, Jerusalem 91904, Israel
2 Geological Survey of Israel, 30 Malkhe Israel, Jerusalem 95501, Israel

The Hatrurim Formation (or the "Mottled Zone") is a unique rock complex, which is composed of high-temperature low-pressure metamorphic minerals corresponding to the sanidinite and pyroxene-hornfels facies. These rocks are the metamorphic product of combustion of the bituminous Maastrichtian to Paleocene marls and chalks of the Ghareb and Taqiye Formations. The colorful rocks of the Hatrurim Formation crop out at several localities in Israel and Jordan. The largest outcrop in Israel is in the Hatrurim basin.

We evaluated the scale of system closure at the time of metamorphism by comparing the chemistry of the protolith (oil shales) to its metamorphic product at the equivalent stratigraphic level in the Hatrurim Formation using isocon diagrams (isocons are diagrams in which the scaled chemical composition of a protolith is plotted versus the composition of the metamorphic product, scaled by the same factors). We collected and analyzed protolith samples of the Lower Ghareb Formation oil shales from the PAMA quarry, Upper Ghareb Formation rocks from un-metamorphosed remnant outcrops from the Hatrurim basin and Taqiye Formation rocks from Har Zin, Har Orahot and Nahal Zin. The correlative metamorphic products were sampled in the Hatrurim basin - gehlenite-larnite, calcite-spurrite and "dense olive" rocks.

Isocon diagrams demonstrate the mobility of different elements during the metamorphic process (specifically their gains or losses; Gresens, 1967; Grant, 1986). The method is based on the assumption that some elements are immobile, or conserved during the metamorphic process. For all these immobile components, the ratios of concentrations in the protolith and metamorphic rocks are equal and are used in determining the mass or volume loss during the process. The concentrations of all immobile species must plot on a straight line that passes through the origin. This line is the isocon and its slope yields the total change in mass due to the metamorphic process.

The isocon diagrams for the gehlenite-larnite, calcite-spurrite and "dense olive" rocks of REE, major, minor and trace elements show that in general their formation was almost completely isochemical except for LOI (organic matter, water and CO_2) minor mobilization loss of some trace elements that was caused by alteration reactions with acidic solutions.

Chemical analysis using laser ablation across bentorite and volkonskoite containing veins in black calcite-spurrite rocks suggest preferred mobilization of Cr into the veins. In addition, the

veins show zoning in respect to Cr which indicates at least two stages mineral precipitation that were related to changes in oxidation/reduction and a change of pH conditions of the fluid leading to differences in the availability of Cr.

Thus, it appears that the system exhibits two competing modes of behavior: on a sufficiently large scale it is isochemical, whereas on a smaller scale open system fractionation exists.

Reservoir mapping and characterization for hydrocarbon exploration, enhanced oil recovery and geological natural gas and CO_2 storage

Gendler M.

Geophysical Institute of Israel, P.O.Box 182, Lod 71100, Israel

Long-term author's experience of reservoir studies on the various petroleum basins of the former Soviet Union (Russia, Ukraine, Turkmenistan, Uzbekistan, Kazakhstan) and Israel is presented in this scientific research.

A combined approach for the mapping and characterization oil and gas reservoir is being proposed. This approach is based on the integration of the geophysical (seismic and well logging) and geological data from a digital database. This technology provides the most effective way for structural and lithofacies mapping, stratigraphic and lithological correlations, petrophysical properties and reservoir reserve estimations.

The basic elements of this methodology are as follows:

* Lithological reconstructions and stratigraphic formation analysis.

* Definition of reservoir petrophysical (porosity, formation fluid properties, net pay thickness) properties.

* Subdivision of hydrocarbon reservoir into sub-reservoirs.

* Tracing lithofacies heterogeneity of reservoir.

* Detection and correlation of high porosity zones, fractures, caverns and karsts development.

* Delineation and mapping of fault zones.

* Expanded Composite Logs construction.

* Construction of the Lithostratigraphic Correlations and Geological Cross-Sections.

* Construction of Reservoir Structure, Lithofacies, Thickness and Petrophysical Maps.

* Development of 3D reservoir geological model.

* Estimation of the hydrocarbon reservoir reserves.

The proposed combined geological and geophysical approach can be very useful at a stage of hydrocarbon exploration, enhanced oil recovery and geological natural gas and CO_2 storage.

Investigation of shallow gas and fluid migration within the Pleistocene-Holocene sedimentary section of the southeastern Levant basin using 3D seismic data

George S.[1], Makovsky Y.[1], Ben Gai Y.[2], Tezcan D.[1]

1 Charney School of Marine Sciences (CSMS), University of Haifa, Haifa 31905, Israel.
2 The Geophysical Institute of Israel, LOD 71100, ISRAEL

The presence of gas in shallow sediment is of interest for two main reasons: (1) their occurrence and underlying indications of fluid flow, may point towards deeper and the possible presence of gas hydrates, (2) gas in unlithified sediments, may reduce the shear strength of the sediments, posing hazards to hydrocarbon exploration. Our work concentrated on the analysis of Southern Israel 3D seismic cube, acquired in 2000 for commercial purpose by WesternGeco and processed through an amplitude preserving workflow. We detected an aboundance of free gas within 1 to 3 km thick post-Messinian sedimentation based on high-amplitude (bright spot) reflections, seismic phase reversal, and acoustic masking. High resolution picking of the sea floor bathymetry, revealed also an abundance of pockmark formations at the western and southern perimeter Palmachim Disturbance. The combination of these observations led to the discovery of active gas seeps in October 2012 by E/V Nautilus. An abundance of, presumably salt deformation related, faulting was identified truncating the sedimentary section from the Messinian salt to the surface. These features correspond with discontinuities in the Messinian layer, seeming at times to penetrate even its base. Reflectivity patterns interpreted by us to represent free gas accumulations seem in several cases to correspond with the deformational features, suggesting together gas leakage through discontinuities in theessinian salt layer.

The oil-shale survey at the HaShfela basin: hydrogeological properties of the Santonian-Maastrichtian sequence

Gersman R., Bartov Y.

Israel Energy Initiatives

As part of the oil-shale survey in the HaShfela basin, Israel Energy Initiatives, LTD. (IEI) has completed the drilling of six appraisal wells. The estimated oil resource in the license area is 40 billion bbl. A major effort in IEI's project is to study the hydrogeological properties of the hydrostratigraphic units and evaluate the integrity of the aquifer confining units.

Previuos studies showed that the Mt. Scopus Group at the Judean Lowland is defined as an aquiclude. It strongly confines the Yarkon-Taninim aquifer within the Judea Group at a depth of 650-700 m throughout the basin. Though many water wells have been drilled into the underlying aquifer and have unavoidably passed through the Mt. Scopus Group, its hydrogeological properties remained poorly studied due the low potential to yield potable water.

The target zone for oil production at the HaShfela basin is found at the Maastrichitian Ghareb Formation. The rock units separating it from the aquifer include the Campanian Mishash Formation and the Santonian Menuha Formation. We studied the hydrological behavior of this section using different approaches: the hydraulic conductivity of the entire section was calculated from slug tests and found to be in the range of 10-10 – 10-11 m/sec. These values were confirmed by laboratory permeability measurements on plugs taken from core. Water salinity was estimated from electrical logs, indicating vertical hydraulic separation between the adjacent units. Water sampled from two boreholes was found to be saline and highly reduced. Visual examination of boreholes showed that natural fractures are mostly found within the rich oil-shale unit and are usually cemented with calcite.

Poor hydrological properties were observed in all of the surveyed locations. The aquicludic nature of the Ghareb, Mishash and Menuha Formations is, therefore, continuous within the study area. It is governed by extremely low bulk permeability, hydraulically-separated sub-units, and impermeable, separated joints and fractures. The thickness of the protective layer is up to 200m, hampering downward mobilization of fluids.

Pleistocene lakes in southern Israel and Jordan: paleogeography, paleohydrology and paleoclimate implications

Ginat H.[1], Mischke S.[2,3], Al-Saqarat B.[3]

1 Dead Sea and Arava Science Center, Kibbutz Qetura, Hevel Eilot 88840, Israel
2 Institute of Earth and Environmental Science, Universität Potsdam
3 Al al-Bayt University, Mafrak, Jordan

Pleistocene lake sediments and associated prehistoric artifacts in the deserts of southern Israel and Jordan are evidence for significantly wetter conditions in the presently hyperarid region. The occurrence of lake sediments at a number of sites in this area provides a unique opportunity to investigate the environmental and climatic conditions in the Pleistocene using a West-East gradient of increasing distance from the Mediterranean Sea as a major moisture source. The extent, water depth, and water chemistry of the Pleistocene lakes in southern Israel and Jordan were reconstructed by sedimentological, geochemical and palaeontological means. A synthesis of the geological and supplementary archaeological data contributes to a better understanding of (1) the early, middle and late Pleistocene environmental and climatic history of southern Israel and Jordan, (2) the role of southern Israel and Jordan in the migration and possibly occupation of hominids on their way out of Africa, and (3) the timing and local expression of ancient lakes.

Our study of the Pliocene and Pleistocene lakes in southern Israel and Jordan is compiling existing but scattered information on ancient lake sediments in the region. This research includes paleoecological analyses of the water bodies and their significance for settlement activities of hominids. This work presents a general view of the ancient lakes in the hyperarid region during time (late Pliocene to late Pleistocene) and space (local basins in the extreme arid region) for the first time.

This report contains geographical and geological background information, a summary of previous research and a description of each one of the ancient lakes. Following 18 months of work we present primary conclusions and plans for the research for 2012.

Some features of seismic, acoustic waves and craters for Sayarim surface explosions

Gitterman Y.

Geophysical Institute of Israel, P.O.Box 182, Lod 71100, Israel

A series of on-surface shots was designed and conducted by GII at Sayarim Military Range (SMR), including two large explosions: ~82 tons of strong IMI explosives in August 2009, and ~100 tons of ANFO in January 2011. It was a collaborative effort between Israel, CTBTO, USA and several European countries, with the main goal to provide fully controlled infrasound sources in different weather/wind conditions, for calibration of IMS infrasound stations in Europe, Middle East and Asia.

Strong boosters and the upward charge detonation scheme were applied to provide a reduced energy release to the ground and an enlarged energy radiation to the atmosphere, producing enhanced infrasound signals, for better observation at far-regional stations. Crater size and local seismic (duration) magnitudes were found smaller than expected for these large surface explosions. Small test shots of the same charge (1 ton) with different detonation directions showed clearly lower seismic amplitudes/energy and smaller crater size for the upward detonation. Many infrasound stations at local and regional distances showed higher than expected peak amplitudes.

For the large-scale explosions, high-pressure gauges were deployed at 100-600 m to record air-blast properties, evaluate the efficiency of the charge design and energy generation, and provide a reliable estimation of the charge yield. Empirical scaled relations for air-blast parameters - peak pressure, impulse and the Secondary Shock (SS) time delay, depending on distance - were developed and analyzed. The charge-scaled parameters were found consistent for all analyzed explosions, except of SS time delays clearly separated for the shot of IMI explosives.

The developed charge design contributed to the success of this unique dual Sayarim experiment, providing the strongest GT0 sources since the establishment of the IMS network, that demonstrated clearly the most favorable westward/eastward infrasound propagation up to 3400/6250 km according to appropriate summer/winter stratospheric wind directions, respectively, and thus verified empirically common models of infrasound propagation in the atmosphere.

The research was supported by the Israel Ministry of Immigrant Absorption.

The pH of the Dead Sea - A liquid junction independent determination

Golan R.[1], Gavrieli I.[2], Lazar B.[3], Ganor J.[1]

1 Department of Geological and Environmental Science, Ben Gurion University of the Negev, Beer Sheva 84105, Israel

2 Geological Survey of Israel, 30 Malkhe Israel, Jerusalem 95501, Israel

3 Institute of Earth Sciences, The Hebrew University, Jerusalem 91904, Israel

---

Throughout the evolution of the hypersaline Dead Sea, mineral precipitation occurred leaving a vast sedimentary record. Precipitation of the alternating aragonite and detrital laminae of the Lisan Formation (the sediments deposited in of the historic hypersaline Lake Lisan the predecessor of the Dead Sea) was attributed to seasonality. The aragonite laminae were precipitated during seasonal oversaturation caused by combination of enhanced input of fresh floodwater bicarbonate with the extremely high concentration of calcium in the lake.

The pH governs the carbonate speciation in most natural solutions and hence the carbonate mineral saturation state and its kinetics. Thus, reliable pH measurements are essential for estimating the kinetics and thermodynamics of aragonite precipitation in the Dead Sea and Dead Sea mixtures with other natural solutions (e.g., Jordan River and seawater). Conducting meaningful potentiometric pH measurements in hypersaline solutions of the Dead Sea type, is however a very challenging geochemical problem.

The conventional pH determination is a measurement of the EMF developed between an H+ sensitive glass electrode and a reference Ag/AgCl electrode dipped in a high ionic strength (I?3 m) KCl solution, connected via a liquid-junction to the measured solution. Calibration of this electrodes pair is traditionally conducted using low ionic strength pH buffers, assuming that the liquid-junction potential of the measured solution is identical to that of the standard. This is certainly not true when measuring high ionic strengths solutions, such as Dead Sea brines (I>9 m) and brine mixtures (Dead Sea brine with Jordan River water and seawater), and introduces a determination error.

In order to conduct a liquid-junction independent pH measurement of the Dead Sea brine we used a pair of ion selective electrodes, following the method proposed by Knauss et al. 1990. Such liquid-junction independent pH measurement is also ionic strength independent of either the calibration standards or the measured solutions. The electrodes pair employed were pH glass electrode and Cl- ion selective electrode and the EMF is proportional to the log activities product of H+ (pH) and Cl- (pCl-).

The electrodes pair was calibrated in several dilutions of Dead Sea brine as follows: 1- Adding to the tested brine solution known aliquots of 32% HCl solution up to excess acidity; 2- Measuring the EMF after each addition; 3- Calculating pHCl after each addition using a Pitzer thermodynamic data base and the MacInnes convention (PhreeqC geochemical modeling code); 4- Plotting the measured EMF (y-axis) as a function of the calculated pHCl (x-axis) that yields an excellent linear calibration curve for calculating the pH.

This method was successfully tested on a large range of dilutions of Dead Sea brine with distilled water and will be used to study aragonite precipitation thermodynamics and kinetics in the Dead Sea and brine mixtures.

Characterizing rock varnish developed on earliest Holocene Negev flint artifacts as a potential paleoenvironmental or paleoclimatic indicator

Goldsmith Y.[1], Enzel Y.[1], Stein M.[2]

1 The Fredy and Nadine Herrmann Institute of Earth Sciences, The Hebrew University of Jerusalem, Edmond J. Safra Campus, Givat Ram, Jerusalem 91904, Israel

2 Geological Survey of Israel, 30 Malkhe Israel, Jerusalem 95501, Israel

---

Rock varnish is a thin coating (1-100s μm) formed primarily in micro-basins on exposed rock surfaces and is common in arid and semi-arid regions of the world. The varnish is composed of clay minerals and largely enriched in Mn, which accumulate in micron-size laminas that vary in their color and Si, Fe and Mn contents. Settling-dust has been proposed as the parent material for varnish. Variations in Mn content in rock varnish laminations have been proposed as possible desert paleo-rainfall indicators; this proposal lacks systematic modern or Holocene analogues isolating climate influence. In addition, despite many years of research, mechanisms of Mn accumulation and alternating Mn-rich and Mn-poor lamina in rock varnish remain unresolved.

To systematically test the varnish chemistry-rainfall dependency, we determined Mn composition in rock varnish formed on flint artifacts produced during the earliest Holocene from eight coeval prehistoric sites in the Negev. These sites lie along a north-south annual rainfall transect ranging between 30-120 mm·yr-1. Then by applying thermodynamic and kinetic reasoning we devised a new geochemical model of rock varnish formation that explains these observations.

The mean Mn content in the varnish is enriched 100× relative to its concentration in its source material - the fine-grained fraction (<20 μm) of the local settling-dust. Vertical profiles of the varnish show 4–6 distinct peaks in Mn concentrations, in all sites, pointing to systematic fluctuations within the varnish along a wide range of environmental settings. In all samples, the Mn content in the outer yellow lamina is enriched from 0% at the varnish surface to ~10% at depth of ~5 μm. We propose, that the amount of wetting cycles by dew or light-rain may explain the Mn variance within the results from the Negev varnish.

Using thermodynamic and kinetic considerations a plausible chemical mechanism of varnish formation is presented. In this model, dust accumulates in micro-basins on exposed rock surfaces. Under the common top-soil pH condition in the Negev and during wetting events, Mn in the dust is mobilized and leached to a depth of ~5 μm under the varnish surface, where it is adsorbed onto clay minerals and oxides. Once the solution dries abrasion removes the upper,

weakly cemented dust sediment, which contains mainly Si, Al and Fe. The Mn is deposited at a depth protected from erosion. Reoccurrences of this process results in a noticeable accumulation of Mn but not Si, Al or Fe. The alternating Mn-rich and Mn-poor laminas form as a result of a competition between the leaching rate of Mn and the accumulation rate of the clay minerals. When moisture is high; lamina with low Mn/clay mineral ratio form, when moisture is low; lamina with high Mn/clay mineral ratio form.

Diurnal Geochemical Fluctuations of the Effluents in the Infiltration basins of the Shafdan plant

Goren O.[1], Gavrieli I.[1], Burg A.[1], Lazar B.[2], Negev I.[3], Guttman J.[3], Kraitzer T.[3]

1 Geological Survey of Israel, 30 Malkhe Israel, Jerusalem 95501, Israel
2 Institute of Earth Sciences, The Hebrew University, Jerusalem 91904, Israel
3 Mekorot National Water Company, Tel Aviv, Israel

Infiltration basins of effluents are common in Soil aquifer treatment (SAT) systems, in which secondary effluents are recharged into an aquifer and recovered after a defined residence time. The SAT system of the Shafdan plant includes six infiltration basins; each basin covers an area of about 200,000 m2 and is divided into about 10 sub-basins that flooded alternately. The recharge regime consists of up to one day of flooding and two days of drying. The water load applied in each flood varies between 30 and 100 cm, depending on the infiltration rate of each sub-basin.

Generally, the chemical evolution of the effluents in SAT systems is attributed to biogeochemical processes that take place along the flow in the vadose zone and in the aquifer. The present work shows that the processes within the infiltration basins themselves have a significant impact on the chemical characteristics of the infiltrated effluents. The aim of this study was to determine the sensitivity of the infiltrated effluent to different conditions in the infiltration basins, such as sunlight, temperature and recharge regime.

The main biogeochemical processes that act in the infiltration basins are photosynthesis and respiration. The intensities of these processes control the redox conditions of the effluents, the pH and the dissolved concentrations of oxygen (DO) and carbon (DIC). The DO concentrations in the basins are enriched compared to the concentrations in the secondary effluent that enters the basins. The DO and DIC concentrations in the basin have an inverse diurnal variation; during the day the DO concentration increases and the DIC concentration decreases due to net photosynthesis, while during the night the DO concentration decreases and the DIC concentration increases due to the respiration. The pH shows similar variation to that of the DO. The isotopic composition of carbon-DIC is also affected by photosynthesis and respiration; the δ13C values increase during the day and decrease during the night. Unlike the DO and DIC, the concentration of dissolved organic carbon (DOC) does not show significant variation in the basin. The nitrogen in the basins appears mainly as ammonium. In the upper part of the vadose zone the concentrations of NH4+ and NO3- were changed significantly between the different sampling campaigns due to changes in the environmental conditions.

Overall, the results emphasize the impact of sunlight on the geochemical conditions of the

effluents in the infiltration basins. The effluents that infiltrate during the day are significantly more oxidized than those infiltrate during the night. Accordingly, in order to optimize the recharge regime of the infiltration basins it is suggested to utilize the sun energy to produce oxygen by flooding during the day-time.

Determination of site response in Timna using microtremor and seismic events.

Gorstein M., Zaslavsky Y., Kalmanovich M., Perelman N.

Geophysical Institute of Israel, P.O.Box 182, Lod 71100, Israel

In regions, characterized by a low rate of seismicity but potentially able to suffer energetic seismic events, it is very difficult to assess site response by experimental methods because of the lack of earthquake occurrence. The problem could be overcome by computing the fundamental frequency of soil by applying the standard HVSR (horizontal to vertical spectral ratio) technique based on ambient seismic noise records (Nakamura, 1989). Assessment of the site amplification effect by means of microtremor measurements reliably identifies the fundamental resonance frequency of the investigated site and provides a fair estimate of the expected amplification level. It is important, however, to understand the limitations of this method like small impedance contrast between soft soil layer and the basement and the weak excitation of soil in cases where the investigated area is located far away from sources of excitation. This is the case of the Timna mines site. In such cases, collection of a suitable data set of seismic events is needed to ensure accurate site response estimation.

The observed data together with any available geological, geotechnical and geophysical information, are used to construct a reliable models of the subsurface and predict the linear and non linear site specific seismic acceleration spectra.

Measuring near-equilibrium rates of silicate mineral dissolution and secondary phase precipitation using silicon isotopes

Gruber C.[1], Zhu C.[2], Jiwchar G.[1]

1 Department of Geological and Environmental Science, Ben Gurion University of the Negev, Beer Sheva 84105, Israel

2 Department of Geological Sciences, Indiana University, Bloomington, IN 47405, USA

One of the most basic problems in studying weathering kinetics is the apparent discrepancy between dissolution rates of silicate minerals measured in the field and dissolution rates measured in laboratory experiments. The rate measured in the laboratory is faster by few orders of magnitude than the rates in the field. The many differences between experimental conditions in the laboratory and natural conditions in the field include: solution/mineral contact, duration of weathering, aging of surfaces, presence and depth of defects and etch pits, formation of leached layers, surface coatings, degree of under saturation, and solution chemistry in micro-pores.

Methods of determination of dissolution rates of silicates are usually based on differences between measurements of Si concentrations. However, the change in solution concentration is affected by both the dissolution of the primary mineral and the precipitation of secondary minerals. Moreover, these concentration differences are small relative to the high concentration of the solutions, under near to equilibrium conditions. As the change in concentration is lower than the uncertainty on ion concentration measurement, the error on the measured rate is large. As a result, the slow rates of mineral dissolution that are observed in the field cannot be determined using standard laboratory methods (Ganor et al., 2007).

This research project proposes and tests a novel method for measuring slow rates reactions of silicate minerals by using stable isotopes of Silicon. This new method overcomes the analytical difficulties by lowering the absolute error on dissolution rates. Moreover, with this method one can eliminate the effect of secondary phase precipitation on the determination of dissolution rate of a primary mineral and it is possible to approximate the precipitation rate of the secondary phase minerals.

Simulations of albite dissolution, at low temperature (3.6°C, 25°C and 50°C), near equilibrium conditions and with precipitation of kaolinite using PHREEQC code were carried out. Simulation results verified the tremendous effect of measuring Si isotope ratio of the experiment solution on reducing reactions rates error. The absolute error on rates reduced to less than one order of magnitude significantly better than the traditional method of change in solution concentration. Furthermore, Simulations of the experimental system showed negligible effect of possible fractionation during secondary phases (clays as kaolinite) precipitation on measured dissolution and precipitation rates in wide range of fractionation factors (0.5‰ - 20‰).

Pseudo-Deterministic Seismic Hazard Analysis for the Dead Sea Basin Area

Harari D., Dor O., Ben-Nun O.

Ecolog Engineering Ltd, 3 Pekeris st., Rehovot

The subject investigation includes the evaluation of Peak Ground Acceleration (PGA) and site amplification parameters for the Dead Sea Basin (DSB) area. The evaluation is based on deterministic detailed multi-scale characterization of the DSB seismotectonic framework and on its collective probabilistic seismic behavior.

The construction of the database includes geometric (length, seismogenic depth, inclination), kinematic (mode and sense of slip) and dynamic (maximum magnitude) information about faults in the DSB based on surface mapping, geophysical imaging and models. The active fault maps (e.g. Bartov et al., 2009; Agnon & Sagy, 2011) show only the fault's intersection with the ground surface, and data in marine and border areas is usually limited or in poor resolution. The project database is a compilation of published data integrated with inferences about the trace of faults. It is assumed that the Jericho and Arava faults are continuous within the DSB and have an overlap zone in its south-central area. Other inferences will be presented and explained.

The seismotectonic model is detailed for the DSB area, and does not take into consideration distant sources (e.g. the Cyprian Trench). The lack of systematic information about earthquake recurrence interval on the individual faults impedes a full probabilistic seismic hazard analysis for the area; therefore the characterization of the DSB & its surrounding faults is deterministic, and relies on Hamiel et al. (2009) for the fault's collective seismic behavior. It is assumed that the Maximum Credible Earthquakes (MCE) occur on the basin's nucleus of lateral motion, the Jericho and Arava faults; and that the Operating Basis Earthquakes (OBE) are primarily of dip-slip origin and occur on all faults with appropriate mechanism. The faults that generate PGA<0.1g at the examined site are not taken into consideration (choice of minimal acceleration of interest for engineering applications).

The choice of reference earthquake scenarios are based on international codes: recurrence interval of 1000 and 2500 years for MCE, and 72 and 144 years for OBE. The corresponding magnitudes for these scenarios are M=6.88 and M=7.29 for the MCE's, respectively; and M=5.7 and M=6.01 for the OBE's, respectively. Following, the potential faults that can generate the scenario earthquakes are identified, and the resultant PGA at the site of interest is calculated. The site response is evaluated based on the local geotechnical conditions. We found that the PGA values are typically, for most cases, 25%-50% higher than those presented by the earthquake building code map, partially due to the use of Next Generation Attenuation Relations (2008). We also found that the typical amplification factor is on the order of 3.

Complex landscape evolution of the central Coastal Plain (Israel) based on buried and relict surfaces

Harel M.[1,2], Amit R.[2], Enzel Y.[1], Porat N.[2]

1 The Fredy & Nadine Herrmann Institute of Earth Science, Hebrew University of Jerusalem, Jerusalem, Israel, 91904

2 Geological Survey of Israel, 30 Malkhe Israel, Jerusalem, 95501

Israel's central Coastal Plain stores thick sequences of terrestrial Pleistocene sediments. Episodic sand supply and dune activity buried and preserved past landscapes of distinct time intervals. These buried sequences archive Quaternary environments, record paleo-landscapes, and hints on external climatic forcing during aeolian, fluvial, and soil forming processes, including dust settling. We analyzed 11 such sequences of Quaternary deposits and their related landscapes across the coastal plain. They include diverse topographic positions, landscape stability, and terrestrial depositional environments during different time intervals. This analysis allows examination of various sedimentary and pedogenic patterns in the Coastal Plain during the middle and late Pleistocene. The chronology of the sediments was determined by OSL, during this or earlier studies. Our results indicate that previously considered buried soils, and therefore defined as paleo-surfaces, are not similar features across the Coastal Plain. We recognized three different stratigraphic and soil-stratigraphic units previously considered of similar origin and evolution:

A) Complete Soil profiles: Soils and buried soils, which show a complete soil profile, developed on a sandy parent material and are characterized by gradual changes of fine particles and CaCO3 content along the profile. These soil profiles accumulated dust and have gradual catenary changes along the past or present topography.

B) Truncated soil profile: Well cemented, CaCO3-rich (calcic) soil horizons on top of sandy dune material. They either partly or completely lost previous upper soil horizons and present distinct sharp contact with the overlying units.

C) Reworked sandy loams: Different units of sandy to clay loams sediments characterized by union or abruptly changing particle size properties along the sequence and have sharp contacts with underlying units.

Type C (reworked sandy loams) can be easily mistaken as buried soils and we suggest that they are fluvial deposits and fills of small local depressions. The high frequency of types B and C in the coastal sedimentary sections indicates that soil erosion, its sediment transport, and widespread redeposition are primary processes in the development of the present characters

of coastal plain topography and sedimentary column. It is not a simple layered sequence of dunes, eolianites (kurkar), and soils as presented before. Interpreting specific environmental conditions of buried surfaces is complex due to coeval processes such as sediment transport, pedogenesis, soil erosion, reworking and deposition of both soils and sediments.

Magnetic Properties of Carbonate Rocks as a Tool for Estimating the Strain field near the Dead Sea Transform, Northern Israel

Issachar R.[1], Levi T.[2], Weinberger R.[2], Marco S.[1]

1 Department of Geophysics and Planetary Sciences, Tel Aviv University, Tel Aviv 69978
2 Geological Survey of Israel, 30 Malkhe Israel, Jerusalem 95501, Israel

The characterization of the strain field is important for understanding the tectonics, seismicity and rock deformation processes along plate boundaries. Yet, the spatial and temporal distribution of the strain field around major faults such as the Dead-Sea Transform (DST) is not well known, basically because kinematic indicators are rare. We therefore apply a new method of the Anisotropy of Magnetic Susceptibility (AMS) for approximating the strain field, by studying the relation between the AMS fabrics and the finite strain of carbonate rocks. This method is based on laboratory experiments and field measurements that show that the minimum axes (k3) of the calcite crystals are parallel to the principal shortening direction in the rocks (i.e., k3∥c-axes). The study was conducted in the Rosh-Pinna region, adjacent to the DST. The measurements were performed in the AMS laboratory at the Geological Survey of Israel. A total of 214 samples from Timrat and Bar-Kokhba formations at 14 outcrops were measured and analyzed. The AMS shows a diamagnetic response typical of pure calcite crystals with well-defined principal axes. We interpret the preliminary results as showing penetrative deformation with principal strain directions affected by the regional stress field, induced by the movement along the DST. We found that the typical direction of the minimum (k3) axes of the AMS fabrics is N~S, indicating the shortening direction of the strain field in the area adjacent to the DST. Furthermore we can recognize a highly developed AMS fabric with well-defined (k1) and (k2) axes in the eastern parts of the study area. This fabric is indicative of a more developed strain, suggesting that the deformation decreases with the distance from the DST. Together with other studies in Israel and worldwide this research establishes the use of AMS measurements as a tool for determining the deformation and strain in carbonate rocks.

Meso-scale fault geometry in the Lisan Formation

Jacoby Y.[1,2], Weinberger R.[2], Marco S.[1]

1 Department of Geophysics and Planetary Sciences, Tel Aviv University, Tel Aviv 69978
2 Geological Survey of Israel, 30 Malkhe Israel, Jerusalem 95501, Israel

Outcrops of the Late Pleistocene Lisan Formation near the Dead Sea provide exceptional three-dimensional exposures of syndepositional fault zone. The Lisan Formation, as non-buried poorly lithifed sediments with its stratified annual laminae, is ideal for studying fault architecture. These sub-horizontal laminae provide an extremely fine and effective stratigraphic pattern, recording the effects of mm-scale deformation features.

We describe detailed three-dimensional structure of one of the normal faults in Masada Plain, which slipped only once. The description is based on measurements of displacement profiles along the exposed fault and at scaled photos. The profiles were produced by measuring the offsets of distinct layer at exposures excavated at 5-cm intervals. Based on these measurements, contoured maps of three-dimensional distribution of in-plane displacement (mm resolution) were produced.

The studied fault dips about 40°, strikes NNE, west side down. The maximum displacement along the fault is 0.5 m. The fault zone is ~0.2-m-wide; composed of gouge and deformation zone that consists of small shear fractures with displacements ranging from 1 mm up to 15 mm, dispersed either singly or clustered. The fractures locally affect mostly the hanging wall. They abut the main fault plane at angles ranging between 10° and 40° but none of them cross it. Generally, the point of maximum fault displacement (Dmax) is located between the fault center (L/2) and one of the tips, and the displacement gradients become gentler near the fault tips. In addition, the Dmax/L ratio is high.

These relationships between three-dimensional fault geometry, spatial fault arrangement and slip distribution near the surface, can provide indicative criteria for understanding rupture kinematics in poorly-lithified sediments. Shear fractures form in porous rocks, as Lisan Formation, by localized inelastic yielding of the host rock. The growth of shear fractures during evolving deformation was followed by linkage producing a through-going fault within the damage zone.

Uplift and exhumation of Mount Hermon: insights from the first (U-Th)/He cooling ages along the northern Dead Sea Transform

Joseph - Hai N.[1], Haviv I.[1], Eyal Y.[1], Weinberger R.[2], Benjamini C.[1], Farley K. A.[3]

1 Department of Structural Engineering, Ben Gurion University of the Negev, Beer-Sheva 84105, Israel

2 Geological Survey of Israel, 30 Malkhe Israel, Jerusalem 95501, Israel

3 California Institute of Technology, Division of Geological and Planetary Sciences, Pasadena, CA91125, USA

The Hermon ridge is a prominent anticlinal structure located at the intersection of the Dead Sea Transform (DST) and the Palmyride fold-and-thrust belt, characterized by intensive deformation including folding, faulting and internal block rotation. The formation of this structure was attributed to tectonic activity of the Syrian Arc fold system and/or to transpression along a DST restraining bend. To date, unequivocal evidence for the timing of tectonic phases across the Hermon structure is still missing.

We utilize (U-Th)/He apatite low-temperature thermochronology combined with geomorphic and structural analysis to constrain the timing, magnitude, and pattern of uplift and exhumation across Mount Hermon. The apatite helium system has the lowest closure temperature among all known thermochronometric systems and constitutes a sensitive thermal recorder of exhumation processes at shallow (1-3 km) crustal levels. Samples for thermochronology were collected mostly from Lower Cretaceous dikes intruding the Jurassic carbonate sequence exposed across the ridge.

Preliminary cooling ages from the hinge of the structure cluster around 20-30 Ma, with older 55-60 Ma ages at the south-east flank. Thermal modeling of the observed cooling age pattern suggests a Late Campanian-Early Paleocene initial folding and uplift followed by significant exhumation starting at Late Oligocene-early Miocene. Average long-term exhumation rates are ~ 30 m/Ma (over 60 Ma) at the flank of the structure with rates of ~ 50-100 m/Ma (over 30-60 Ma) at the hinge. Future samples and 3D thermo-kinematic modeling will constrain how these rates varied with time and shed light on differential uplift of fault-bounded blocks.

Geomorphic analysis across the ridge including stream profiles, relief at various scales, average slope, channel steepness index (ksn) and swath profiles, delineate apparent gradients in erosion rates and potentially young structures. More than 200 dip measurements, busking structural analysis, fold axis reconstruction and a stratigraphic cross section help define the structure of the ridge more accurately and limit the total amount of exhumation.

Observation of Site Effects at the Schools of Qrayot and Earthquake Hazard Assessment

Kalmanovich M., Zaslavsky Y., Gorstein M., Perelman N., Giller V., Aksinenko T. , Ataeva G., Dan H., Giller D., Shvartsburg A.,

Geophysical Institute of Israel, P.O.Box 182, Lod 71100, Israel

After the occurrence of large destructive earthquakes, it has long been understood that near-surface sedimentary layers significantly amplify earthquake ground motion. This is particularly important for Israel since most urban areas located on sedimentary basins with strong impedance contrast between the soft sediment and underlying bedrock. At the request of the Ministry of Education, the Seismology Division of the Geophysical Institute of Israel carried out in 2011 (November-December) a series of measurements and calculation to assess the seismic hazard for 15 schools located in Qiryat Motzkin, Qiryat Ata and Qiryat Bialik. The site response to seismic waves was determined empirically using ambient noise measurements at 86 locations. Generally, within the study areas we obtained two peaks appearing at different frequencies range: 0.5-0.8 Hz with amplification factor 2-3 and 1.5-6 Hz with amplification 3-6. These frequencies are associated with two impedance contrast: one at deeper and the other at shallow strata. Observed H/V ratio functions were modeled using computer program SHAKE. To develop the analytical subsurface model for different schools we used regional and local geological information and results of the refraction survey providing information on shear wave velocities in the upper layers. For each school we obtained a fair resemblance in frequency, amplification and shape between analytical function and H/V ratio. These analytical functions were used for seismic hazard assessment using Stochastic Estimation of Earthquake Hazard (SEEH) procedure (Shapira & van Eck, 1993, Natural Hazard, 8, 201-215). In accordance with the calculated acceleration response spectra and with respect to geological characteristics of site, we divided the schools into five groups. Each group is characterized by soil-column model.

Sediment reworking events as possible indicators for seismic activity in the Northern Gulf of Aqaba-Eilat

Kanari M.[1], Bookman R.[2], Ben-Avraham Z.[1], Tibor G.[3], Niemi T.M.[4], Goodman Tchernov B.[2] , Hartman G.[3], Galloway J.L.[4], Al-zoubi A.[6], Abueladas Abdelrahman M.S.[1]

1 Department of Geophysics and Planetary Sciences, Tel Aviv University, Tel Aviv 69978
2 The Dr. Moses Strauss Department of Marine Geosciences, Haifa University, Mt. Carmel, Haifa 31905, Israel
3 Israel Oceanographic & Limnological Research Ltd., Tel-Shikmona, P.O.Box 8030, Haifa 31080, Israel
4 Department of Geosciences, University of Missouri-Kansas City, USA
5 GeoSense, Environmental and Engineering Geophysics, LTD
6 Surveying and Geomatics Department, Al-Balqa' Applied University, Al Salt, Jordan

---

We aim to identify and date sediment reworking events in submarine cores, e.g. slumping, turbidites or tsunami/seiche deposits in the Northern Gulf of Aqaba-Eilat (NGAE), located at the southern part of the Dead Sea Transform. Based on seismic and bathymetric analyses, prior studies suggest that the offshore Evrona and West Aqaba faults situated within the gulf are recently active. Tectonic activity, as well as other possible triggers (e.g. climatic or gravitational) may result in reworking of the submarine sediments.

In order to contribute to the Holocene earthquake record of the NGAE (i.e. long and short term recurrence intervals) we aim to identify tectonically induced sediment reworking events in cores and correlate them across the Gulf to specific climatic / tectonic events.

We analyze cores retrieved in the frame of USAID-MERC research (TA-MOU-08-M29-036), located on and off the submarine canyons of the Eilat sub-basin detected in multibeam bathymetry data. In addition, a paleoseismic trench was recently excavated at the palm plantations of kibbutz Eilot, following an estimated location of the onland continuation of the submarine Evrona fault in light of GPR survey and offshore seismic data interpretation.

Grain size distribution of core sediments is used to identify depositional sequences typical of sediment reworking events. Radiocarbon dating of core sequences is expected to reveal the timing of sediment mass-flow/ transport events and possibly match correlative historical earthquakes. Deeper and older dated sequences will assist in determination of the Holocene seismic record of the NGAE region.

Three to four events of sediment reworking are identified in core MG10-P27 (submarine canyon, 530 mbsl) as grain size analysis implies. The on-land trench revealed detailed stratigraphy, yet no fault was traced in it. However, the strata revealed three horizons containing what appears

to be liquefaction features at several locations along the trench log, possibly attributed to one or more earthquakes. Radiocarbon dating of both core sediments and trench strata is currently in progress; Comparison of core and trench sediments and their ages may yield cross-validation of these two data sources.

Methane bubble growth and migration within shallow muddy aquatic sediments: a theoretical study

Katsman R., Makovsky Y.

The Dr. Moses Strauss Department of Marine Geosciences, Haifa University, Mt. Carmel, Haifa 31905, Israel

Shallow gassy marine sediments abundantly found on continental margins of Israel and worldwide, are a source of major concern for their contribution to destabilization of coastal and marine infrastructure and global warming. Biogenic gas accumulation and migration within muddy aquatic sediments is associated with intensive sediment fracturing, affecting structural integrity, load-bearing capabilities, and slope stability of the sediments. Prediction of these destabilizing or even catastrophic events is especially important in a context of globally-intensifying Israeli offshore infrastructure. We built a fully-coupled LEFM-reaction-transport numerical model permitting to study the detailed physics of gas accumulation and migration in muddy marine sediment. We systematically examine interplay between methanogenesis, methanotrophy, gas solubility, and sediment fracturing controlling the bubble dynamics. Simulations shows that during the initial stage of bubble growth fracture increment subsides in the bubble bottom part, and bubble form evolves from the circular one to the form of the 'inverted tear drop'. Each fracturing event is accompanied by the instantaneous pressure drop within the bubble, followed by the continuous stage of pressure elevation induced by solute transport to the growing bubble. Surface tension was found to be negligible in comparison with pressure developed within the bubble even for the small circular bubble (8mm in diameter). Calculated bubble vertical size that controls initiation of bubble rise from the location of its nucleation demonstrates a good agreement with values reported in the literature.

Re-evaluation of the inland retreat rate of Israel's Mediterranean coastal cliff

Katz O., Mushkin A.

Geological Survey of Israel, 30 Malkhe Israel, Jerusalem 95501, Israel

The Israeli coastal cliff extends about 50 kilometers along the eastern Mediterranean shores. The cliff is comprised of late Quaternary eolianites and paleosols and reaches heights of up to 50 meters. In places, time-averaged inland cliff-top retreat rates of up to a few tens of centimeters per year have been measured usually by comparing aerial photos from the last decades. Commonly, these locally constrained retreat rates have been: 1) extrapolated as representative of the entire cliff length, and 2) adopted by hazard-mitigation and planning authorities. Here, we re-evaluate the current understanding of coastal-retreat patterns and rates along Israel's Mediterranean cliff line using a suite of field observations, aerial photography and recently obtained airborne & ground based high resolution LiDAR measurement of cliff morphologies.

First, we constrain the decadal-scale retreat rates along the entire coastal-cliff of Israel by comparing the cliff-top location in 1945 and 2004 using aerial photos. We find a statistically significant spatial correlation between: 1) calculated low retreat rates (less than 0.1 m/year) and field-based criteria indicating overall stability, e.g., slope angle of 45° along the upper half of the cliff, talus cover along the lower part of the cliff and developed vegetation cover, and 2) high retreat rates and field criteria indicating recent instability ,e.g, fresh landslide scars and 'hanging' valleys , which provides independent support for the calculated retreat rates. Calculated 60 years average cliff-top retreat rates (in bins of few hundred meters) of less than 0.1, 0.2 and 0.3 m/year along 58, 77 and 85% of the cliff length, respectively, reveal that extended stretches of the cliff line did not experience detectable retreat in the past 60 years, thus implying relative stability of ~50% of Israel's costal cliffs during this time period. Low retreat rates at longer time scales are also supported by numerous archeological sites along Israel's coastal cliff, built more than 103 years ago, that exhibit an architectonic coherence with the present-day cliff line and thus also argue against high retreat rates of 10-1-100 m?yr-1 which would translate to at least 102-103 m of retreat during the last millennium.

In summary we suggest that straight forward spatial and temporal extrapolations of locally derived retreat rates to the entire coastal cliff line may have led to overestimation of cliff activity. In light of our results it appears that the overall short and long term retreat rate of Israel's coastal cliff is lower than a few tens of centimeters per year, while locally higher retreat rates can occur with extreme events of up to 8 meters of cliff top retreat resulting from strong winter storms.

Oil sand exploration project in Inner Mongolia, China

Kolodner K., Barun D.

Geo-Prospect LTD.

Oil sands are a mixture of clay, sand and water with 10-20 percent bitumen. More than 2 trillion barrels of the world's petroleum lies in oil sands. Oil sands are found worldwide. Alberta, Canada, has a booming oil-sand industry with more than 1 million barrels of synthetic oil are produced there every day. That volume means that Canada is the number 2 oil producer in the world, second only to Saudia.

The exploration project in China was near by one of the largest petroleum-producing basins in China. Oil migration took place upward, parallel to the dip, toward the local structural highs as well as toward marginal areas where several oil fields were discovered. The existence of traps at the time of hydrocarbon migration enabled their accumulation in the different oil fields.

The exploration contained ~150 boreholes and Geophysical survey included an airborne electromagnetic - magnetic survey.

The residual magnetic data was used to identify major basement blocks and related fault systems. The basin exhibits the typical structural style of a rift basin which is characterized by the presence of elongated uplifted blocks that are separated by narrow graben features. The results show a series of NE-SW oriented narrow blocks, gradually descending to the basin and a system of transfer faults with small lateral shifts, perpendicular to the normal faults. They probably form conduits for oil migration.

Corresponding maps of electrical resistivity were drawn on the basis of raw electromagnetic data. It was proved that certain resistivity values and lithology are related. Electrical resistivity criteria for oil prospecting were developed on the basis of electromagnetic statistical analysis of the subsurface in comparison with oil content data. As a result, two main oil domains were indicated.

The oil bearing sands were found in three intervals. The top surface of the oil-sand occurrences forms an elongated oval ridge structure, trending NE-SW. There is a good correlation between the amount of oil and the elevation of the top-oil surface: Locations with high net oil column appear at the crest of the ridge and ones with a low net-oil column are generally on the slopes of the structure.

The physical and chemical properties of these Chinese oil sands are of paramount importance for their economic evaluation. Overall, 850 cores were sampled for characterization. The higher quality and the least degraded oils are characterized by low viscosity, high API gravity, high

saturates and aromatics, and low asphaltenes.

The combination of the high saturated and aromatic hydrocarbon content (high API gravity), high hydrogen content, exceptionally low sulfur, nitrogen, and metal contents, indicates that these Chinese oil sands contain good quality heavy oils rather than extra heavy oils usually found in typical Canadian and Venezuelan oil sands.

Groundwater recharge in the southern coastal aquifer: soil and vadose-zone point of view

Kurtzman D.[1], Turkeltaub T.[1,2], Baram S.[2], Dahan O.[2],

1 Institute of Soil, Water and Environmental Sciences, Agricultural Research Organization ARO, The Volcani Center, Bet Dagan 50250, Israel

2 Department of Environmental Hydrology & Microbiology, Zuckerberg Institute for Water Research, Blaustein Institutes for Desert Research, Ben-Gurion University of the Negev, Sede Boqer, Israel 84990

Soil overlying the southern coastal aquifer vary from sand dunes in the west, small areas of red medium soil (Hamra) to large areas of Vertisols (cracking clays) at the center and east. This talk combines studies from this region in which groundwater recharge was investigated through vadose zone sampling, monitoring and modeling, as well as some surface observation on soil cracks.

The first study concentrates on the lighter soils of the west. In this study vadose zones under a natural sand dune (Ashdod), a citrus orchard and a rain-fed crop field (Nir Galim) were monitored with vadose zone monitoring systems (VMS). VMS enables continuous measurements of the vadose zone water content and frequent sampling of pore water at selected points across the entire vadose zone. Flow and chloride transport models through the vadose zone were calibrated to the monitoring data at the three sites and recharge was investigated using historical meteorological data and through scenarios of land-use and climate change. Some interesting results of this investigations are: multiyear average recharge under the orchard is only 10% of average surface inputs (precipitation and irrigation); Landuse change on the natural sand dune to intensive vegetable greenhouse will reduce increase chloride flux to groundwater 11 folds (irrigation water of 200 mgCl/l); a 25% drop in rainfall will lead to ~54% drop in average recharge under rain-fed crop field.

Recharge through Vertisols in the central and eastern parts of the southern coastal aquifer is more complex due to the nature of the cracking clays and the underlying vadose zone. Vadose zone under irrigated crop land was found to be wetter and les saline than nearby uncultivated vadose zone under Vertisols (Revadim). Modeled matrix fluxes through the non cultivated vadose zone were extremely low (~2 mm/yr). The only way to explain the existence of a fresh water aquifer before the intensive cultivation period is recharge of fresh water through preferential paths. Observation on fracture networks in the region (Beer Tuvia) revealed that most of the network doesn't seal during the winter and percolation of storm water through preferential paths is possible. Comparison of VMS data from a non cultivated clayey site and other sites support fast percolation through non cultivated Vertisols. Intensive cultivation

in this region (starting 1950-1980) shifted the deep percolation mechanism to matrix flow that flushed the previously saline dry vadose zone, causing salinization of the aquifer since the 1960s. Examination of groundwater chloride data from the 1930's shows that the most saline area in this part of the aquifer (400-500 mgCl/l) was under the most cultivated Vertisols, suggesting that traditional cultivation had similar effect on recharge under Vertisols, but not as extreme than the effect of modern irrigated intensive cultivation.

The late Pleistocene hydrological history of Lake Kinneret based on Sr/Ca and $^{87}Sr/^{86}Sr$ in ostracods from Ohalo shore, Israel

Lev L.[1,2], Almogi-Labin A.[2], Stein M.[2], Ben-Avraham Z.[1]

1 Department of Geophysics and Planetary Sciences, Tel Aviv University
2 Geological Survey of Israel, Jerusalem, 30 Malkhe Israel St., Jerusalem

The late Pleistocene hydrological history (e.g. salinity and water sources) of Lake Kinneret is recorded in sediments and fossils (e.g. Melanopsis and ostracod shells) that were deposited in the lake. A 5 meters deep trench that was dug at the Ohalo –II archeological site (dated to ~22.5 ka B.P) was used for this study. The trench covers the time interval of the last glacial period (~22-27 ka B.P), including the high-stand time interval of Lake Kinneret when its level reached ~ 160 m below mean sea level and the lake merged with the saline Lake Lisan. More than 200 samples were recovered from the trench. We measured major and trace elements (Mg, Sr, Ca) and strontium isotopes in ostracod valves of Cyprideis torosa. The Sr/Ca ratios are used to infer the ratios in the lake waters. For this we applied Sr/Ca partition coefficient of 0.7 that is deduced from living ostracods and their Lake Kinneret habitat water. Sr/Ca water ratios during the late Pleistocene are lower than the Sr/Ca values of the Holocene and modern lake-water (Sr/Ca~0.002 compared with ~0.007, respectively). Sr/Ca values that were measured in contemporaneous Lisan aragonites also showed lower values compared to modern Dead Sea (Sr/Ca~0.006 compared to ~0.01). We distinguish 3 major periods based on the change in the Sr/Ca ratios: (1) relatively high values of Sr/Ca (>0.0039) predating the high lake stand (27-26 ka B.P); (2) somewhat lower and constant Sr/Ca values (0.0035±0.0004) during the high lake stand and immediately after that (26-23 ka B.P); (3) decreasing Sr/Ca values (from ~0.0037 to ~0.0031) at the top of the core that postdate the archeological site. $^{87}Sr/^{86}Sr$ ratios in the ostracods, ~ 0.7080, are constant throughout the entire studied interval. These values are much higher than the values that were measured in Holocene lake waters (~0.7076). They are the same as those of Lake Lisan indicating that strontium in the last glacial Lake Kinneret was affected by Dead Sea brines.

Reliable Monitoring of Fresh-Saline Water Interface in Coastal Aquifers

Levanon E.[1,2], Yechieli Y.[2], Salev E.[2], Friedman V.[3], Gvirtzman H.[1]

1 Institute of Earth Sciences, The Hebrew University, Jerusalem 91904, Israel
2 Geological Survey of Israel, 30 Malkhe Israel, Jerusalem 95501, Israel
3 Hydrological Service, Israel Water Authority

This study deals with the reliability of monitoring of the fresh-saline water interface (FSI) in coastal aquifers, considering the effect of tides in long-perforated boreholes. Electric Conductivity (EC) fluctuations at the coastal aquifer of Israel, as measured in long-perforated borehole, were found to be in the same periodicities as sea tide, but two orders of magnitude larger than sea level or groundwater level fluctuations. On the other hand, direct measurements in the aquifer through buried EC sensors demonstrate very small fluctuations in EC. This implies that EC measurements within the long-perforated boreholes might be distorted due to a vertical flow in the borehole, while actual fluctuations of the FSI within the aquifer are two orders of magnitude smaller. This vertical flow occurs due to sea tide fluctuations – On high tides, the hydraulic head of saline water on the lower part of the borehole increases, so upward flow occurs in the borehole. On low tides, the hydraulic head of saline water decreases and induces downward flow. Fast – Fourier – Transform analysis demonstrates that sea tide fluctuations are the driving force for water level and EC fluctuations within the borehole.

Considering these field data, we suggest that monitoring of fresh - saline water interface adjacent to the sea through long-perforated boreholes is unreliable. EC fluctuations in short-perforated boreholes (1 m perforation on the upper part of the FSI) were somewhat larger than in the aquifer, but much smaller than those in the long-perforated borehole. The short-perforation diminishes the vertical flow and the distortion and therefore more reliable for monitoring of the FSI at shoreline vicinity.

Developing new earthquake scenarios for Israel using Hazus loss-estimation software

Levi T.[1], Katz O.[1], Bausch D.[2]

1 Geological Survey of Israel, 30 Malkhe Israel, Jerusalem 95501, Israel
2 FEMA Region VIII, Denver Federal Center, Bldg 710, Denver, CO 80225

Israel is situated along the tectonically active Dead Sea Transform (DST) experiencing magnitude 6-7 earthquakes with recurrence time of hundreds to thousands years. Worldwide, mitigation of future earthquake damage, improving of population survival and evaluation of expected earthquake effects is done using modern earthquake loss estimation computer techniques. Consequently these techniques have become common and are widely used to quantify potential, social and economic losses from earthquakes. However, so far in Israel only preliminary damage and loss estimation scenarios were developed. The present study simulates modern damage and loss estimation scenarios for various earthquakes affecting Israel, for the first time by using the Hazus loss estimation software.

To accomplish the above, first step was obtaining information regarding the Israeli geography, geology, infrastructure, buildings, demographic and economic and implementation of the data into the Hazus databases. The input files of the program were fitted and supplied for every census track with data records of central hospitals, medical care stations, police and fire and rescue services facilities, central bus stations, highway and railway bridges, ports, airport facilities, pumping water stations, waste water facilities and fuel farms. In addition a landslide susceptibility map was developed and incorporated into the Hazus data-base as well. Then, two synthetic earthquakes were simulated: "Ein Gev" and "Ayelet HaShahar" scenarios, both resemble, Mw=7.0 and focal depth of 10 km.

The preliminary results show clearly that the location and the seismic durability of the examined facilities have a major influence on the amount and type of damage, whether caused to a single facility or to the group of devices and buildings. Yet, it is shown that even for low seismic building codes; strong earthquakes will apparently not severely affect the entire country. For example, in the "Ayelet Ha Shahar scenario" a total of 20 police stations and 5 fire and rescue services stations may be damaged severely and collapse. One day after the earthquake, 89 of the 278 police stations and 21 of the 60 fire and rescue services stations are expected to have a functionality level less than 60%.

Landslides are expected to develop in steep slopes at a radius of about 50 km including damage in major population centers.

The results of the simulations show excellent ability of Hazus to resolve the expected different damage levels and loss for various types of buildings and infrastructures for each specific census tract in Israel as well as locate sites of expected landslides. The loss information provides decision-makers and emergency authorities a tool for planning and exercising emergency actions following an earthquake.

Late Pleistocene palaeoclimate of the Dead Sea area (Israel): speleothem and stromatolite records

Lisker S.[1], Vaks A.[2], Bar-Matthews M.[3], Porat R.[1], Frumkin A.[1]

1 Geography Department, The Hebrew University, Jerusalem
2 Oxford University, UK
3 Geological Survey of Israel, 30 Malkhe Israel, Jerusalem 95501, Israel

---

Calcite speleothems are rare in the nowadays arid to hyper-arid rain-shadow Dead Sea area of eastern Israel. Speleothem ages (U-Th) from caves on the Dead Sea Fault Escarpment and two caves from arid rain-shadow areas surrounding the Dead Sea, span the last three glacial cycles between ca. 354 to 12 ka and suggest episodic wet local palaeoclimate mainly during the glacial periods of Marine Isotopic Stages (MIS) 6 and 4 to 2.

U-Th ages of stromatolites deposited in the Late Pleistocene Lake Lisan and preserved in caves of the Dead Sea Fault Escarpment, suggest that regional relatively wet climate affected the lake catchment area during the late part of MIS-3 lasting until middle MIS-2, as well as at MIS-5 to 4 (interglacial-glacial) transition.

Speleothem deposition periods from 38.4±0.5 to 16.4±0.3 ka, i.e. late MIS-3 to early MIS-2, representing moist periods in the lake area, are coeval to regional wet conditions inferred by the stromatolite record. A direct connection is thus implied between local and regional climate at the latest Pleistocene based on correlation between two independent data sets. This connection implies that glacial climate has generally been moister than interglacial climate during the last glacial-interglacial cycle at both local and regional scales around the Dead Sea and its predecessors.

The Meged Oil Field – Introduction

Luskin T., Shteingolts V., Soferstein M.

Givot Olam Oil, Ltd.

The Meged Field is located in central Israel and lies within the Galil rift zone, which forms the southwestern extension of the Palmyra rift at the northern part of the Arabian plate. The Palmyra rift formed during the extensional opening of the intercontinental rift zone on the Neo-Tethys passive margin, during the Late Permian – Late Triassic period and extended across Syria and northwestern Iraq. The Galil rift is separated from the South Palmyra by the latest Dead Sea transform fault system.

Seismic and geological data demonstrate that Central and Northern Israel are an integral part of the Palmyra Rift with thick Triassic and Paleozoic sections.Notably, Meged oil is conclusively tied to a Silurian source rock and suggests that the Galil Rift contains a Palaeozoic Silurian source capable of charging the Lower Mesozoic reservoirs. A present day dome shaped Meged structure with a four-way dip closure incorporates several structural developmental stages 1. early Jurassic inversion along the bounding fault, forming large areas of significant vertical relief, 2. later modified during the Late Cretaceous - Miocene "Syrian Arc" compression and 3. subsequent Tertiary tilting down to the west. The main reservoir units in the Meged field are contained within the Middle and Upper Triassic Saharonim and Mohilla Formations sealed by an upper Mohilla anhydrite unit.

A gross oil column in the fractured carbonate reservoirs of the Meged Field is over 600 m thick, as confirmed by the Meged-5 well. During 7-month production in 2011, the Meged-5 well produced more than 150,000 bbl of high quality oil, from zone 8b only.

Pervasive evidence of methane seepage along the base of Israel's Mediterranean slope – preliminary results of E/V Nautilus 2011 cruise

Makovsky Y.[1], Ben Avraham Z.[1], Ballard R.D.[2], Austin J.[2], Coleman D.[2], Almogi-Labin A.[3], Tchernov D.[1], Tezcan D.[1], Spiro B.[1], Ezra O.[1], Antler G.[4], Rubin M.[1], Tsadok R.[1], Fuller S.A.[2], Phillips B.[2], Qupty N.[1], Sade H.[5], David N.[1,5], Scheinin A.[1], Sivan O.[4], Hübscher C. [6], and Project Nautilus participants.

1 Charney School of Marine Sciences (CSMS), University of Haifa, Haifa 31905, Israel. yizhaq@univ.haifa.ac.il

2 Sea Research Foundation Institute for Exploration, Institute for Exploration, Mystic, RI, USA.

3 Geological Survey of Israel, 30 Malkhe Israel, Jerusalem, 95501, Israel.

4 Geological and Environmental Sciences, Ben-Gurion University of the Negev, Beer-Sheva 84105, Israel.

5 Israel Oceanographic and Limnological Research, Haifa, Israel.

6 Institute for Geophysics, Center for Marine and Climate Research, University of Hamburg, 20146 Hamburg, Germany.

Features related with methane seepage are prominent throughout the Nile delta, but so far have not been observed along the Israeli continental slope north of Gaza. A five days cruise in Octber 2011 onboard the Ocean Exploration Trust E/V Nautilus collected high definition video and hand and short core samples at water depths of 500 to 1300 m of the Israeli Mediterranean utilizing the vessel's state-of-the-art ROV operation. The cruise was led by a combined team of the Institute For Exploration, Charney School of Marine Sciences, Israel Oceanographic and Limnological Research, the Geological Survey of Israel and Ben Gurion University of the Negev. This cruise was a follow up of E/V Nautilus 2010 cruise, previously reported. ROV dives, carried out at depths of 1100 to 1200 m on the western edge of Palmahim Disturbance on seismically observed pockmarks and bright spot reflections, revealed active gas seepage sites characterized by semi-periodic gas bubbling, carbonate chimneys, dark gas saturated sediment patches and a characteristic biogenic community. Sediments cores collected within the dark patches purtray high concentrations of methane with Carbon isotopic values suggesting a biogenic origin, and oxygen depletion in near surface water. Seepage regions are also surrounded by wider areas of unusually intense seafloor burrowing. At a depth range of 600 to 800 m along the northern slope of the Palmahim Disturbance ramp we mapped low lying heterometric rock ledges, boulders and rubble hard rocks, settled with rich deep water fauna and particularly deep water corals. Preliminary examination of one tubular feature

collected in the region revealed a chimney-like morphology, dolomite composition and δC13 values as low as -40, suggesting a methanogenic origin. Yet no evidence of active gas seepage was found in the vicinity of these reefs. Offshore northern Israel, approximately opposite to Acco, we surveyed a set of meters-scale pockmark features at a water depth of 1100 m, along a north-south striking seafloor escarpment. Within one of these pockmarks we found a dark patch of sediments inhabited by tube warms, and sampled high concentration of methane. Farther west we documented an area of intense burrowing at the top of a seismically observed structural bulging. Taken together our observations suggest that active or recent gas seepage extend along the entire base of the Mediterranean continental slope of Israel, and are possibly associated with leakage through structural pathways in the Messinian salt layer.

Liquefaction on the Mediterranean shore of Israel: possible onshore evidence for past tsunami

Marco S.[1], Katz O.[2], Dray Y.[3]

1 Department of Geophysics and Planetary Sciences, Tel Aviv University, Tel Aviv 69978
2 Geological Survey of Israel, 30 Malkhe Israel, Jerusalem 95501, Israel
3 Restoration of Ancient Technology, Binyamina, Israel

In search for liquefaction in the clastic sediments of the coastal plain of Israel we excavated trenches behind a 4th century Byzantine dam on the Crocodile Creek, some 850 m inland of the Mediterranean shore. The abundant silt and sand in the region with very shallow ground water were evaluated as susceptible for liquefaction in the past, but these previous searches failed to find field evidence for it. We discovered a series of liquefaction features in the form of "flame structures" penetrating an overlying clay-rich soil. Peculiar asymmetric shapes and in places zig-zag shapes characterize the individual injections, most of which trend eastward and southward. The liquefaction is most prominent several meters from the point where the dam is badly damaged on the seaward side as if it had been hit and possibly breached by a large wave. The size of the flame structures diminishes with distance from the damaged part of the dam until complete disappearance some 100 m away from it. One plausible explanation is that earthquake vibrations triggered the liquefaction by increasing the pressure in water-saturated silt and forcing it upward into the overlying soil. The other option is that a sudden inflow of seawater induced shear at the bottom of the lake triggering Kelvin-Helmholtz Instability. As a result of the instability the silt intruded the overlying sediment. Three arguments support the tsunami mechanism. One is the asymmetry of the flame structures and their dominant vergence away from the break in the dam, the second is their gradually diminishing amplitude with distance from the dam, and the third is their similarity to structures that were reported from Indonesia after the great 2004 tsunami and other palaeotsunami observations. We regard these observations as evidence for the vulnerability of the densely populated coastal plain to liquefaction and also to tsunami waves in low-laying places. Based on the stratigraphic position, archaeological findings, and historical accounts we regard the earthquake of November 25, 1759 the most plausible trigger for the liquefaction, probably as tsunami induced structures.

Observations of seismic activity in Southern Lebanon

Meirova T., Hofstetter R.

Geophysical Institute of Israel, P.O.Box 182, Lod 71100, Israel

Recent seismic activity in southern Lebanon is of particular interest since the tectonic framework of this region is poorly understood, and seismicity in this region is very infrequent, while to the east the Roum fault is seismically active. Since early 2008 an intense seismic activity occurred there continuing until end of 2010 including several swarm-like sequences, and continuous trickling seismicity over many other days, amounting in total to more than 900 microearthquakes in the magnitude range of 0.5<Md<5.2. The length of the region of activity is about 40 km long mainly in the N-S direction, located about 10 km west of the Roum fault.

The largest earthquake with magnitude Md = 5.2 occurred on February 15, 2008, and is relocated at 33.327 N, 35.400 E at a depth of 9 km. The mean-horizontal peak ground acceleration observed at two nearby accelerometers exceeded 0.05 g, where the strongest peak horizontal acceleration was 55 cm/sec2 at station Manara (~55 km SE of the epicenter). Application of the HypoDD algorithm yields a pronounced N-S zone, parallel to the Roum fault. Focal mechanisms, based on full waveform inversion, of the strongest earthquakes present strike-slip faulting.

Seismic attenuation in Israel from coda waves

Meirova T., Pinsky V.

Geophysical Institute of Israel, P.O.Box 182, Lod 71100, Israel

Ground-motion simulations or studies on the nature of ground motion should incorporate attenuation parameters of the media. The quantification of the seismic attenuation and the study of the physical mechanisms underlying the processes of seismic energy dissipation are important in the seismic risk analysis. We used the Multiple Lapse Time Window Analysis technique to determinate regional attenuation in the crust in the frequency range 0.5 -16 Hz. The method also allows estimating the relative contributions of intrinsic and scattered attenuation.

Our study shows a few remarkable finding. Scattering and intrinsic attenuation in the central and southern Israel are comparable, while in the northern Israel both the scattering and intrinsic energy dissipates by different pattern. The scattering attenuation in the southern and central Israel does not affect the trend of energy decay with distance and practically is negligible respect to the intrinsic absorption, whereas in the North the scattering attenuation is a notable. This effect could illustrate the presence of large scale heterogeneity in Northern Israel, when the seismic wavelength is lower than average size of heterogeneity. The quantitative estimate of frequency dependent Q value for central and southern Israel was modeled as $Q=145f^{0.92}$. For northern Israel the estimate of this parameter is $Q=83f^{0.92}$.

Tsunami Early Warning and Mitigation System in Israel

Meirova T.[1], Rosen D.[3], Salamon A.[2]

1 Geophysical Institute of Israel, P.O.Box 182, Lod 71100, Israel
2 Geological Survey of Israel, 30 Malkhe Israel, Jerusalem 95501, Israel
3 Israel Oceanographic & Limnological Research Ltd., Tel-Shikmona, P.O.Box 8030, Haifa 31080, Israel

---

Following the government decision in 2007 to set up Tsunami Warning System in Israel (TWSI) the system will be developed as a part of the Tsunami Early Warning and Mitigation System in the North Eastern Atlantic, the Mediterranean and Connected seas (NEAMTWS).

The main objective of the initial phase is to have in place a system for dealing with tsunamis having destructive potential far from the source, i.e. with impact times longer than 30 minutes after the first alert that a tsunami may have been generated. However, most of the historical tsunamis that hit the Levant are considered local and as such are outside the mandate of the NEAMTWS and should be considered by the local authorities (Salamon, 2010). In the next phase the TWSI would be capable of producing tsunami warning alerts for locations within 10 minutes travel time of the source that is especially important in the case of tsunamis with local sources.

The first effort will be devoted to developing and integrating the basic elements of a local warning system. The system architecture for TWSI will consist of the following elements: National Tsunami Warning Focal Point and National Tsunami Warning Center, Tsunami National Contact, Centers for Technological and Scientific services and National Civil Protection organizations.

Evolution of the Arabian-Nubian Shield and the provenance of Paleozoic sandstones in Southern Israel and Jordan: Zircon U-Pb-Hf perspectives

Morag N.[1], Kolodner K.[2], Avigad D.[1], Gerdes A.[3], Belousova E.[4], Harlavan Y.[5]

1 Institute of Earth Sciences, The Hebrew University of Jerusalem, Jerusalem 91904, Israel
2 Geo-prospect Ltd., Jerusalem 91036, Israel
3 Institut für Geowissenschaften, Johann Wolfgang Goethe Universität, D-60438 Frankfurt am Main, Germany
4 GEMOC, Department of Earth and Planetary Sciences, Macquarie University, NSW 2109, Australia
5 The Geological Survey of Israel, Jerusalem 95501, Israel

The Arabian-Nubian Shield (ANS) basement of southern Israel records over 300 m.y. of Neoproterozoic crustal evolution, which includes two major igneous cycles: an early island-arc cycle at ca. 880-740 Ma and a later post-collisonal cycle at ca. 660-580 Ma. Although the main phase of island-arc magmatism is dated between 880 and 740 Ma, the occurrence of rare 900-1000 Ma detrital zircons with positive εHf(t) values in the Elat schists indicates the onset of arc magmatism in the ANS by early Tonian time, much earlier than previously recognized. Zircon εHf(t) values in the studied basement rocks are mostly positive, supporting previous isotopic evidence for the overall juvenility of the northern ANS. Nonetheless, detrital zircons in the oldest metasedimentary units, derived from the erosion of island-arcs, display a wide range of εHf(t) values from +1 to +13, which may indicate a certain degree of contamination by an older crustal component. This option is supported by the occurrence of rare zircon xenocrysts with pre-Neoproterozoic ages and/or negative εHf(t) values. Zircon εHf(t) values in post-collisional granitoids and volcanics resemble those retrieved from the island-arc rocks, although less scattered (+5 to +9), and their origin is therefore consistent with both reworking of the earlier island-arc crust and crystallization from mantle-derived melts.

Zircons from the Cambrian–Ordovician sandstones, overlying the ANS basement, yielded predominantly (~70%) negative εHf(t) values incompatible with a juvenile source. Therefore, most of these detrital zircons were derived from distant terrane(s) comprising reworked pre-Neoproterozoic crust, rather than from the adjacent ANS. As the studied Cambrian–Ordovician section is located at the northern tip of the ANS, sand must have been transported several thousand kilometers before deposition. This finding implies that the ANS and adjacent parts of the Pan-African orogen in NE Africa were completely warned down by the onset of Cambrian deposition, and that the topography over vast areas in northern Gondwana was relatively leveled such as to allow massive transfer of sand across the continent.

The role of extreme winter storms in the overall retreat pattern of an actively eroding eolianite coastal cliff-line in the eastern Mediterranean

Mushkin A.[1], Katz O.[1],

1 Geological Survey of Israel, 30 Malkhe Israel, Jerusalem 95501, Israel

Eolianite cliffs along the Mediterranean coast of Israel form an actively eroding 55-km-long linear feature with local average retreat rates of up to 0.3 m/year over the past 60 years. Here, we investigate the effect of extreme winter storms with decadal-scale recurrence intervals, on the overall retreat pattern of this 'weak rock' coastal cliff-line. Repeat high-resolution (1-2 cm) ground based LiDAR surveys before and after an extreme '20-year' winter storm that occurred in the eastern Mediterranean during December 2010 allowed us to characterize syn- and post-storm erosional effects at cm-km scales.

The LiDAR surveys documented cliff instability initiated by syn-storm erosion of basal cliff notches that propagated up-cliff during the months that followed and lead to post-storm activity, which constituted >75% of the total storm-related cliff erosion. The latter occurred primarily as discrete catastrophic gravity driven slope-failure events that range in volume between 100-103 m3. The cliff-line returned to its long-term activity level ~5 months after the storm. Locally, storm induced landward cliff retreat reached 7 m, which is comparable to the total retreat previously documented along this coastal stretch during the past 60 years. Yet, in a broader spatial context, cliff-retreat associated with the December 2010 storm accounts for <5% of the total retreat documented for this cliff-line during the past 60 years, thus implying only a secondary role for extreme winter storms in the overall volumetric retreat of this coastal cliff line. Nonetheless, the preferred occurrence of peak storm-associated erosion at local capes suggests that extreme winter storms may have a central role in maintaining the large-scale linearity of Israel's coastal cliff-line.

Direct dating of late-Pleistocene activity along the Qiryat Shemona fault, the Dead Sea Transform in northern Israel

Nuriel P.[1], Weinberger R.[1], Rosenbaum G.[1]

1 School of Earth Sciences, The University of Queensland, QLD 4072, Australia
2 Geological Survey of Israel, 30 Malkhe Israel, Jerusalem 95501, Israel

Direct dating of brittle fault activity is of fundamental importance to tectonic reconstructions and paleoseismic studies. One way to address this issue is by constraining the timing of fault striations, but this requires a better understanding of the striation formation mechanism and associated mineralization. We present results from a microstructural, geochemical and geochronological study of calcite precipitates associated with striated fault planes from the ~N-S striking Qiryat Shemona fault zone, a major segment of the Dead Sea Transform in northern Israel. Analyses were carried out at the Stable Isotope Geochemistry Laboratory and the Radiogenic Isotope Laboratory, at the University of Queensland. We recognize four types of coexisting calcite precipitates, including calcite cement in dilation breccia, calcite in striated groove morphology, calcite gouge associated with hydraulic fracturing and pressure solution, and calcite coating of the fault surface. Geochemical data indicates various precipitation mechanisms associated with formation of syn-tectonic (calcite cement and striations), co-seismic (calcite gouge), and inter-seismic (calcite coating) precipitates in the fault zone. Using U-Th dating of samples from several fault-plane localities, we delineate four well-defined deformation ages in the period from 220 to 60 ka. The present results were integrated with previous results that show the following: (1) ~W-E striking calcite-filled extensional veins were emplaced perpendicular to the adjacent Qiryat Shemona fault between 358 and 17 ka (Nuriel et al., 2012; Journal of Structural Geology); and (2) the late-Pleistocene Hazbani basalts are folded along ~N-S trending axes next to the Qiryat Shemona and Tel Hai faults (Weinberger et al., 2009, Tectonics; Weinberger et al., 2010; Israel Journal of Earth Sciences). The intergrated analysis provides evidence for a transition from an early (pre-Pleistocene) phase of almost pure strike–slip to a late (Pleistocene) phase of con¬vergent strike–slip faulting (transpression). The latter style of faulting is associated with strain partitioning as follows: (1) ~N-S shearing along the Qiryat Shemona and Tel Hai bounding strike-slip faults; (2) ~E-W shortening within the adjacent blocks and formation of mini fold and thrust belt; and (3) ~N-S perpendicular extension due to relaxation and formation of calcite-filled veins. The faults investigated in this study show activity at the last 60 ka and should, thus, be considered as potential active faults for seismic hazard assessments.

Experimental assessment of dynamic characteristics of two monuments in Avdat national park.

Perelman N., Zaslavsky Y.

Geophysical Institute of Israel, P.O.Box 182, Lod 71100, Israel

The ability to evaluate the vulnerability of existing structures during an earthquake and to estimate parameters of ground motion from historical earthquakes that damaged archeological structures depends on analytical models of the structures involving their dynamic characteristics. The present work is focused on reliable empirical estimates of resonance frequencies and damping ratios of two ancient structures located in Avdat National Park in the Negev: the Column and the Portal. We utilized various means of excitation in the horizontal direction: "man-power" impact at the top of the Column and Portal, impact by sledgehammer striking at the base of the Column and the Portal and low amplitude vibrations produced by ambient excitations.

The use of velocity seismograms obtained by standard short period seismometers and processing techniques based on the Fast Fourier Transform enabled identification of resonance frequencies and damping of the Column and Portal. The Fourier velocity spectra obtained from various forced excitations of the Column indicated two peaks at the surprisingly low frequencies of f1 = 3.0 to 3.8 Hz and f2 = 4.2 to 5.3 Hz. The frequency f1 is interpreted as the first mode bending motion in the X and Y directions of the Column and f2 may be related to the vibration of the entire Column as a "rigid body" because of detachment under the base.

The frequency of about 14.5 Hz (Y direction) and 21 Hz (X direction), which are clearly seen in the spectra of motion of the Portal from different means of excitation are interpreted as the fundamental frequencies of the Portal. We estimated the equivalent viscous damping for the first modes of vibration at various excitation levels as îcolumn=3.6% - 5.8% and îportal=1.7% - 5.4%.

We have obtained stable, high resolution results in determining resonance frequencies and damping of both structures.

Thermal and optical luminescence of fault gouge: preliminary experimental results

Philip E.[1], Porat N.[2], Agnon A.[1], Reches Z.[3]

1 Department of Geology, Hebrew University, Jerusalem 91904, Israel
2 Geological Survey of Israel, 30 Malkhe Israel, Jerusalem, 95501, Israel
3 School of Geology and Geophysics, University of Oklahoma, Norman OK, 73019, USA

Recognizing past events of intense shear along faults is essential for better understanding of earthquake physics and seismic hazards. Yet, only a few geological features, e.g., pseudotachylites, have been accepted as indicating intense shearing conditions. We present here an attempt to develop a new method to recognize past earthquakes. We hypothesize that intense shear would modify the luminescence of the gouge particles which formed during the shear event. To test this hypothesis, we measured the Optical Stimulated Luminescence (OSL) and Thermoluminescence (TL) of gouge powder that formed in shear experiments under controlled conditions. We conducted a series of experiments on a laboratory fault that was sheared by a rotary friction apparatus, which is capable of simulating earthquake conditions. The experiments were conducted under dark conditions on samples of sandstone and quartzite composed mostly of quartz. The experiments were run under slip velocities of 1 to 20 cm/s, normal stresses 0.15 to 2.8 MPa, and for few seconds to 10 minutes. The gouge formed during the shear process was collected after slip distances of few centimeters to few hundreds of meters. These samples, as well as the original non-sheared rocks, were analyzed with OSL and TL methods. The preliminary results show complete or partial OSL signal resetting (1-3 orders of magnitudes). Further, TL results of heating experiments show a resetting signal that can be related to the maximal temperature on continuous heating. These results can be compared to distinquish between conductive heating and shearing. These preliminary results suggest that OSL and TL signals are likely to be reset by the fast shear of earthquakes. We plan to apply these methods to field cases, and if successful, OSL/TL could provide good estimates of age, slip-rate, and temperature of past earthquakes

Detailed mapping of deep Jurassic structures in the Eastern Levant Basin with multi-azimuth seismic data

Politi M.[1,2], Agnon A.[1], Reshef M.[3]

1 Nadin and Freddy Harman Institute of Earth Sciences, The Hebrew University, Jerusalem, 91904
2 Adira Energy Ltd, 12 Abba Hillel st., Ramat Gan 52506
3 Department of geophysics, Tel Aviv University, Ramat Aviv, Tel Aviv 69978

During hydrocarbon exploration at the Eastern Levant Basin, a need for a detailed and accurate image of deep Jurassic reservoir formations has been identified.

The deep targeted structures are characterized by intense fracture systems and minor faults with small vertical displacements. To acquire high quality and reliable imaging we used modern multi azimuthally methods (dual and full azimuths) using modern acquisition technologies (multi streamer, Ocean Bottom Cable – OBC). The data acquired has been processed in the depth domain with an emphasis on de-noising of undesirable noises, Pre-Stack Depth Migration (PSDM) supported by a detailed and accurate velocity analysis. The integration of multi-azimuths into a 3D image has yielded a high resolution image, and detection of anomalies caused by anisotropy of seismic energy propagation within sediments, contributing to better insight and understanding of the spatial subsurface model. A comparison of data processing results firstly presented here to recently processed 2D lines using modern data processing techniques presents a clear advantage of the multi-azimuths data, permitting accurate and detailed imaging of deep structural elements in the subsurface

Data Exchange Improves Regional and Global Seismic Monitoring

Reich B., Feldman L., Avirav V., Hofstetter R.

Geophysical Institute of Israel, P.O.Box 182, Lod 71100, Israel

---

The Seismology Division, Geophysical Inst. of Israel, operates and maintains the Israel Seismological Network (ISN) in a continuous mode since 1981. The ISN comprises 42 short-period stations (include Meron array), 8 broadband stations, 57 accelerometers, and 10 infrasound stations. In the last 30 years more than 7,000 regional earthquakes, mainly in the Middle East and the Eastern Mediterranean region, and 14,500 teleseisms were recorded by the ISN, being an integral part of the seismological database. In parallel we sort out about 92,300 man-made explosions, mainly quarry explosions. In the last 30 years the Seismology Division is closely cooperating with national and international seismological organizations, i.e. ISC, NEIC, EMSC, ORFEUS, GSD, GFZ, INGV, NOA etc., in data exchange (parametric and waveforms) for the rapid and routine determination of epicenters and for the enhancement of local, regional and teleseismic monitoring. Any location of moderate to strong earthquake involves data coming from many seismic networks. We present several moderate to strong earthquakes that occurred over the globe in the last years, where some of them were catastrophic and devastating

Precipitation Kinetics of Sulfate-Bearing Minerals under Environmental Condition of CO_2 Geological Storage

Rendel P.[1], Wolff-Boenisch D.[2], Gavrieli I.[3], Ganor J.[1]

1 Ben-Gurion University of the Negev, P.B 653, Beer-sheva, 84105.
2 Geological Survey of Israel, 30 Malkhe Israel, Jerusalem, 95501.
3 Institute of Earth Sciences, University of Iceland, Sturlugata 7, 101 Reykjavík, Iceland.

Carbon Capture and Storage (CCS) has been widely recognized as one of the main technologies to mitigate climate changes. Deep-saline aquifers are the preferred potential repositories for excess CO_2, currently being emitted to the atmosphere from anthropogenic activities, Large-scale injection of CO_2 into subsurface reservoirs would induce a complex interplay of multiphase flow, capillary trapping, dissolution and chemical reactions that may have significant impacts on both short-term injection performance and long-term fate of CO_2 storage. To ensure the viability of geologic CO_2 storage, we need a holistic understanding of reactions at supercritical CO_2 water-rock interfaces and the environmental factors affecting these interactions.

The major objectives of the research are to study the kinetics of CO_2 brine-rock interactions and derive respective rate laws under the typical conditions of CO_2 storage sites. These rate laws may be used in modeling the storage sites and operating them in a way that will minimize scaling and consequence reduction of injectivity.

A new experimental system was set up at the BGU Water-Rock interaction laboratory allows studying the interaction between CO_2, brine and minerals under CO_2 supercritical conditions. Consisting of a 300ml continuous stirred reactor combined with two 30m long plug flow reactors, both fully capable to deal with high pressure, temperature and corrosive conditions maintaining a continuous and computerized data acquisition of various variables including: pressure, temperature, stirring, in-situ pH, and ORP. The experimental setup allows the measuring of dissolution and precipitation rates of diverse minerals under a wide range of environmental conditions as found in CO_2 storage sites (pressure, temperature, pumping rates, brine and rock composition) offering the possibility to sample liquid and solid samples for further chemical and morphologic analysis.

Keywords: CCS, CO_2, water-rock interaction, Kinetics, Super-critical, Dissolution, Precipitation

High resolution magnetic survey in lake Kinneret (Sea of Galilee)

Rofe M.[1], Ben-Avraham Z.[1], Tibor G.[2], Rybakov M.[3]

1 Department of Geophysics and Planetary Sciences, Tel Aviv University, Tel Aviv 69978
2 Israel Oceanographic & Limnological Research Ltd., Tel-Shikmona, P.O.Box 8030, Haifa 31080, Israel
3 Geophysical Institute of Israel, P.O.Box 182, Lod 71100, Israel

---

Lake Kinneret is located in Kinnarot-Bet Shean basin along the Dead Sea Fault, at the northwestern part of the large volcanic field Harrat ash Shaam. The magnetic field of the lake was measured by Ben-Avraham et al. in 1980. A new high resolution magnetic survey was conducted in 2008 along more than 2,400 km of dense (5-100 m spacing) grid lines. This study presents the new results of this survey.

A comparison between these surveys revealed general similarities and some new information. Both of the magnetic maps show two smooth magnetic domains: positive in the east (corresponds to normal magnetization) and negative in the north and west (probably corresponds to reverse magnetization). Nevertheless, along the northern and western shore of the lake there are large amplitude anomalies of shorter wavelength. The separation between the magnetic domains (defined by the 0 nT contour line) in the southern part of the lake revealed a significant difference.

The northwestern part of the lake is a region of particular interest, as its magnetic anomalous pattern offshore possibly reflects a sub-bottom continuation of the Cover Basalt covering the Korazim block onshore. An enlarged view of this region shows large amplitude anomalies (up to 587 nT) that appear as minima and maxima (magnetic dipoles) throughout the entire marine area. Positive and negative anomalies form a linear shape, which broadens southwards from the northwestern margin. Modeling results show that one of these anomalies is caused by a magnetized body at approximately 500 m depth, perhaps a sub-channel filled with basalt flows. A normal fault delineating the northwestern margin of the basin was previously suggested as the Kfar–Nahum fault, where a steep bathymetric scarp exists along the shore. Such faulting may suggest that the Early Pliocene (5–3 Ma ago) volcanic phase preceded the formation of the Kinnarot-Bet Shean basin. We address this issue by examining the magnetic field variations over transition between marine and land areas.

An area of 2 square km was measured with very dense (5-30 m spacing) grid lines, assuring micro-magnetic results. A high resolution (1 nT contour interval) pattern reveals local magnetic anomalies (100-800 m wavelength). The possible sources of these anomalies are shallow lithological variations.

Stratigraphy and lithology of the Neogene sedimentary sequence in Nahal Tavor area

Rozenbaum A.G.[1,2], Sandler A.[1], Zilberman E.[1], Stein M.[1,2]

1 Institute of Earth Sciences, The Hebrew University, Jerusalem 91904, Israel
2 Geological Survey of Israel, 30 Malkhe Israel, Jerusalem 95501, Israel

The stratigraphy, lithology and environments of deposition of the Neogene sedimentary sequence in the lower Galilee are revisited. This sequence, bounded between the Middle Miocene Lower Basalt and the Early Pliocene Cover Basalt, was studied in Nahal Tavor area. A detailed lithological description of two sections is presented, including thin-section examination and mineralogical composition (XRD). The sections comprise the following units: 1) the Lower Basalt; 2) a pyroclastic unit, possibly correlative to the "Umm Sabune Conglomerate"; 3) the Bira Fm.; 4) the Gesher Fm.; 5) a sequence of a conglomerate and red paleosols; and 6) the Cover Basalt. In addition, two occurrences of the Intermediate Basalt are recognized. The pyroclastic unit is 15 m thick and consists of sand to pebble size pyroclastic fragments and some carbonatic material. Ar-Ar dating of two volcanic bombs yielded total fusion ages of 13.0 and 12.4 Ma, with no plateau age. The Bira Fm., ~60 m thick, consists of bedded to laminated, soft to indurate carbonate rocks. The lower 35 m is dominated by dolomites and the upper 25 m by limestone. Most beds contain 1-20% of pyroclastic fragments, which gradually decrease from the base to the top. Beds and lenses of bentonite are interbedded, representing aquatic weathering of fine pyroclastic material. Gastropods and/or bivalve appear at least in 60% of the beds. Three sedimentary cycles were identified in the Bira Fm., each begins with detritic carbonates, some showing cross bedding, and terminates with beds rich in molluscs mainly bivalves (more than 60% in a bed); the upper one is correlated with the "lumachelle bed". These bivalve-rich beds indicate temporal connection to the open sea and near-shore facies. No unconformity was recognized between the Bira and Gesher Fms. The Gesher Fm., ~50 m thick, consists of soft dolomite, sparitic and oolitic limestone and some opal/chert lamina. The structure is bedded to laminar with some brecciated beds. Only a few beds contain macrofossils, including fish remains. Bentonite lenses and beds, increase toward the upper part, along with pyroclasts. It seems that the volcanic activity, mainly of pyroclastic material, continued after the termination of the Lower Basalt flows, declined during the end and the beginning of the Bira and Gesher Fms., respectively, and increased again in the middle Gesher Fm., preceding the eruption of the Cover Basalt flows. The results obtained so far suggest that the Bira Fm. was deposited in a shallow water body, mostly isolated from the open sea. Full isolation led to evaporitic environments at the lower part of the Gesher Fm., which gradually turned into a freshwater body in this area.

The effect of coastal groundwater salinization and freshening on nutrient behavior, experimental study

Russak A.[1,2], Yechieli Y.[2], Lazar B.[3], Herut B.[4], Sivan O.[1]

1 Department of Geological and Environmental Sciences, Ben Gurion University of the Negev, Beer Sheva

2 Geological Survey of Israel, Jerusalem

3 Institute of Earth Sciences, Hebrew University, Jerusalem

4 Israel Oceanographic and Limnological Research, Haifa

An experimental setup was designed aiming to identify and quantify the effect of salinization and freshening of coastal aquifers on nutrient behavior. Sediments and groundwater were collected from the coastal aquifer of Israel (Poleg and Nitzanim areas), as well as seawater from the same sites. One set of the column experiment was performed under aerobic conditions and the other two under anaerobic conditions by bubbling N2 gas into the injected water. Under anaerobic condition, during salinization, ammonium (NH4+) was highly enriched, up to 80 µmol ·L-1, due to desorption from the sediment by cation exchange process (similar pattern as Ca2+). Nitrate (NO3-) was depleted due to denitrification at low salinities, and consequently nitrite (NO2-) was enriched. At higher salinities NO3- concentrations were also low due to denitrification and its original low concentration in seawater. Phosphate (PO43-) was highly enriched, by up to 6 µmol ·L-1, probably due to its release via processes like organic matter oxidation and dissolution of manganese oxide or calcite, which release the adsorbed PO43-. Under aerobic condition NO2- and NH4+ remained at about 1 µmol·L-1, within the background range of seawater and freshwater. It is speculated that the NH4+ desorbed from the sediment during salinization (cation exchange) was nitrified and thus the concentration remained low. Phosphate was enriched to about 2 µmol ·L-1, probably due to desorption from the sediment by anion exchange.These experimental results show that salinization and freshening of groundwater affect the nutrient levels via ion exchange, and under anaerobic conditions, denitrification and oxides dissolution processes have additive impacts.

Where is the Carmel Fault?

Salamon A.[1], Aksinenko T.[2], Zaslavsky Y.[2], Kalmanovich M.[2], Shvartsburg A.[2], Giller V.[2], Dan H.[2], Giller D.[2], Zviely D.[3], Ankori E. Medvedev B.[2] Frieslander U.[2] Zilberman E.[1] Baruch O.[1]

1 Geological Survey of Israel, 30 Malkhe Israel, Jerusalem 95501, Israel
2 Geophysical Institute of Israel, P.O.Box 182, Lod 71100, Israel
3 Recanati Institute for Maritime Studies, University of Haifa, Haifa, 31905, Israel

---

While all geological, seismological, geophysical, and morphological evidences point towards the presence of a significant fault in between the Carmel Mountain and the Zevulun Plain, the exact surface trace of this fault has not yet been identified and mapped. Being a suspected active fault in terms of the Israeli Building Code 413 that crosses the city of Haifa and significant infrastructure facilities, its potential for surface rupture cannot be underestimated. Yet so far no unequivocal evidences were found to allow determining its status.

In light of this gap, we conducted a comprehensive project in order to trace as accurate as possible the expected surface location of the Carmel Fault between the Kibutz Yagur and the Mediterranean Sea, with a special emphasis on the associated uncertainties. The data was collected by several methods, analyzed and evaluated by a GIS platform:

i. Geological mapping: no clear surface expression of the fault was found. At the most we identified shallow dolomites of the Yagur Formation in an open pit prepared for a new structure of the Rambam Hospital. Therefore, the location of the main fault must be further northeastwards.

ii. Borehole data: analysis of the lithology of numerous drills conducted mainly for geotechnical purposes in and around the Haifa Port area, allowed to identify the transition zone between holes that penetrated the Yagur dolomites and holes with no dolomites at all. That zone is assumed as the probable location of the fault.

iii. High resolution reflection profiles: examination of the existing shallow seismic profiles, some of which were contributed by the private sector, pointed towards the zone where the fault, if exists, disturbs the shallowest layers.

Preliminary evaluation of the data so far achieved, including existing ambient noise measurements (site specific), showed gaps of data and directed us to perform further ambient noise measurements.

iv. Ambient noise cross sections: this method allows to construct S-wave velocity model of the subsurface along a given set of measurement points, and identify the places where the

velocity model changes drastically between points. The zone of such changes is interpreted as the zone where the fault is located.

Combining all the data together allowed us to portray the surface projection of the uppermost part of the Carmel Fault as it is exhibited through the various methods. The result is a narrow strip, several tens to a few hundred meters wide, which is interpreted as the zone of uncertainty of where the Carmel Fault is located.

Disharmonic structures along the arava valley. A key for understanding the tectonic activity along the dead sea rift valley.

Salmon M.[1], Ginat H.[2], Eyal Y.[1]

1 Department of Geological and Environmental Science, Ben Gurion University of the Negev, Beer Sheva 84105, Israel

2 Dead Sea and Arava Science Center, Kibbutz Qetura, Hevel Eilot 88840, Israel

---

Disharmonic structures are structures that cannot be explained by a simple faulting or by sedimentary disconformities. In the same outcrop different layers are deformed differently by the same stress. The study focused on various disharmonic structures exposed along the western part of southern Arava edge, between Be'er Ora in the south and Kibbutz Yahel in the north, in proximity to the Arava highway in the east. The research was assisted by a geological & topographical mapping accompanied with accurate GPS measurements.

The rocks in these outcrops, mainly consisting of Menuha & Mishash formations (Santonian), are restricted by a series of listric and sub-parallel horizontal faults. The bedrock in which these structures are found consists mainly of the Gerofit formation (Turonian). The missing section in the base of the outcrops may reach 50 to 120 m. Additional, intra-structure missing sections within the structure may reach 40 m

Most of these outcrops are located in a narrow strip, approximately one kilometer wide, at the margin of the Arava rift, near the cliffs that border its western edge, and in various structural places. Some of these outcrops coincide with local watershed lines, and a few are located at the bottom of the Arava Valley. In a few of these outcrops rock units from the formations Hazera & Ora (upper Canomanian and lower Turonian ages) can be found. These unique structures developed as the byproducts of a complex mechanism that includes a normal, listric and sub-parallel faulting. Changes in the main fault strike results in extension perpendicular to the main strike-slip faults, and formation of grabens. Local disturbances, in the form of very shallow negative flower structures and pull-apart, are caused by secondary East-West trending faults sub-perpendicular to the main South-North faults. These structures are part of the disharmonic folding.

The rock units that are involved in these structures suggest that the main faulting activity associated with the formation these structures took place during the early Miocene period, prior to the final design of the regional truncate surface. This activity took part during the early stage of the development of the Dead Sea and Arava Rift Valley.

A revised chronostratigraphy of the Neogene sequence in the eastern Lower Galilee

Sandler A.[1], Zilberman E.[1], Rozenbaum A.G.[1,2], Stein M.[1,2], Jicha B.[3], Singer B[3]

1 Geological Survey of Israel, 30 Malkhe Israel, Jerusalem 95501, Israel
2 Institute of Earth Sciences, The Hebrew University, Jerusalem 91904, Israel
3 Department of Geoscience, University of Wisconsin-Madison, 1215 W Dayton St., Madison WI 53706

The sedimentary sequence between the Lower Basalt and the Cover Basalt in the Lower Galilee and the North Valleys contains records of key events in the regional Neogene geological history. New 40Ar-39Ar ages are obtained to establish an accurate chronology of the Neogene marine invasions, precipitation of the thick evaporate sequence in the Zemah-Kinneret basin, and the structural evolution of the lower Galilee. The current contribution focuses on the western margins of the Dead Sea Rift between Kokhav HaYarden in the south and Poriyya in the north where 21 samples were collected from basalt flows and pyroclastic units. Fourteen samples yielded plateau ages and 7 yielded less reliable (~) total fusion ages.

Truncated basalt flows separated by conglomerate units with reddish paleosols build the upper part of the Lower Basalt at the foot of the Kokhav HaYarden escarpment, and at a nearby continuous core borehole. The lower part of this interval was dated to 11.90±0.06 and 11.16±0.09 Ma, and its uppermost flow to ~10.1 Ma. Three Intermediate Basalt flows were recorded and dated in the overlying sequence: 10.07±0.05 Ma within the Umm Sabunne Fm., 9.09±0.06 Ma (~9.0 at the borehole) and 8.48±0.09 Ma within the Bira Fm. The Cover Basalt base was dated to 5.10±0.06, somewhat younger than a previously published age (Heimann et al., 1996).

A ~100 m thick section at Nahal Yavne'el is comprised of two pyroclastic units, separated by a basalt flow and overlain by relatively thin Cover Basalt. The base of the Cover Basalt there yielded identical ages of 4.59±0.07 and 4.60 Ma±0.04, whereas the flow yielded ~5.1 Ma, indicating that the upper pyroclastic unit is the Fejjas Tuff. The lower unit consists of coarse fragments, apparently related to an eruption center with volcanic breccia, exposed near Kvuzat Kinneret. A volcanic bomb within the Fejjas Tuff at the Kinneret-Poriyya road-cut was dated to 4.89±0.33 Ma. The Fejjas Tuff extends westward to Sarona, where the base of the overlying Cover Basalt was dated to 4.96±0.11 Ma. A thin paleosol separates between the top Gesher Fm. and the base of the Cover Basalt in a core borehole drilled ~5 km north of the road-cut. The base of the Cover Basalt is dated there to 4.60±0.05 Ma.

Based on the new ages it is concluded that the activity of the Lower Basalt flow magmatism

decreased between 13 and 10 Ma while pyroclastic activity increased. The deposition of the Umm Sabunne Fm., which consists mainly of pyroclastic components, did not exceed ~0.5 Ma. The deposition of the consequent Bira Fm. commenced before ~9.5 Ma, but its termination has not yet been determined. The Fejjas Tuff is younger than 5.1 Ma, the oldest flow of the Cover Basalt.

Structure of the Levant Basin based on residual gravity anomalies

Segev A., Rybakov M.

Geological Survey of Israel, 30 Malkhe Israel, Jerusalem 95501, Israel

Gravity data were compiled from satellite gravity and compared with shipboard gravity data. The gravity effect of the water layer is calculated in 3-D mode and removed from the Free Air gravity data. The complete Bouguer gravity data have a reliability and accuracy that enables interpolation to a 5 mGal contour interval. By removing the effect of the Moho interface and mantle below, we calculated the residual Bouguer gravity (RBG). The regional RBG anomalies in the Levant basin (LB) actually reflect density variations within the ~14 km thick sedimentary succession together with the ~10 km crystalline oceanic crust. Considering the latter has relatively homogeneous basaltic composition, the major existing RBG anomalies in the LB essentially indicate density variations almost entirely within the sedimentary succession. The major Phanerozoic lithofacies belts across the Afro-Arabian continental margin significantly contribute to the major density variations. It emphasizes the carbonate lithofacies belt (20-30 mGals) offshore Lebanon, central Israel plus Yam high, northern Sinai and northern Egypt. The highest RBG anomalies (>50 mGal) are associated with prominent positive reduced-to-pole (RTP) magnetic anomalies: Cyprus, Niklas, Eratosthenes and offshore Lebanon indicate the presence of basic magmatic bodies. The Herodotus Basin and the Eratosthenes-Niklas areas are typified by RBG >40 mGal and generally positive RTP magnetic anomalies. The Pleshet, Dolphin and Baltim Basins (central LB), are most likely Cretaceous grabens, occupying the lowest RBG anomalies (down to -25 mGal). We interpret these lows as a result of very thick (>3 km) Oligocene siliciclastics that accumulated there during the Oligocene regional truncation of the Afar plume province. Minerva and Sour lows northwest from these deep heavily loaded basins, as well as Jaffa and north Sinai low RBG anomalies, or basins, on the southeast, are suggested to represent tectonism and flexural response to the central LB Oligocene loading. These basins were later (since the Pliocene) affected and filled by the loading of the Nile sedimentary cone. Leviathan SW-NE moderate positive RBG anomaly, as well as the perpendicular Hermes High are located in an undisturbed magnetic area suggesting an absence of magmatic bodies. The cause for these anomalies is probable pre-existing tectonics and isostasy. Jonah ridge is characterized by small RBG anomaly and high RTP magnetic anomaly, both strengthening the existence of volcanic ridge close to the continental-oceanic transitional zone. The internal structure of the LB based on the RBG anomalies is strongly influenced by Cenozoic sediments that accumulated within tectonic basins. It is suggested that this structure has very important implications for the thermogenic oil and gas potential in the LB.

Coastal-cliff retreat dynamics at Olga beach characterized through monthly high-resolution ground based LiDAR campaigns

Shahar N., Katz O., Mushkin A.

Geological Survey of Israel, 30 Malkhe Israel, Jerusalem, 95501

Our study quantitatively constrains the variety of cliff-erosion processes associated with an extreme winter storm event (~20-30 yr return interval) that struck the Eastern Mediterranean on Dec 11-13 2010. We focused on a 150-m-long cliff stretch near Olga in central Israel and used a total of 10 high-resolution (1-2 cm) ground-based LiDAR scans from before the storm and up until 329 days after it carried out at ca. monthly intervals.

The pre-storm LiDAR scan at this site documented a near vertical cliff face up to 25 m above sea level comprised primarily of a late Pleistocene eolianite with prominent cross-bedding structures (Dor Eolianite); a <10-m-wide beach stretch between the cliff base and the water line was interrupted midway by a pile of talus material associated with a 20-m-long landslide scarp in the cliff face directly above. The first post-storm LiDAR scan was carried out 30 days after the storm and revealed extensive cliff erosion along the entire stretch. Syn-storm cliff erosion totaled 970 m3 .

We distinguish between post- and syn-storm erosion based on the presence, or lack of talus material below the eroded cliff-face, respectively: As significant post-storm weather events did not occur in this region up until the first scan - material that was removed from the cliff and was not observed at the cliff-base (e.g., talus) is assumed to have been removed during the storm itself, and is thus categorized as syn-storm activity. Accordingly, cliff erosion with associated talus material is categorized as post-storm activity.

Massive syn-storm erosion of 250 m3 also occurred on the pre-existing midway talus pile. Post-storm activity up until the first scan was fairly minor. The next post-storm LiDAR scans which took place 58, 105 and 135 days after the storm recording a single 53 m3 rock slide event, a massive 1312 m3 rock slide and another 985 m3 rock slide event respectively, documented two major post-storm changes: 1) Erosion and removal of St from the base of the cliff, and 2) major rockslide events which affected the entire cliff height and resulted in up to 7m of inland cliff-top retreat. The remaining scans documented overall cliff stability. Nonetheless, prominent cliff-parallel fractures are visually apparent and appear to be at highest risk of future collapse.

Quantitative Analyses of Macrofauna and Depositional Environments of the Bira Formation at Nahal Tavor

Shaked-Gelband D.[1,2], Edelman-Furstenberg Y.[1], Mienis H. K.[3], Sandler A.[1], Zilberman E.[1], Stein M.[1,2], Starinsky A.[2]

1 Geological Survey of Israel, 30 Malkhe Israel St., Jerusalem, 95501
2 Institute of Earth Science, Hebrew University of Jerusalem, Givat Ram, Jerusalem, 91904
3 National Mollusc Collection, Hebrew University of Jerusalem, Givat Ram, Jerusalem, 91904

A sequence of Neogene sedimentary rocks in the Lower Galilee and the North Valleys, wrapped between major basalt units, contains the unrevealed records of geological key events. During this period major marine invasion(s) formed on-land water bodies that deposited sequences of lacustrine/lagoonal sediments.

A sequence of the Bira Formation was described and sampled in a tributary of Nahal Tavor. This sequence includes abundant beds rich with gastropods and bivalves, far more than known from previous works. Forty two layers were sampled, and so far, in 32 of them the macrofossils were sorted, identified and counted. Quantitative analyses of community structure included species richness, species evenness, species dominance, feeding types and life habitats. Variations in the density of shell-packing as well as the assemblage composition provided knowledge on the changes in the depositional environment.

In addition, the isotopic composition of strontium was measured in a few samples from Nahal Tavor, Tel Kashish and Poriyya (both fossils and matrix). The results show intermediate values, which suggest a mixed supply from sea water and basaltic fresh water.

A total of 51 molluscan taxa were identified, 30 gastropods and 21 bivalves. The molluscan assemblages range from assemblages with a dominance of 1-2 species and very low species richness (2-8) to those with no dominant species and a high richness (24 species).

The molluscan assemblages of the Bira Formation in this area indicate periods of open connection with the ocean and periods of restricted, or no connection. In general, the section shows estuarine/fresh water environments. Fresh to brackish water gastropods (Melanoides, Melanopsis, Theodoxus, Lymnaeidae, Bithynia) are the dominant group throughout the section. There are at least five marine intercalations in the Bira Fm. The three intercalations examined so far are characterized by a dominance of 60-100% marine bivalve species (Ruditapes, Mytilidae). The upper part of the Bira sequence is characterized by a stronger marine control indicated by the presence of several densely-packed shell beds, i.e., "lumachelle". These first results clearly show that despite the few marine intercalations, the Bira Foramtion in this area is basically non-marine.

Geometrical Focusing as a Mechanism for Significant Amplification of Ground Motion in Sedimentary Basins

Shani-Kadmiel S.[1,4], Tsesarsky M.[1,2], Louie J. N.[3], Gvirtzman Z.[4]

1 Department of Geological and Environmental Science, Ben Gurion University of the Negev, Beer Sheva 84105, Israel
2 Department of Structural Engineering, Ben Gurion University of the Negev, Beer-Sheva 84105, Israel
3 Nevada Seismological Laboratory, University of Nevada, Reno, USA
4 Geological Survey of Israel, 30 Malkhe Israel, Jerusalem 95501, Israel

---

In this study we investigate the parameters which lead, by mechanism of geometrical focusing, to exceptionally high ground shaking during strong earthquakes. We have previously shown that the deeper structure of sedimentary basins can produce a range of intra-basin effects, i.e., edge-effect above faults and other steep structures, diversion of seismic energy by convex diapirs or magmatic intrusions and convergence of seismic waves above "bowl-shaped" sub-basins (Shani-Kadmiel et al., 2012). We find by means of analytical solution the point at which seismic energy converges and employ a 2-D finite difference numerical solution for a more detailed analysis in the time and frequency domains.

Our results indicate that effective geometrical focusing occurs for a very specific set of interface eccentricities and velocity ratios, converging seismic energy at ±0.5 km from the surface. In cases where the span of the convergence zone is sufficiently small and close to the surface, this mechanism leads to significant amplification of PGV at the center of the basin by up to a factor of 3.5. The spectral amplification ratio of ground motions as a result of effective geometrical focusing is frequency dependent such that amplification is proportional to frequency up to the corner frequency of the source. Effectively focusing basins with low velocity ratio equate the travel-time of body- and surface-waves causing them to converge at the center of the basin. Overlapping resonant frequencies of these phases cause a ground motion pulse with exceptionally large amplitude.

Reference:

Shahar Shani-Kadmiel, Michael Tsesarsky, John N. Louie, and Zohar Gvirtzman, 2012 in press. Simulation of Seismic-Wave Propagation through Geometrically Complex Basins: The Dead Sea Basin. Bulletin of the Seismological Society of America, 102, accepted 13 January.

Deep percolation of nitrate, under citrus orchards: vadose zone observations and modeling

Shapira R., Kurtzman D.

Institute of Soil, Water and Environmental Sciences, ARO, Volcani Center

During the last decade, high nitrate concentration is the main cause, for disqualification of drinking water wells in Israel. Fertilization excess or inefficient utilization, of Nitrogen (N) inputs at the surface, may increase N leach and contaminate the underlying aquifer.

In this study we obtained continuous undisturbed sediment cores from agricultural land above the Israeli coastal aquifer. In total, 15 boreholes of 9 meter depth were drilled using a direct push rig, at five different sites. Each site consists of three boreholes, two relatively close (<30 m), and the third relatively far (>100 m). Four sites are located within citrus orchards (three in Hamra soil of the Sharon region and one in Vertisol of the Yehuda low land), and one site is located within a field of variable crops in the Sharon. Soil cores were cut to samples that represent 30 cm out of the vertical profile, enabling a detailed analysis of the root zone and deep vadose zone.

Water content, chloride (Cl) and nitrate profiles show large heterogeneity within the sites. Nevertheless closer profiles have a higher correlation than distant profiles of the same plot. High Cl concentrations below root zone (average 490-1480 mg/l), indicate relatively low recharge below the orchards (90-325 mm/year). Unlike the Vertisol profiles, those of Hamra show significant correlation between Cl and nitrate, suggesting large fractions of nitrate that are not withdrawn by the roots. Ammonium concentration profiles are negligible under all sites, apart of one orchard, that is being irrigated using treated waste water (TWW) since around 1980. Relatively uniform dissolved organic carbon (DOC) profiles were found in heavy soils, whereas in lighter soils these profiles are high at the top, and decrease sharply within the top three meters to low concentrations in the deep vadose zone.

Three sites were chosen for calibration of one-dimensional models of water flow (Richards equation with root water uptake) and transport of Cl, ammonium and nitrate (advection dispersion equation with source/sink terms for reactions and uptake threw the vadose zone). Fitting of observed and modeled water contents was obtained using physical data (bulk density, hydraulic conductivity and grain size distribution) and moderate parameter fitting. Dispersivity was calibrated using the chloride profiles. Fitting modeled nitrate profiles to those observed, required restriction of the maximum allowed concentration for nitrate root uptake. This result is in-line with the correlation between Cl and nitrate profiles. The calibrated models were used to simulate optional fertilization scenarios. Simulation of 50% N fertilizers, showed

72% reduction of N leach, while N root uptake decreased by only 22%. Lower amounts of N inputs may further reduce N fluxes to groundwater. A good start may be farmers' consideration of N in the irrigation water as fertilizer.

Probability based estimation of earthquake risk parameters to be used in earthquake preparedness operations.

Shapira A.[1], Steinberg D. M.[2], Begin Z. B.[3]

1 National Steering Committee for Earthquake Preparedness, PM Office, Jerusalem.
2 School of Mathematical Sciences, Tet Aviv University.
3 Ministerial Committee on Earthquake Preparedness, Government of Israel, Jerusalem

---

Responders to the event of a destructive earthquake would much appreciate having a reference earthquake damage scenario that will quantify the earthquake risk towards which they will prepare. One approach, commonly used, is to define an earthquake of magnitude M and location X which corresponds to a certain probability of occurrence and prepare for its consequences, i.e., defining a reference event to yield a reference scenario (using e.g. HAZUS). However, when considering preparedness on a national or regional level, there is usually no one reference event that should be applicable for all sites (communities) in the country. Furthermore, the damages associated with a reference event may not reflect the damages that are "likely" to happen in the next T years. In order to get an idea of the likely damages, we need to study the damage distribution, not the earthquake distribution.

To overcome these difficulties, we developed a novel approach in which we aim at assessing the probability of exceeding specified damages (earthquake risk) within a predefined period rather than computing damages from a reference scenario. Consequently, we quantify the earthquake risk parameters, such as number of severely damaged houses or number of fatalities, which correspond to an acceptable probability, to be determined by the decision makers.

The results obtained provide a uniform risk reference to be targeted in preparedness and readiness operations. It has to be emphasized that those risk parameters are not predictions of damages likely to occur in any single earthquake. In most cases they will be lower than those estimated from a maximum probable earthquake.

The emergence of collapsed sinkholes on mudflats along the shore of the Dead Sea

Shoval S., Kaz G.

The Open University of Israel

The emergence of collapsed sinkholes on mudflats along the shore of the Dead Sea is related to subsiding of the near-surface sediments into subsurface cavities. The sinkholes on the mudflats appear in a local Holocene rock unit known as Ze'elim Fm. The mudflats were formed by exposure of the littoral clayey sediments along the shore of the Dead Sea due to the regression of the sea water. The emergence of the sinkholes was ascribed to the fast drop of the Dead Sea base-level, which leads to the formation of the subsurface cavities due to dissolution by groundwater within subsurface rock salt layer.

The present study reveals that the emergence of sinkholes on mudflats is very much controlled by the properties of the clayey sediments of the mudflats. Their subsidence involves two types of movements – subsurface flowing and near-surface collapsing. Within the subsurface saturated zone at the base of the sinkholes the wet clayey sediments behave as a mud and move into the soaked cavities by subsurface flow, as a viscous fluid. The ability of the subsurface wet clayey sediments to flow into the cavities resulting from their muddy properties encouraged by fine grained and loose texture, saturation with saline water and richness in expandable smectite layers. As a result of removing of sediments in the subsurface, within the above near-surface unsaturated zone the dry and unconsolidated sediments collapse down and the holes of the sinkholes become open to surface.

Study the long-term re-hydroxylation and rehydration in pottery of different archeological ages in view of re-hydroxylation dating

Shoval S.[1], Paz Y.[2]

1 The Open University of Israel
2 The Israel Antiquities Authority

Re-hydroxylation dating has been proposed in the literature as a developing technology for dating fired clay ceramic. Therefore, the study of the long-term re-hydroxylation and rehydration in ancient pottery in relation to their archeological ages is of interest. In the present study, the accumulation of the re-hydroxylation and the rehydration in the pottery is quantified by measuring the weight-loss of the corresponding de-hydroxylation and dehydration process using thermal analysis apparatus. The advantage of this apparatus in separation of the weight-loss occurs by the de-hydroxylation from that of the dehydration in the course of controlled heating of the pottery.

Pottery of different archeological ages: Chalcolithic, Bronze, Iron, Persian and Roman Periods as well as traditional vessels were measured. Two groups of pottery were examined, noncalcareous and calcareous pottery. In each of these groups the weight-loss due to de-hydroxylation and due to combined dehydration and de-hydroxylation increases generally with the increase age of the pottery. However, some pottery has exceptional weight-loss in relation to their archeological ages, which is related to variations in the composition of the pottery, the level of the firing and the burial conditions in the site. From the results, it seems that the re-hydroxylation dating is not sensitive enough for pottery of adjacent archeological periods and some pottery behave exceptional.

Pseudo-amorphous and crystalline phases in the ceramic composition of noncalcareous pottery

Shoval S.[1], Paz Y.[2]

1 The Open University of Israel
2 The Israel Antiquities Authority

Pseudo-amorphous and crystalline phases in the ceramic composition of Bronze Age noncalcareous pottery from Canaanite sites were studied using FT-IR and micro-Raman spectroscopy. These methods are advantageous in identification of the pseudo-amorphous thermal phases which are lack XRD peaks. The application of second-derivative and curve-fitting techniques improves the identification. The FT-IR spectroscopy makes it possible to distinguish between meta-smectite and metakaolinite and to estimate the firing temperature of the pottery. The Micro-Raman spectroscopy is sensitive to the structural degree of ordering of the thermal phases and enables point analysis of peculiar components in the composition of the pottery.

Two groups of pottery were analyzed: Brown Cooking Ware and ceramic 'Metallic Ware'. Pseudo-amorphous meta-clays are found to be the main phase in the ceramic material of the pottery. The Brown Cooking Ware is rich in meta-smectite and the ceramic 'Metallic Ware' is rich in mixture of metakaolinite with some meta-smectite. That finding indicates that they were fired from raw material containing smectite and smectite with kaolinite, respectively. The crystalline phases in the ceramic material contain some amounts of re-carbonated calcite (up to 3%) and some reformed clay minerals. The 'Metallic Ware' contains some gehlenite, indicating that it was fired from raw material containing some calcite. Initial minerals in the ceramic material are quartz silt and some anatase. Proto-mullite and mullite were not detected in the composition of the pottery.

The emergence of collapsed sinkholes on mudflats along the shore of the Dead Sea

Shlomo S.[1], Paz Y.[2]

1 The Open University of Israel
2 The Israel Antiquities Authority

The emergence of collapsed sinkholes on mudflats along the shore of the Dead Sea is related to subsiding of the near-surface sediments into subsurface cavities. The sinkholes on the mudflats appear in a local Holocene rock unit known as Ze'elim Fm. The mudflats were formed by exposure of the littoral clayey sediments along the shore of the Dead Sea due to the regression of the sea water. The emergence of the sinkholes was ascribed to the fast drop of the Dead Sea base-level, which leads to the formation of the subsurface cavities due to dissolution by groundwater within subsurface rock salt layer.

The present study reveals that the emergence of sinkholes on mudflats is very much controlled by the properties of the clayey sediments of the mudflats. Their subsidence involves two types of movements – subsurface flowing and near-surface collapsing. Within the subsurface saturated zone at the base of the sinkholes the wet clayey sediments behave as a mud and move into the soaked cavities by subsurface flow, as a viscous fluid. The ability of the subsurface wet clayey sediments to flow into the cavities resulting from their muddy properties encouraged by fine grained and loose texture, saturation with saline water and richness in expandable smectite layers. As a result of removing of sediments in the subsurface, within the above near-surface unsaturated zone the dry and unconsolidated sediments collapse down and the holes of the sinkholes become open to surface.

Geomorphological settings of wave-shape notches, developed on the carbonate slopes of Mt. Carmel, Israel

Shtober Zisu N.[1], Amasha H.[1], Frumkin A.[2]

1 Department of Israel Studies, University of Haifa, Mt. Carmel, Haifa, 31905, Israel
2 Geography Department, The Hebrew University, Jerusalem, 91905, Israel

Notches, (in Hebrew: Tsnirim) are horizontal erosion features common along carbonate cliffs of the Mediterranean climate zone In Israel. These morphological features are shaped like half tubes that extend over tens or hundreds of meters, along stream valley slopes. Although this morphological phenomenon is widely observed, little is known about its origin and the processes that shaped it. The term "notch" is used in the relevant literature to describe horizontal "C"-shaped indentations, developed on slopes or cliffs, regardless of their location or shaping mechanism. However, as most studies relate the origin of notches to coastal processes, they are rarely discussed in the context of inland sites.

In Israel, inland notches can be found in the Carmel Mountain area, as well as in the Galilee and in the Judean Mountains.

The present study is designed to identify the evolution and the processes which shaped these enigmatic landforms. To this end, the study is assumed to identify, quantify and classify this phenomenon in terms of geomorphological and bioerosional settings, using a multidisciplinary approach.

Previous studies attributed the formation of Mt. Carmel notches to a Late Tertiary transgression which eroded the lower levels of the Mountain by marine processes, whereas recent observations suggest the implausibility of a coastal/marine origin. The present study suggests that notches are dissolution/weathering cavities cut into particular types of limestone or dolomite beds, in accordance with the strata' susceptibility to weathering, i.e. the specific chemical and mineralogical properties of the lithic substrate, which might favor bioerosional processes.

Within the Carmel Mountain, notches are found at altitudes of between 116 to 425 m.a.s.l. Most notches are concentrated in the Nahal Oren, Nahal Haruvim and Nahal Hod catchments, although some were also observed in the Galim, Rushmia, Rakefet and Mearot channels' canyons. Their height may reach 10 meters, but most common notches are 2-3 meters high and 1-2 meters deep. They are always developed in dolomite or hard limestone and always follow a particular exposed stratum; most notches are found in the Yagur (dolomite) Formation, limestone beds of Arqan Formation, and in both Muhraqa and Sumaq members (Bina Formation).

The small scale structure and roughness of carbonates fault mirrors

Siman-Tov S.[1], Aharonov E.[1], Emmanuel S.[1], Sagy A.[2]

1 Institute of Earth Sciences, The Hebrew University, Jerusalem 91904, Israel
2 Geological Survey of Israel, 30 Malkhe Israel, Jerusalem 95501, Israel

---

The surface roughness and the small-scale features of fault planes are significant factors in controlling frictional stability and earthquake mechanics. In this research we look at the nano-to-micro structures of carbonate fault planes using AFM (Atomic Force Microscopy) and SEM (Scanning Electron Microscope), showing that these planes are composed of cohesive nano powders that also result in highly smooth surfaces. We propose that both the smoothness of these faults and their nano-grained structure are very significant during slip motion.

Many mature fault surfaces (large total slip and wide shear zone) have "mirror-like" appearance, i.e. at certain angels they reflect light perfectly even at field exposures. To better understand the roughness, the structure, and the formation of mirror surfaces, samples were collected from three "mirror" carbonate fault planes along the Dead Sea Rift and analyzed with nano characterization tools. AFM scans of the samples, and spectral analysis that we performed on topography profiles, revealed that on the micro-scale the mean surface roughness amplitude is a few tens of nanometers, which indeed, according to the "Rayleigh roughness criterion" makes them reflect light almost like mirrors. In fact we propose that one can use "mirror like" appearance of faults and the "Rayleigh roughness criterion" to constrain their micro-scale roughness to below ~50 nms.

In addition, the AFM scans showed that the surface topography changes from a smooth surface with striations on it at the micron scales, to hilly topography on the sub-micron scales. This change of topography at small scales was also demonstrated by the spectral analysis of the roughness. The nano features that were observed by AFM scans, were also observed in SEM Images. These showed that the hills are in fact stacked nano-powders that cover the surfaces. If these nano-powders are the result of a co-seismic process, it could have a special significance to the physics of slip in mature faults. SEM images also showed the change from striated surfaces in scales larger than microns, to nano features with no striations at the smaller scales. This agrees with the loss of brittleness predicted under ~1 micron.

We also performed TEM measurements normal to the interface, showing that the layer of nano-grains is about 500 nms deep, and covers a layer of highly twinned calcite micro-crystals, with a rough interface between the two layers. The TEM images suggest that the nano-grains may form by detaching boundaries between twins. This suggests a coupled ductile-brittle

deformation that forms the nano-powder. Further research is needed to fully understand the formation of these nano-particles in shear zones and how they influence slip during seismic events.

Corroboration for the influence of a component of solar irradiance on subsurface radon signals

Steinitz G.[1], Sturrock P.[2], Martin C.[3], Piatibratova O.[1], Kotlarsky P.[1]

1 Geological Survey of Israel, 30 Malkhe Israel, Jerusalem 95501, Israel
2 center for Space Science and Astrophysics, Stanford University, Stanford CA USA
3 Department of Geology, La Laguna University, Tenerife, Spain

Rn-222 occurs at highly varying levels as a trace component in subsurface air (geogas). Nuclear radiation from radon in geogas and in experiments using air+radon within a confined volume exhibits systematic temporal variations. These variations are composed of periodic and non-periodic signals spanning from annual and semi-annual to daily and sub-daily durations. Analysis of extensive data sets from three key sites 200 km apart in the arid desert of southern Israel and from a 5-year experiment using alpha and gamma detectors demonstrate that the periodic variations, observed to a depth of >100 meters, are related to an above surface driver probably due to a component of solar irradiance.

New confirmations are based on recognizing further cyclic phenomena, some of which are not linked with Earth related periodicities. A likehood analysis of the alpha and gamma time series in a long-term experiment is performed. A Combined Power Statistic formed from the gamma, alpha-H and alpha-L sensors inside the experimental tank shows that the time series of the nuclear radiation contains an annual periodicity as well as a clear semi-annual and possibly a ternary-annual periodicity. The same analysis also resolves additional periodicities in the frequency range of 10-15 yr-1 in the gamma time series which are indicative of a relationship to rotation of the sun around its axis. Observation of solar periodicities in the temporal pattern of the nuclear radiation of radon is a significant independent substantiation for the notion of the influence of a component in solar irradiance.

An independent confirmation of the solar effect in the experimental data is obtained by observing day time and night time patterns. "Specgrams" of the power as a function of frequency and hour of day show that the peak of the annual periodicity occurs at daytime while the semi-annual and solar periodicities are seen to be prominent at night. This is interpreted to indicate a differentiation in the nuclear radiation from radon as a function of rotation of Earth. – i.e. when Earth faces the sun and when the sun is completely obstructed. This feature is also demonstrated using Continuous Wavelet Transform (CWT) analysis on separate time series composed of day-time and night-time measurements

Using the CWT analysis tool the day- and night-time difference in radon time series is also detected at subsurface geological sites from Israel, Tenerife and Italy. These sites are from different geological and geophysical scenarios, different elevations and span depths from several meters to around 1000m below the surface.

Hydrocarbon Potential and Prospectivity of the Southern Dead Sea - Results of an Integrated Basin Analysis

Tannenbaum E.[1], Gardosh M.[2], Bruner I.[3], Kremien R.[1]

1 Ginko Oil Exploration LTD, 11 Menahem Begin St., Ramat Gan, Israel
2 Ministry of Energy and Water, 234 Jaffa St, Jerusalem, Israel
3 Ecolog Engineering LTD, 3 Pekeris St. Tamar Park, Rehovot, Israel

Minor quantities of oil and gas and various types of heavy oil shows were found in the Southern Dead Sea Basin (SDSB), although large accumulations of hydrocarbons were not yet discovered. In 2002 Ginko Oil Exploration L.P. acquired a Temporary Permit for exploration in an area that extended from Ein Gedi to Neot Hakikar. The company conducted an integrated basin analysis, led by the late Dr. Eli Tannenbaum , to evaluate the hydrocarbon potential and identify drilling prospects in the Zerach Permit area.

The analysis included systematic study of the SDSB using advanced exploration techniques, some of them applied in Israel for the first time. The main steps of the study were: (a) reprocessing approx. 300 km of selected 2D seismic lines using "multi-focusing" stacking procedure; (b) time and depth mapping of seven seismic horizons; (c) compilation of the basin's structural and stratigraphic framework; (e) 2D and 3D modeling of subsidence history; (f) 2D and 3D modeling of thermal history, hydrocarbon migration and entrapment. In a following stage of the project a regional gravity dataset was analyzed and an airborne High-Resolution Magnetic survey (HRAM) was acquired to identify potential structural traps.

The results of the integrated basin analysis showed significant potential for hydrocarbon generation, migration and entrapment. Modeling suggested that generation of oil from the organic-rich Senonian Bituminous Rocks (SBR) started 4 Ma ago and is still taking place. It was estimated that up to 1 BBOE may be trapped in commercial-size accumulations. Various prospective areas were identified on the margin and within the basin; the latter were subdivided to shallow, deep and ultra-deep prospects. Two favorable areas for exploration were outlined: Metzada-Mor in the north and Amiaz-Sedom in the south. One well was drilled on the basin's margin, Zuk Tamrur-4, and discovered small amount of oil. Other potential traps within the basin were not tested by drilling.

Master plan for floodwater utilization in the Central and Northern Arava Valley

Tatarsky B.[1], Simon E.[1], Iviansky Y.[1], Agbaria R.[2]

1 Tahal Consulting Engineers Ltd.
2 Israel Water Authority

During the period 1975-1998 six percolation reservoirs were constructed along the central and northern Arava Valley: Nekarot (1975), Eshet (1986), Tzokim (1994), Idan (1997), Neot Tmarim (1998) and Hatzeva (1998). The original aim of the project, initiated and spearheaded by the Jewish National Fund (JNF), was to promote enhanced groundwater recharge by infiltration from the reservoirs to the local alluvial aquifer. Two main advantages were expected to be gained from the scheme: (a) preventing flash floods from reaching the saltpan at Kikar Sdom, where they are lost to the utilizable water storage; and (b) promoting aquifer recharge close to consumers, thus minimizing the energy and costs involved in conveyance. Subsequently, a secondary use was developed for the reservoirs in the form of direct utilization of the water by farmers. This involved construction of pumping stations, filtration and chlorination systems next to three of the six reservoirs.

In time serious doubts regarding the efficiency of the reservoirs began to be expressed. One of the main concerns was the accumulation of a considerable amount of both fine and coarse material in the reservoirs, transported by the high energy of the flows during every flood. This has two negative impacts: blockage of the reservoir bottoms to infiltration of water to the subsurface, and reduction of the effective storage volume of the reservoir. Moreover, the local drainage authorities encountered many operational difficulties that had not been foreseen in the early stages and that were found to have a significant effect on the utilization opportunities and maintenance costs of the systems.

Much effort has been invested in maintaining, operating and monitoring the reservoirs and the aquifer, mainly by three authorities: (a) the local drainage authorities; (b) Mekorot Water Co. Ltd.; and (c) the Hydrological Service. However, no entity has to date taken full responsibility for the system as a whole, while management policy has never been defined.

Many studies have been carried out in the past on various aspects of the percolation reservoir scheme in both the academic and private sectors. The studies include a broad range of issues dealing with physical, quality and engineering aspects.

The present study comprises two main stages (and objectives):

Stage 1: to analyze the efficiency of each reservoir and determine whether it is contributing to

or harming the utilizable water storage.

Stage 2: to suggest alternatives to the current scheme in order to improve water utilization, and recommend an optimal alternative for each reservoir based on engineering and economic analyses.

The current address presents the interim conclusions of the first stage, which was completed recently.

The study is commissioned and sponsored by the Israel Water Authority.

Lithological constrains for gas hydrate distribution on the mid-Norwegian margin: influencing slope stability and geo-hazard through time

Waldmann N.[1], Haflidason H.[2]

1 The Dr. Moses Strauss Department of Marine Geosciences, Haifa University, Mt. Carmel, Haifa 31905, Israel

2 Department of Earth Science, University of Bergen, All?gaten 41, N-5007 Bergen, Norway

Gas hydrate is stable in marine sediments on many Arctic continental slopes under present temperature and pressure fields. Yet, changes in the physical conditions have been shown to trigger dissolution and emanation of methane into the ocean. Access to a huge database of 2D and 3D seismic records, covering the entire mid-Norwegian margin, now provide an exceptional opportunity to test the relationship between methane release and slope stability. On the mid-Norwegian margin wedges of thick glacigenic units were deposited during past glacial intervals and covers older sequences of fine-grained hemipelagic siliceous ooze. This stratigraphic architecture combined with subsidence, large amount of biogenic methane, deep thermogenic methane reservoirs and thermal processes, provide a natural laboratory where to study the development and dynamics of methane hydrates and other digenetic processes through Cenozoic time.

Gas hydrate bearing sediments are commonly detected in our seismic profiles by the presence of cross-cutting bottom simulating reflectors (BSR's). We also recognize the presence of a second, deeper BSR. This reflector has previously been interpreted as a fossil base of the gas hydrate stability zone caused by hydrate dissociation during postglacial sea level rise and increase bottom water temperature. Several submarine slides confine the spatial distribution of present day gas hydrates, whereas the occurrence of the second BSR is patchy and discontinuous, but appears to be detached from the mass wasting structures. This observation indicates the possible link between methane dissociation and migration from the deeper BSR to the present-day gas hydrate stability depth with ocean floor destabilization at different temporal scales. The presence of a diagenetic-related BSR deeper in the stratigraphical sequence may also suggest thermal gradient increase at depth, thus providing a complementary scenario for methane hydrates dynamics through time.

A Holocene record of tectonic activity in Tierra del Fuego, Southernmost South America (54ÆS)

Waldmann N.[1], Ariztegui D.[2], Austin Jr. J.[3], Anselmetti F.[4], Moy C.[5]

1 The Dr. Moses Strauss Department of Marine Geosciences, Haifa University, Mt. Carmel, Haifa 31905, Israel
2 Section of Earth and Environmental Sciences, University of Geneva, Rue des Maraichers 13, 1205 Geneva, Switzerland
3 Institute for Geophysics, Jackson School of Geosciences, University of Texas at Austin, TX 78759, Texas, USA
4 Eawag, Swiss Federal Institute of Aquatic Science and Technology, Ueberlandstrasse 133, 8600 Duebendorf, Switzerland
5 Geology Department, University of Otago, 360 Leith Walk, 9054-Dunedin, New Zealand

High-resolution seismic imaging and sediment coring in Lago Fagnano, located along the Magallanes-Fagnano plate boundary in Tierra del Fuego, have revealed a chronologic catalog of Holocene mass-wasting events. These event layers are interpreted as resulting from slope instabilities that load the slope-adjacent lake floor during mass flow deposition thus mobilizing basin floor sediments through gravity spreading. A total of 22 mass flow deposits have been identified combining results from an 800 km-long dense grid of seismic profiles with a series of sediment cores. Successions of up to 6 m-thick mass-flow deposits pond the basin floor spreading eastward and westward following the main axis of the eastern sub-basin of Lago Fagnano. An age model on the basis of information from previous studies and from new radiocarbon dating allowed establishing a well-constrained chronologic mass-wasting event catalogue covering the last ~15000 years. Simultaneously-triggered basin-wide lateral slope failure and the formation of multiple debris flow and megaturbidite deposits are interpreted as the fingerprint of paleo-seismic activity along the Magallanes-Fagnano transform fault that runs along the entire lake basin. The slope failures and megaturbidites are interpreted as recording large earthquakes occurring along the transform fault since the early Holocene. The results from this study provide new data about the frequency and possible magnitude of Holocene earthquakes in Tierra del Fuego, which can be applied in the context of seismic hazard assessment in southernmost Patagonia.

Late Holocene sediment cycles and vegetation change in the Zraq Qa'a Jordan

Woolfende W.[1], Ababneh L.[2]

1 Fulbright Alumnus and Emeritus Scientist, USFS, Bishop, California
2 Research Specialist, Academy of Natural Science, Philadelphia, PA, USA

Shifts in aquatic and terrestrial vegetation associations and hydrology during the past >3100 yr are indicated by the pollen and sediment sequences in a core retrieved from the Azraq wetland, Jordan. The pollen sequence provides evidence for a relatively stable wetland during the period of study until ca. AD 1400 when the wetland apparently declined as desert shrubland expanded. Springs continually supplied fresh water that maintained the shallow pools and marsh. In periods of increased winter precipitation, runoff from the surrounding wadis may have inundated the wetland and deposited silts and clays. During dryer episodes the influx of winter storm water would have been much less but the springs would have still provided water to the wetland and deposited peat. This is shown by the sequences of clay, silty and sandy clay loam, and peat in the core. However, an interruption in the sedimentary cycle is noticed around 250 B.C. that suggests a change in the landscape use and relation during that period.

Constraining regional paleo peak ground acceleration from back analysis of prehistoric landslides: Example from Sea of Galilee, Dead Sea transform

Yagoda - Biran G.[1], Hatzor Y.H.[1], Amit R.[2], Katz O.[2],

1 Department of Geological and Environmental Science, Ben Gurion University of the Negev, Beer Sheva 84105, Israel

2 Geological Survey of Israel, 30 Malkhe Israel, Jerusalem 95501, Israel

Accurate estimation of expected peak ground acceleration (PGA) in seismically active regions is a challenging task. The best way to estimate, quantitatively, expected PGA is by investigating instrumental data of past strong earthquakes in a given area. In some regions of the world however recorded data are scarce, and if they exist, they are typically available only since the late 19th century. As such they are hardly representative of the true seismicity in the studied region. We propose here an analytical approach to constrain the lower threshold of paleoseismic PGA on the basis of back analysis of old landslides. To perform the analysis we use a mapped landslide with geomorphic features that have been preserved in the field, the slip surface of the landslide, a good reconstruction of the slope geometry and ground water level prior to failure, and the mechanical properties of the sheared material. We perform static and pseudo-static limit equilibrium back-analyses using standard solution procedures to obtain lower bounds of paleoseismic PGA required to induce slope failure. Back analyses of three different landslides around the Sea of Galilee (SOG) return similar PGA results that range between 0.15 and 0.5 g, thus constraining the threshold paleoseismic PGA range for this region. The analytically inferred regional PGA is supported by results of an independent numerical analysis of earthquake-toppled columns in a nearby Byzantine church.

Using results from a recent paleoseismic trenching study performed on one of the studied landslides and a modified attenuation relationship for the study area we localize the possible loci of moment magnitude Mw=7.0 earthquakes that can explain the studied failures along the boundaries of the SOG, and find that they coincide with traces of the Eastern and Western Margin faults of the Dead Sea transform around the SOG. The temporal relationships between the observed failures are discussed on the basis of dated colluvial sediments, geomorphologic constraints, and archeological evidence.

About "myth" accompanying the results obtained from the ambient noise measurements for the microzoning of an earthquake hazard

Zaslavsky Y., Gorstein M., Ataeva G., Aksinenko T., Kalmanovich M., Perelman N.

Geophysical Institute of Israel, P.O.Box 182, Lod 71100, Israel

Many examples of destructive earthquakes clearly show that local site conditions often cause a great damage. The necessity for detailed mapping of the earthquake hazard in urban areas derives from the fact that the geological inhomogeneity dominates the spatial distribution of the intensity of damage and the amount of casualties. In most cities around the world direct information from the strong motion recordings is usually unavailable. The same situation exists in Israel, where the great variability in the subsurface conditions across a town/city and the relatively high costs associated with obtaining the appropriate information about the subsurface, strongly limits proper earthquake hazard quantification.

Over the years, we have conducted site investigations in several thousands of sites in urban areas. These investigations demonstrate that the horizontal-to-vertical (H/V) spectral ratio from the ambient noise can be a useful tool for the assessment of the ground motion characteristics on soft sediments. This information, together with any available geological, geotechnical and geophysical information, helps constructing a reliable model of the subsurface, which is then integrated in the processes of the seismic hazard assessment.

Nevertheless, various researchers conclude that whereas the prominent peak of the H/V ratio is well correlated with the fundamental resonance frequency, the amplitude of this peak is not as stable and accurate estimate of the amplification level as the one obtained from the spectral ratio of earthquake records. These "myths" are produced by ignorance of many factors that influence on measurements and analysis of ambient noise. When one or more of these factors drop out from the view of the researchers, different "myths" could be "born" .Our experience dispels them by focusing on several of these factors: identity of the registration channels, coupling between seismometers and soil, recordings length of the ambient noise, selection of the spectral analysis time window for obtaining reliable H/V ratio, underground pipe lines and construction, soil-structure interaction, effect of rain and wind.

Quantification of the site effects in the Israeli building code, using the Vs,30 parameter. – A seismological view

Zaslavsky Y.[1], Gorstein M.[1], Perelman N.[1], Ataev G.[1], Aksinenko T.[1], Shapira A.[2]

1 Geophysical Institute of Israel, P.O.Box 182, Lod 71100, Israel
2 National Steering Committee for Earthquake Preparedness, Prime Minister's Office

Modern building codes for seismic design, including the recently updated Israeli Standard (SI 413), adopted new site amplification factors and new procedure for site classification. The new site classification system is based on five soil classes, defined in terms of the average shear wave velocity through the top 30 m of the soil profile (Vs,30).

In the last decade, the Seismology Division of the Geophysical Institute of Israel launched conducted site investigation in more than 5500 locations, located in 30 towns and neighboring villages. These investigations demonstrate a high variability in the subsurface condition across a town/city.

Soil column models were used to calculate the uniform hazard linear and non linear site specific acceleration spectra (10% exceedance in 50 years). Computations are made, as in series of the previous studies, using the SEEH procedure (SEEH – Stochastic Estimation of the Earthquake Hazard) developed by Shapira and van Eck [Natural Hazard 8, 201-215, 1993].

Site corrections, defined as the ratio between the maximum ordinate of the non-linear acceleration spectrum at the surface to the acceleration spectrum on bedrock at the same period are calculated from synthetic accelerograms that served as input to the 1-D multi-layers soil column model, in two period ranges: 0.1-0.7 sec (corresponds to the period of 0.2 sec) and 0.8-1.2 sec (corresponds to the period of 1.0 sec).

Our study has demonstrated that the geology across is complex and highly variable over short distances questioning the usefulness of using Vs,30 to classify sites and applicability of adopting site correction values that appear in e.g. the American codes in Israel for soils of the same class. Additional soil parameters may strongly affect amplification effects.

Neoproterozoic basement and Lower Paleozoic siliciclastic cover of the Menderes Massif (Western Taurides): coupled U-Pb-Hf zircon isotope geochemistry

Zlatkin O.[1], Avigad D.[1], Gerdes A.[2]

1 Institute of Earth Sciences, The Hebrew University, Jerusalem 91904, Israel
2 Institute of Geosciences, Mineralogy, J.W. Goethe University, Frankfurt 60438, Germany

It is commonly accepted that the Tauride Block (southern Anatolia) was originally a part NE Africa – Arabia prior to opening of the Eastern Mediterranean in the Triassic. The Neoproterozoic basement of the Taurides, overlain by Paleozoic platform sediments, is exposed in the Menderes Massif. It comprises metasediments and intrusive granites. The oldest Neoproterozoic unit, a Paragneiss, contains significant amounts (~30%) of Archean-aged zircons and εHf(t) values of about a half of its Neoproterozoic zircons are negative suggesting derivation from distal Pan-African terranes dominated by reworking of an old crust. In the overlying, mineralogically-immature Core Schist, the majority of the detrital zircons are Neoproterozoic, portraying positive εHf(t) values indicating derivation from a juvenile source, resembling but not identical to the Arabian Nubian Shield. The period of sedimentation of both units is constrained between 570 to 550 Ma (Late Ediacaran). The Core Schist sediments, ~9 km thick, accumulated in less than 20 my implying a tectonic-controlled sedimentary basin evolved adjacent to the juvenile terrane. Granites, now orthogneisses, intruded the basin fill at 550 and 545 Ma, they carry 560-1000 Ma and 2.0-2.5 Ga inherited zircons and exhibit ±0 εHf(t=550 Ma) and TDM ages of 1.4 Ga consistent with anatexis of various admixtures of juvenile Neoproterozoic and Late Archean detrital components.U-Pb-Hf detrital zircon signal of a Paleozoic quartzite located in the base of a pre-Carboniferous silisiclastic cover resembles that of far-traveled Ordovician sandstones in Jordan, supporting pre-Triassic paleorestorations placing the Tauride with Afro-Arabia. The detrital signal of the overlying carbonate-bearing Quartzitic sequence (Devonian-Early Carboniferous?) is dominated by a local fingerprint: the majority of its detrital zircons yielded U-Pb-Hf values identical to that of the underlying granitic gneiss implying exposure of Menderes-like granites. The hiatus between both units possibly reflects the pre-Carboniferous unconformity known in the Levant. The U-Pb-Hf detrital zircon content of the Menderes Neoproterozoic and Lower Paleozoic metasediments fits a Gondwana provenance, consistent with derivation from Neoproterozoic Pan-African orogens, most likely from various segments along the East African Orogen and the Sahara Metacraton. ~550 Ma granites are not known in the northern Arabian-Nubian Shield where igneous activity mostly ceased by 580 Ma. Granites possessing TDM ages of 1.4 Ga are also uncommon there. This implies that the Menderes does not represent a straightforward continuation of the Arabian-Nubian Shield. 260-250 Ma lead-

loss and partial resetting of the U-Pb system of certain zircons in both basement and cover units was identified. It is interpreted as a consequence of a Permian - Early Triassic thermal event coeval with paleo-Tethys closure north of the Tauride and with the onset of Neo-Tethys opening in the Levant.

Visual methodology for identifying damage of historical earthquake: the case of 1927 in old photographs of Jerusalem

Zohar M.[1], Rubin R.[2], Salamon A[1]

1 Geological Survey of Israel, 30 Malkhe Israel, Jerusalem 95501, Israel
2 Department of Geography, Hebrew University, Jerusalem

Many localities in Jerusalem have been severely damaged during the 1927 Jericho earthquake, however this is known mainly from written and eyewitness reports and only a few photographs. The methodology presented here allowed us to widen significantly our ability to trace the damaged localities by identifying the appearance of iron anchors in old photographs. The anchors were reported to have been installed after the 1927 earthquake in damaged structures in order to prevent further deterioration.

The search focused on the Jaffa Gate area for being relatively preserved since the beginning of the 20th century and well documented by numerous accounts. The findings were mapped and classified on a GIS platform and a set of inspected buildings containing the anchors was generated. Overall 5 variants of anchors were identified: (1) Iron Rails; (2) Thin Rods; (3) 'X' formed anchors; (4) 'S' formed anchors; and (5) Round Clamps.

Each of these buildings was examined in relation with the historical sources and the old photographs. The photographs were then classified into two groups: those taken prior to the earthquake and those taken as close as available after the occurrence. This way we were able to single out the anchors that were installed right after the earthquake and those that were placed in later times. For the 'post- earthquake' anchors, it is reasonable to assume that they were used for retrofitting damaged building. Such were the Iron Rails, Thin Rods, 'X' and 'S' formed pipes. Ideally, this is also supported by written sources. On the other hand, no 'post-earthquake' Round Clamps were identified, and they are dated to 'post-1967' times.

This new approach enabled us to map in high resolution the spread of damage caused by the 1927 earthquake around the Jaffa Gate, much better had we limited ourselves to the inspection of written sources. The potential of this new methodology can now be further applied for damage and risk analyses in other parts of Jerusalem as well as in other old cities.

S-shape distribution of the longshore sand transport at the Mediterranean coast of Israel

Zviely D.[1,2], Kit E.[2]

1 The Leon Recanati Institute for Maritime Studies, University of Haifa, Haifa 31905, Israel.
2 Faculty of Engineering, School of Mechanical Engineering, Tel-Aviv University, Ramat-Aviv, Tel-Aviv 69978, Israel.

The Mediterranean coast of Israel, with the exception of Haifa Bay and few small rocky headlands, has a straight shoreline that gradually changes its orientation from northeast to almost north. The coastal section from Ziqim to Haifa Bay and its inner continental shelf (0 to about 30 m depth) considered the northern flank of the Nile littoral cell. This region is mainly composed of Nile-derived quartz sand. Sand from the Nile Delta moves eastward to the northern Sinai, then northeastward to the Israeli coast by longshore currents. These currents are generated by the radiation stresses of breaking waves and shearing stresses of local winds. Wave-induced currents are generated in the surf zone, generally limited to about 10 m depth. Since radiation stresses are generally at least an order of magnitude greater than shear stresses, these stresses predominate in the surf zone during storms. Beyond this region, however, to about 30 m depth, shelf currents are generated by local winds. The wave-induced and wind-induced longshore currents occur in both directions. However, the net longshore sand transport (LST) runs northward along the entire coast, up to Haifa Bay. This northward net LST results from waves of larger size approaching from west-southwest and southwest compared to their counterparts from west northwest and northwest.

As a result of this net LST direction, sand accretion has developed at the southern side (up-stream), while the northern side (down-stream) of marine structures along Israel's southern coast has eroded. Along Israel's central and northern coasts, however, this morphological phenomenon is less dominant - even inverted around some small coastal structures. This apparent contradiction led some researchers to the mistaken claim that net LST north of Netanya runs southward. Such claims - if correct - would require a convergence zone between Tel-Aviv and Herzliya, where huge amounts would accumulate. Coastal and seabed observations in this region fail to detect any such accumulation.

In the last years new LST computations for the Israeli coast were performed based on high-quality directional wave data. The results of these assessments where supported by coastal observations gathered from aerial photographs, beach surveys and bathymetric charts. The LITDRIFT model of Danish Hydraulic Institute enables to get the cross-shore distribution of the LST was used in the recent studies. S-shape distribution revealed in these computations

indicates that, although the integrated net sediment transport in the central and northern parts of Israel is directed to the north, the net transport is to the south in a narrow strip between the coastline and seabed contour of 2 to 3 m depth. This S-shape distribution, explains sand accretion observed at the northern side of small coastal structures between Herzliya and Carmel coast.